EXPLORING ALTERNATIVES TO PVPP FOR FINING PHENOLIC COMPOUNDS IN WINES

by

SAMADHI CHINTHANA CHANDRASEKARA

THESIS

SUBMITTED TO FLINDERS UNIVERSITY

FOR THE

MASTER OF BIOTECHNOLOGY

02nd JUNE 2025

FLINDERS UNIVERSITY

COLLEGE OF MEDICINE AND PUBLIC HEALTH

TABLE OF CONTENTS

LIST OF ABBREVIATIONS

MWCNTS	Multi-walled Carbon Nanotubes
PVPP	Polyvinylpyrrolidone
HPLC	High-performance Liquid Chromatography
TFA	Trifluoroacetic acid
ACN	Acetonitrile
AC	Activated Carbon
G	Graphene nanoplatelets
CNTs	Carbon Nanotubes
OH-CNTs	Hydroxyl-functionalized Carbon Nanotubes
COOH-CNTs	Carboxyl-functionalized Carbon Nanotubes
NH_2-CNTs	Amine-functionalized Carbon Nanotubes

LIST OF FIGURES

LIST OF TABLES

ABSTRACT

The wine industry is looking to sustainable and environmentally friendly alternatives as a global trend. Polyvinylpolypyrrolidone (PVPP) is a synthetic polymer commonly used to remove phenolic compounds from wine. Due to its plastic-based nature and inability to biodegrade, it is important to find a sustainable and environmentally friendly alternative to replace PVPP. This study identified a range of carbon-based nanomaterials, including graphene (G), activated carbon (AC), carbon nanotubes (CNT), and functionalized carbon nanotubes (OH-CNTs, COOH-CNTs and NH_2-CNTs), as potential alternatives to PVPP for removing phenolic compounds from white wines.

This study applied an experimental plan with seven fining agents at five concentration levels (200-2,000 mg/L) in Riesling and Chardonnay wines, which were used as a matrix. Scanning electron microscopy (SEM) revealed distinct morphological characteristics for each nanomaterial. Nanoparticle tracking analysis (NTA) proved that various fining agents impacted particle size distribution.

UV-Vis spectroscopy demonstrated the effectiveness of reducing total phenolic content at 280 nm absorbance levels, showing that various carbon alternatives were as effective as PVPP. High-performance liquid chromatography (HPLC) analysis of several phenolic compounds, including tyrosyl, caftaric acid, caffeic acid, and quercetin, revealed that AC produced the greatest percentage reduction at the highest concentration (2,000 mg/L). Meanwhile, functionalized CNTs exhibited varying efficiencies based on their surface functionality. The optimal concentration range for using PVPP in white wines is generally 100-800 mg/L. While higher concentrations may enhance phenolic removal, they can also lead to the over-stripping of desirable phenolics, resulting in wines with diminished mouthfeel, reduced aromatic complexity, and imbalanced sensory profiles. Additionally, excessive fining agents use increases production costs, generates more lees, and may complicate subsequent stabilization steps. Therefore, using the minimum effective dose is recommended for balancing wine quality. These results highlighted the importance of selecting fining agents based on the specific objectives of the winemaking process. The results confirmed that, based on effectiveness and cost, carbon-based nanomaterials, especially graphene and carbon nanotubes, are sustainable alternatives to PVPP for use in wine fining. This research provides valuable information for developing a more sustainable approach to winemaking while preserving or improving wine stability and quality.

DECLARATION

I certify that this thesis does not contains material that has been submitted for a degree or diploma at any university earlier without acknowledgement, Moreover, the work presented here will not be submitted by me for another degree or diploma in the future without Flinders University's approval, best of my knowledge and belief, does not contain any material previously published or written by another person except where due to reference in made in the text.

ACKNOWLEDGEMENT

My sincere gratitude and heartfelt appreciation are hereby extended to the following individuals, who have continued to support me throughout this research work.

Associate Professor Agnieszka Mierczynska-Vasilev, Principal Research Scientist at the Australian Wine Research Institute (AWRI), South Australia, for the expert guidance and encouragement given to me throughout this research project. Her sage advice and thoughtful ideas aided the successful completion of this project.

Professor Krasimir Vasilev, Professor of Biomedical Nanotechnology in the College of Medicine and Public Health, Flinders University, for the expert guidance and encouragement given to me throughout this research project.

Professor Alistar Standish, Course Coordinator, Master of Biotechnology in College of Medicine and Public Health, Flinders University, for the valuable guidance at all times.

I would like to thank to other staff from the Australian Wine Research Institute, South Australia, for assisting with instrumentation.

I am deeply indebted to all my family and colleagues for providing me with unconditional motivation and support to pursue this achievement.

CHAPTER 1

LITERATURE REVIEW

1.1 Background

The fining process is a crucial step in winemaking, as it eliminates unwanted phenolic compounds and polyphenols that can negatively impact the sensory qualities of the wine. Currently, Polyvinylpolypyrrolidone (PVPP) is the most widely used synthetic polymer in the wine industry for reducing specific phenolic compounds associated with issues like browning, astringency, and pinking (Cosme et al., 2019). However, due to its plastic-based composition and associated environmental concerns, there is a growing demand for alternatives, particularly greener and more sustainable options. Polyphenols and phenolic compounds in wine, including anthocyanins, tannins, and catechins, significantly influence its sensory characteristics, especially colour, taste, and stability (Merkytė et al., 2020). Consumers are often willing to invest in high-quality bottles because wine is a highly valued product that reflects cultural significance and sensory appeal (Geană et al., 2019). While these phenolic compounds are essential for enhancing the wine's profile, an excess can lead to undesirable characteristics. The finning process aims to remove or reduce these compounds, with PVPP being highly effective for wine clarification and stabilization (Ferreira et al., 2018). However, growing environmental awareness and regulations regarding plastic pollution have intensified the search for sustainable alternatives (Mocke, 2023).

The nanotechnology suggests that carbon-based nanomaterials, such as carbon nanotubes (CNTs), functionalized CNTs, and graphene, could serve as promising alternatives to traditional fining agents (Luchian et al., 2024). These materials possess unique physical and chemical properties, including a high surface area and significant aggregation potential, which could contribute to their effectiveness in reducing phenolic compounds in wine. Notably, the single-layer carbon atoms arranged in a 2D lattice structure of graphene demonstrate the ability to diminish these compounds (Mamvura et al., 2012). However, these innovative fining agents remain in the experimental stage regarding their application in the wine industry.

This research addresses significant environmental and technical challenges in the wine industry. By exploring the potential of graphene and CNTs as alternatives to traditional fining agents, it aims to develop a sustainable approach that maintains or even enhances wine quality. These new fining agents, by offering superior binding properties compared to PVPP, may

potentially facilitate more effective removal of phenolic compounds. Their reusability and lower environmental impact could make them particularly appealing in the context of modern sustainable winemaking (Cosme et al., 2019).

1.2 Overview

1.2.1 Hypothesis and Aims

This research aims to investigate the potential of graphene, carbon nanotubes, and functionalized carbon nanotubes as sustainable and environmentally friendly alternatives to polyvinylpolypyrrolidone for fining phenolic compounds in wines. The central hypothesis points out that graphene and carbon nanotubes, due to their unique physicochemical properties, can either match or exceed the performance of PVPP in enhancing wine stability and quality.

Nanomaterials typically range in size between 1 to 100 nm and possess distinctive crystalline structures that confer high resistance to extreme temperatures and low pH levels (Luchian et al., 2024). These attributes make them particularly valuable in both the pharmaceutical and wine industries. Their well-defined pore structure and dimensional properties facilitate favourable adsorption kinetics (Luchian et al., 2011), enhancing the selective adsorption process that can effectively modify the phenolic profile of the wine.

Furthermore, the functionalization of CNTs can further enhance their effectiveness by introducing various chemical groups that improve their binding capabilities with phenolic compounds. This versatility allows for targeted fining, enabling winemakers to tailor the fining process to specific wine types and desired flavor profiles. Additionally, the eco-friendly nature of carbon-based nanomaterials aligns with the industry's increasing focus on sustainability and reducing environmental impact.

Overall, this research seeks to provide a comprehensive evaluation of these innovative nanomaterials, offering insights into their practical applications in winemaking and contributing to the development of more sustainable practices within the industry.

1.3 Wine and Winemaking Process

1.3.1 Wine

Winemaking and the consumption of wine have been part of human civilization for centuries (Anderson, 2018). Renewed for its rich variety of colour, aroma, taste, and cultural significance, wine is produced through the fermentation of grape juice or must, where grape sugars are transformed into ethanol and carbon dioxide (Waterhouse et al., 2024). Although Australia possesses ideal conditions for grape growing, its wine production and exports did not gain significant momentum until the 1890s. Between 1980 and 2000, Australian wine production quadrupled, with exports accounting for two-thirds of the total production. Now, Australia's wine industry is positioned as a dominant player in the global wine industry (Anderson, 2018). According to the Australian wine export report, during the 12 months of 2024, the export value increased by 34% to 2.55 billion dollars compared to 2023. Also, the total volume of wine increased by 7% to approximately 649 million litres (Wine Australia, 2023).

1.3.2 The Winemaking Process

The transformation of grape juice into wine is one of humanity's oldest biotechnological practices, dating back to the dawn of civilization. Over time, numerous winemaking technologies have been developed, contributing to the remarkable diversity of wine products we see today (Mills et al., 2008).

The first step in winemaking is the grape harvest and crush. While the procedures for making white and red wine are largely similar, there are key differences in processing. For white wines, techniques such as cold settling, filtration, or centrifugation are employed to separate the juice from the skins and clarify it. The clarified juice is then transferred to a barrel or fermentation tank, where alcoholic fermentation begins, either through the wild yeasts present in the juice or with the addition of a starter culture. The fermentation process for white wines typically lasts from one to two weeks, with temperatures gradually increasing from 10 to 18°C.

In the production of red wine, after pressing the grapes, the skins remain in contact with the ferment to infuse colour into the wine. Alcoholic fermentation begins either through the action of natural yeasts or by adding a starter culture, similar to the process for white wine. During fermentation, solids rise to the top of the tank, forming a "cap". Winemakers often push this cap down into the liquid to enhance the extraction of red pigments and influence the wine's taste profile. Once the appropriate period has passed, the wine is separated from the skins, and

fermentation continues in a different container. The wine is considered "dry" when all the primary sugars in the juice have been converted into alcohol (Mills et al., 2008). Following fermentation, the winemaking process involves aging, blending, fining, stabilization, filtration, sterilization, and bottling (Waterhouse, 2002). Figure 1.1 displays the production process flow chart of white and red wine.

1.3.2.1 Wine Aging

Aging is a critical step in the winemaking process, during which significant and diverse physicochemical changes occur that can lead to considerable financial costs for producers (Pereira et al., 2010). Many phenolic compounds in wine are unstable during aging, undergoing a series of reactions such as oxidation, polymerization, and pigmentation. These modifications can significantly alter the wine's organoleptic qualities. Sensory perception and the age of red wine are key factors in assessing the quality and characterization of alcoholic beverages derived from grapes (Chira et al., 2012).

Figure removed due to copyright restriction.

Figure 1.1 Flow chart illustrating the overall production process of wine making and the diverging production streams leading to white and red wine prior to the stage of bottling. This flow chart clearly maps each pivotal production phase and identify significant inputs and outputs along the vinification route (Mills et al., 2008).

1.3.2.2 Finning Process in Winemaking

Fining is a crucial step in the winemaking process, aimed at producing a wine that approaches perfection in taste, colour, and clarity. Ideally, the fining process should not compromise the wine's essential aromatic and flavour compounds (Castillo-Sánchez et al., 2008).

During fining, agents bind with the unwanted compounds in the wine, which then gradually settle at the bottom of the fermentation tank, forming a sediment known as lees. Once the lees have settled, they can be completely removed, ensuring that undesirable substances are while

these proteins exhibit considerable diversity, most are structurally related and classified as pathogenesis-related (PR) proteins. Their tendency to form haze or cloudiness further emphasizes their critical role in maintaining wine stability and clarity (Ferreira et al., 2001).

Coagulation of proteins in white wines can occur due to unfavourable storage conditions, leading to aggregation. Denatured protein may precipitate, forming amorphous sediments or deposits, or they may flocculate, resulting in a suspended haze in the bottled wine. This haze reduces the wine's commercial value and can make it unacceptable for sale. In the highly competitive global wine market, wine must appear clear and free of visible sediments to attract customers.

One common solution to the issue of protein instability is the use of bentonite, which effectively removes proteins responsible for haze formation. This practice has become integral to the production of white and rose wines (Ferreira et al., 2001). However, bentonite fining has notable disadvantages, including issues related to waste disposal challenges and, more importantly, significant wine losses - typically, between 3 to 10 % of the wine volume is lost with the bentonite less (Waters et al., 2005). In Australia alone, losses to the wine industry from bentonite fining have been estimated at $100 million per year, with global losses reaching approximately $1 billion (Majewski et al., 2011).

In response to the challenges, several alternative approaches have been developed (Van Sluyter et al., 2015) (Vincenzi et al., 2005). Recent research has focused on using zeolites and magnetic nanoparticles to remove haze-forming proteins from wines (Mierczynska-Vasilev et al., 2019).

1.3.3 Wine Sugars

The primary grape sugars found in wine are hexoses, specifically fructose, and glucose, both of which are reducing sugars. These sugars accumulate during the ripening of grapes, starting from nearly undetectable levels. In dry wines, typical sugar concentrations range from 0.2 - 4.0 g/L for fructose, and 0.5 - 1.0 g/L for glucose (Waterhouse et al., 2024). These sugars not only contribute to the wine's sweetness but also play a crucial role in fermentation, where yeast converts them into alcohol and carbon dioxide. The balance of these sugars can significantly influence the overall taste and quality of the wine (Jordão et al., 2015).

1.3.4 Phenolic Compounds in Wine

Phenolic compounds in wine can be categorised into two groups: simple phenolic compounds, which have a single aromatic ring containing one or several hydroxyl groups, and polyphenolic

compounds, which feature multiple aromatic rings in their structure (Waterhouse, 2002). These compounds are secondary metabolites found in grapes, and their formation and modification can occur during the winemaking process.

Phenolic compounds significantly contribute to the quality of the wine, enhancing sensory attributes such as taste and colour. They also play a crucial role in wine's aging potential and overall stability. Furthermore, moderate wine consumption, particularly of polyphenol-rich wines, has been associated with health benefits, including a reduced risk of chronic disorders such as diabetes mellitus, metabolic syndrome, and cardiovascular diseases (Visioli et al., 2020).

The most abundant constituents of the non-alcoholic fraction of red wine are polyphenolic compounds. However, their overabundance can create challenges for wine, particularly in relation to colour and aroma. (Gil et al., 2019).

Wine phenolics are classified into two main groups based on their chemical structures: flavonoids and non-flavonoids (Burin et al., 2011). Each group contains several sub-groups. Key categories of non-flavonoids include phenolic acids and stilbenes, while flavonoids encompass anthocyanins, flavan-3-ols, and flavonols. The most common phenolic compounds used to assess the quality and authenticity of wine include phenolic acids, flavonoids, tannins, and stilbenes (Merkytė et al., 2020). Figure 1.2 shows the primary structures of the non-flavonoids and flavonoids in wine.

Figure removed due to copyright restriction.

Figure 1.2 The primary structures and classification of phenolic compounds in wine: (A) hydroxybenzoic acid, (B) hydroxycinnamates (Merkytė et al., 2020), (C) hydrolysable tannins (Lozada-Ramírez et al., 2021), (D) cis- and trans-stilbenes (Merkytė et al., 2020), (E) monomeric flavan-3-ols (Zhao et al., 2023), (F) flavones, (G) flavonols, (H) anthocyanidins (Merkytė et al., 2020).

1.3.4.1 Phenolic Acids

The two major types of phenolic acids found in grapes, and wine are hydroxycinnamic acids and hydroxybenzoic acids. Among the hydroxycinnamic acids, caffeic, coumaric, and ferulic acids generally occur as conjugates with tartaric acid esters or diesters. In contrast, the hydroxybenzoic acids are characterised by a general C6–C1 structure and mainly exist in their free forms in wine. The well-known examples of hydroxyl benzoic acids include gallic, vanillic, gentisic, syringic, salicylic, and protocatechuic acids. The concentration of these phenolic acids directly influences the sensory profile of the wine, impacting descriptors such as colour, bitterness, and astringency in mouthfeel (Muñoz-Bernal et al., 2023).

1.3.4.2 Flavonoids

All wine flavonoids belong to the class of polyphenolic compounds, characterised by multiple aromatic rings with attached hydroxyl groups. Flavonoids typically consist of 15 carbon atoms and feature a common structure of two aromatic rings linked by a three-carbon chain. The principal classes of flavonoids used as chemical indicators in wine include anthocyanins,

flavonols, and flavan-3-ols (Merkytė et al., 2020). These flavonoids play a crucial role in determining the colour, flavour, and overall quality of the wine.

1.3.4.3 Tannins

Tannins can be categorized into two major chemical groups: hydrolysable tannins and condensed tannins. Both types contribute to the sensory property of astringency in wines, with proanthocyanidins playing a significant role in this characteristic and being essential for red wine quality. Astringency, regarded as the most important organoleptic feature in red wines, is not a distinct taste but rather relates to mouthfeel or tactile sensation. It is often described as a sensation of dryness or roughness (Muñoz-Bernal et al., 2023).

The variability of tannins is influenced by their isomer structure, which depends on the framework of their bonds and the type of monomers involved. Tannins also contribute directly to wine flavour by adding bitterness and play a crucial role in stabilizing red wine colour through the formation of complexes with anthocyanin (Merkytė et al., 2020).

1.3.4.4 Stilbenes

Stilbenes represent a small class of grape compounds, with resveratrol being the most important member of this group. These compounds share a similar origin to cinnamic acid derivatives and are formed in must and wine during the winemaking process (Rentzsch et al., 2009). Their high antioxidant, anticarcinogenic, and antimutagenic properties make them valuable for health promotion in the human diet (Visioli et al., 2020). Table 1.1 represents the common phenolic compounds in red and white wines and its concentrations.

Table 1.1 Common concentrations of phenolic compounds in red and white wines (Waterhouse, 2002).

Figure removed due to copyright restriction.

1.4 Challenges Related to Phenolic Compounds in Wine

1.4.1 Browning Reaction of Polyphenols

Both red and white wines tend to shift from their typical colour to a brownish hue over time. This discoloration, commonly called "browning", is characterized by an increased absorbance in the yellow region of the visible spectrum, particularly around 420 nm (Skouroumounis et al., 2005). Browning is a significant concern in winemaking and is primarily caused by phenolic compounds, including cinnamates (Li et al., 2008).

Two types of browning can be distinguished in wine: enzymatic and non-enzymatic. Enzymatic browning involves oxidoreductases, mainly polyphenol oxidase (PPO), and typically occurs at the beginning of the winemaking process, such as during crushing and maceration. PPO and other enzyme activities generally decrease during fermentation due to ethanol production. Consequently, any browning observed after vinification is usually attributed to non-enzymatic oxidation (Li et al., 2008). Figure 1.3 shows the Effects of phenols on wine.

Figure removed due to copyright restriction.

Figure 1.3 Effects of phenols on wine: (a) Complex relation between flavan-3-ols and sensory characteristics such as aroma, taste, and colour. (Zhao et al., 2023), (b) The Non-enzymatic browning process in wine. It takes place during aging through chemical oxidation. The phenolic compounds get oxidized and form reactive quinones, with metal ions, it act as the catalysts. Quinones further polymerize and contribute to the browning of the wine. (c) The enzymatic browning process, initiating during crushing, release enzymes and phenolic substrate and enabling them to react with oxygen. With glutathione depletion, residual quinones react and produce brown pigments. (Li et al., 2008).

1.4.2 The Sensory Quality of Wine

Wine phenolic compounds are key secondary metabolites responsible for essential sensory attributes such as colour, astringency, and bitterness, all of which significantly impact the quality of the finished product. (Cosme et al., 2019). However, excessively high concentrations of these phenolic compounds can lead to undesirable taste or appearance issues. These challenges can often be mitigated by reducing the concentration of the phenolic compounds through the use of fining agents, such as polyvinylpolypyrrolidone (Durán-Lara et al., 2015). Additionally, during the process of vinification, odourless precursors present in both grapes and musts are hydrolyzed, releasing varietal aromas, including varietal thiols. This release of aromatic compounds can also be regulated by fining treatments (Gil et al., 2019).

1.5 Limitations of PVPP

1.5.1 Polyvinylpolypyrrolidone (PVPP) in Winemaking

Polyvinylpolypyrrolidone, or PVPP, is a specialized fining agent predominantly used in alcoholic beverage production, particularly in winemaking. This partially cross-linked synthetic polymer, derived from polyvinylpyrrolidone (PVP), has a strong affinity for binding polyphenolic compounds (Gil et al., 2019).

PVPP is primarily used to reduce polyphenol levels in wines, effectively addressing issues related to browning and off-flavours. It can be applied at various stages of the winemaking process, including in grape must, during fermentation, or to the final wine. However, its most common applications occur either at the must stage or during fermentation (Seabrook & van der Westhuizen, 2018).

Since its commercial introduction in 1961 as an adsorbent for phenolics in beer, PVPP has been widely adopted to enhance beer stability and prevent haze formation. Its application has also extended to winemaking (Ferreira et al., 2018). In 2014, white wine production represented 32 % of global wine output, with a total of 270 million hectoliters, with an estimated PVPP usage of 1,037 tons for this application (Cosme et al., 2012). This highlights the significant role PVPP plays in improving the quality and stability of wines.

1.5.2 Problems Associated with PVPP in Winemaking

Polyvinylpolypyrrolidone (PVPP) is widely used in winemaking to enhance quality by reducing polyphenol levels, effectively addressing issues related to browning and off-flavours. However, its application leads to several significant limitations and challenges.

Firstly, PVPP generates substantial amounts of waste, much of which is directly discharged into municipal wastewater treatment plants. While research on the environmental effects of PVPP is limited, studies on similar polymers suggest potential ecological risks. Based on current consumption rates, approximately 20,000 tons of PVPP will need to be disposed of over the next 20 years, a figure that is likely a conservative estimate (Ferreira et al., 2018).

Moreover, as a plastic material, PVPP is lightweight, durable, strong, and inexpensive, qualities that make it useful but also highly problematic. Its durability poses decomposition challenges, leading to increasing instances of PVPP pollution in the environment. Vanharova's study revealed that in soil environments, PVP-based material exhibited only approximately 4% biodegradation over a 70 days, showing slow decomposition rates. (Vanharova et al., 2017). This raises concerns about PVPP's contribution to global plastic pollution, particularly in the wine industry, which is increasingly focused on sustainability and environmentally friendly practices (Ferreira et al., 2018).

Another significant challenge is the rising cost and unsustainable availability of PVPP. This situation raises questions about the long-term viability of relying on this synthetic fining agent, which has been essential in many winemaking processes (Cosme et al., 2019). Winemakers may need to explore alternatives, such as natural fining agents like bentonite or egg whites, or innovative approaches to clarify and stabilize wines.

Additionally, while PVPP effectively clarifies wine, it can also lead to the loss of desirable flavour and aroma compounds, impacting the overall sensory profile. Its effectiveness can vary depending on the wine's composition, resulting in inconsistent outcomes. The risk of over-fining is another concern. Overuse of PVPP can lead to overly sterile wines, stripping them of character and complexity, which is particularly important for premium wines (Van Buiten & Elias, 2024).

In summary, given these challenges, winemakers must carefully consider the use of PVPP in their processes, balancing its benefits against its environmental and economic implications. Exploring alternative fining methods may be essential for promoting both wine quality and sustainability in the industry.

1.6 Alternative Fining Agents

The process behind wine stabilization and achieving clarity over time involves the physical and chemical precipitation of unsuitable compounds and particles that contribute to cloudiness in wine. While clarification can occur naturally, it typically takes a considerable amount of time

and may not yield the desired clarity, astringency, bitterness, and stability (González-Neves et al., 2014). Additionally, fining agents are used to eliminate haze formation caused by wine proteins and reduce colour intensity.

Fining agents function as binding agents, facilitating the binding and precipitation of polyphenols and tannins. They react chemically or physically to form new complexes that can be separated from the wine after settling to the bottom of the vessel (Ghanem et al., 2017).

When selecting fining agents, several characteristics and concerns must be considered, including their safety for health, compliance with permitted additives, ease of separation from wine, minimal alteration of the wine's composition, and insolubility in the final product. Alternative fining agents can be categorized into existing and novel fining agents.

1.6.1 Existing Fining Agents

Gelatine- The addition of gelatin to white wine helps reduce phenolic compounds associated with bitterness and astringency. In red wine, gelatin is used as a colourant-reducing agent. It primarily interacts with larger polyphenolic compounds, and the amino acids present assist in the interaction between wine tannins and gelatin. These large molecular-weight substances eventually precipitate to the bottom of the solution (Rossi & Singleton, 1966). Among protein-based fining agents, gelatin is the most aggressive. Therefore, over-fining and excessive colour removal is easily achievable.

Isinglass - Isinglass is a collagen-based preparation derived from sturgeon collagen (Boulton et al., 2013). It is mainly used to clarify white wines, resulting in a brilliantly clear appearance with minimal effects on astringency. Isinglass easily interacts with monomers and smaller polyphenolic compounds, contributing to a soft mouthfeel and reducing harsh taste sensations. However, over application can lead to residual protein in the wine, increasing the risk of protein haze (Bisson, 1996).

Table 1.2 Common fining agents used in the wine industry, their origin, and usage in winemaking (Sanborn et al., 2010).

Figure removed due to copyright restriction.

Figure removed due to copyright restriction.

Activated Carbon (AC) - Activated carbon is a highly porous solid characterized by a structure in which atoms are densely packed, allowing for extensive surface area and varied pore sizes (Sing, 2013). Research indicates that activated carbon is effective in adsorbing and removing phenolic compounds from water thanks to its superior adsorption capacity (Mukherjee et al., 2007). In the wine industry, activated carbon serves a crucial role in deodorizing and decolorizing wines, helping to eliminate unwanted flavours and aromas (Boulton et al., 2013). Its relatively low cost (Abu-Nada et al., 2021) and effectiveness make it a popular choice among winemakers for improving the overall quality of their products. Due to its high porosity, activated carbon can effectively bind to a range of compounds, making it a versatile tool in the winemaking process. However, careful dosage is essential to prevent the removal of desirable flavours and to maintain the integrity of the wine. AC may eliminate some essential phenolic compounds, which may cause reduced desirable sensory characteristics in the wine.

1.6.2 Novel Approaches to Wine Fining

Recent literature has highlighted the effective use of carbonaceous materials, such as activated carbon, graphene, and carbon nanotubes, in capturing pollutants, including dyes, phenols, and

oil spills. These innovative materials have demonstrated significant potential for removing various contaminants, and their application techniques are rapidly evolving (Abu-Nada et al., 2021).

In the context of winemaking, novel approaches for fining are emerging that leverage these advancements to enhance the clarification and stabilization of wine. By utilizing these cutting-edge techniques and materials, winemakers will be able to improve wine quality while addressing environmental concerns and increasing efficiency in the fining process.

1.6.2.1 Graphene

Graphene was first created as a single-layer sheet in 2004 by Geim and Novoselov (Novoselov et al., 2004). It consists of carbon atoms arranged in a two-dimensional honeycomb lattice, which imparts remarkable properties, including exceptional electrical and thermal conductivity, mechanical strength, and flexibility. Graphene's large surface area, approximately 2630 m^2/g, enables it to adsorb a wide range of organic compounds effectively, making it highly desirable for various applications, including filtration, sensors, and energy storage.

The adsorption capabilities of graphene are enhanced by its functional groups, which can be modified to improve interactions with specific molecules. This versatility allows graphene to be tailored for targeted applications, such as the removal of pollutants from water or the enhancement of wine quality.

Recent studies have demonstrated that graphene exhibits exceptional adsorption capabilities for organic compounds, attributed to its large surface area and unique structural properties, making it one of the most effective adsorbents available (Kong et al., 2021).

According to Apul et al., 2013, graphene materials maintain substantial adsorption potential even in distilled and deionized water containing natural organic matter (NOM), which competes with target molecules for adsorption sites. In the context of wine fining, graphene's ability to retain significant adsorption potential in the presence of NOM is particularly noteworthy. This positions graphene as a promising candidate for innovative fining agents for wine, as it may not only improve wine clarity and stability but also address environmental concerns associated with traditional fining agents.

There are two primary mechanisms by which graphene acts as an effective adsorbent in the removal of phenolic compounds. The first mechanism involves electrostatic attraction. This

mechanism involves the interaction between charged sites on graphene and the charged groups of phenolic compounds. Oxygen-containing functional groups on graphene can create negatively charged sites that attract positively charged regions of phenolic compounds, facilitating their adsorption.

The second mechanism is based on pi-pi interactions, which occur between the electron-rich benzene rings of phenolic molecules and the graphene surface. These interactions enhance the binding of organic adsorbents, thereby increasing the efficacy of graphene in adsorbing phenolic compounds (Wang et al., 2019).

1.6.2.2 Carbon Nanotubes (CNTs)

Carbon nanotubes were first synthesized in 1991 by Iijima (Iijima, 1991), prior to the discovery of graphene. They can be produced using chemical vapor deposition methods (Liu et al., 2014). CNTs have attracted considerable attention in recent years within the environmental science field due to their high surface area, chemical stability, and unique absorption characteristics. There are two primary types of CNTs, single-walled CNTs (SWCNTs) and multi-walled CNTs (MWCNTs), both of which are extensively reported for their ability to absorb organic compounds, including phenolic compounds (Apul et al., 2013).

Single-walled carbon nanotubes are one-dimensional nanometer-sized materials recognized for their exceptional tensile strength, resilience, large surface area, thermal stability, and limited solubility (Niyogi et al., 2002). In contrast, multi-walled carbon nanotubes consist of multiple layers of carbon atoms arranged in concentric cylinders, which enhance their mechanical strength and thermal conductivity. MWCNTs typically have a greater surface area and can be more cost-effective than SWCNTs, making them attractive for various applications, including environmental remediation. Their structural complexity allows for enhanced interactions with organic compounds, further improving their adsorption capacities. Consequently, both SWCNTs and MWCNTs represent valuable materials in the pursuit of effective adsorbents for environmental applications, drug delivery, sensors, energy storage, composite materials, electronics, and even food-related uses.

1.6.2.3 Functionalized Carbon Nanotubes

Functionalized carbon nanotubes are advanced nanomaterials renowned for their unique chemical and physical properties, making them suitable for various applications. The process of functionalization, which involves modifying the sidewalls and end caps of carbon nanotubes, enhances their capabilities by introducing various functional groups.

For instance, amine-functionalization allows for the attachment of larger polymeric compounds, improving the effectiveness of the nanotubes in various applications. Notably, amine-CNTs significantly enhance the binding ability with phenolic compounds by forming covalent bonds between the phenolic groups and the CNTs, which enhances their potential use in applications such as water purification and wine fining (Chidawanyika & Nyokong, 2010).

In addition to amine-functionalization, hydroxyl (OH)-functionalized CNTs have gained attention for their ability to increase solubility and improve interaction with polar substances. Hydroxyl groups can enhance the adsorption of organic compounds, including phenolic substances, by providing additional hydrogen bonding sites. This modification broadens the range of potential applications for CNTs, especially in fields such as environmental remediation and food safety.

Carboxylic acid-functionalized CNTs represent another important type, known for their ability to form stable interactions with various molecules due to the presence of carboxyl groups. These functional groups facilitate the attachment of other compounds and enhance the overall reactivity of the CNTs. The COOH groups can engage in hydrogen bonding and electrostatic interactions, further broadening the range of applications for functionalized CNTs, particularly in environmental remediation and chemical sensing. Research has demonstrated that low-symmetry phthalocyanines can be covalently attached to carboxylic acid-functionalized SWCNTs. This covalent binding occurs through direct reactions between the functional groups on the nanotubes, eliminating the need for coupling or activating agents.

Overall, functionalized CNTs, including amine, hydroxyl, and carboxylic acid modifications, present a promising avenue for developing more efficient adsorbents and improving the performance of various materials across diverse fields.

1.7 Brief Overview of the Characterization Methods

1.7.1 Brief Overview of the Nanoparticle Tracking Analysis (NTA)

The physicochemical properties of carbon nanomaterials, including carbon nanotubes and graphene, are critical to their functionality and applications, as well as their effectiveness as fining agents. Key aspects of this characterization include particle surface area, size, surface charge, and morphology.

To analyse these properties, techniques such as Nanoparticle Tracking Analysis (NTA) and Zeta potential are widely employed. NTA has gained popularity due to its ease of use and

ability to provide reproducible results (Bhattacharjee, 2016). This method directly measures nanoparticle size distribution and concentration by observing and tracking the Brownian motion of nanoparticles in suspension (Mansfield et al., 2015). The diffusion coefficient (Dt) obtained through NTA is subsequently used to calculate particle size via the Stokes-Einstein equation. NTA detects Dt by monitoring the movement of nanoparticles relative to scattered light, captured as video using charge-coupled device (CCD) cameras (Bhattacharjee, 2016).

1.7.2 Brief Overview of the Zeta Potential Measurements

The Zeta potential (ZP), also known as the electrokinetic potential, is another critical measurement used to determine the surface charge of nanoparticles. ZP represents the potential at a slipping or shear plane of a colloidal particle moving in an electric field. It indicates whether nanoparticles possess a positive or negative charge based on their movement toward respective electrodes during electrophoresis. Importantly, ZP does not measure charge density but rather the potential at the nanoparticle surface. pH is a significant factor influencing ZP measurements, particularly in aqueous dispersions (Bhattacharjee, 2016).

1.7.3 Brief Overview of the Scanning Electron Microscopy (SEM)

Morphological analysis of nanomaterials is typically conducted using Scanning Electron Microscopy (SEM). SEM is a versatile analytical tool widely used in research to examine the surface characteristics of materials. During SEM analysis, a sample is bombarded with high-energy electrons, and the emitted secondary electrons are collected for analysis. This process was provided details information about the material's properties, including surface texture (topography), appearance, size and morphology, composition, crystallographic structure, and orientation. While topography focuses on superficial features such as texture and smoothness, morphology addresses the overall shape and dimensions of the particles. It is important to note that SEM detects only the electrons that scatter from the surface of the sample (Sharma et al., 2018).

1.7.4 Brief Overview of the High-Performance Liquid Chromatography (HPLC) and UV-Vis Spectroscopy

Both High-Performance Liquid Chromatography (HPLC) and UV-Vis spectroscopy were utilized to quantitatively assess the reduction of phenolic content in wines. Additionally, the statistical technique of ANOVA was applied to determine significant differences in performance among the various finning agents.

HPLC has evolved into one of the most advanced and widely used methods for analytical separation. It operates on the principle of a mobile phase and a stationary phase. In modern applications, the stationary phase can be either solid or liquid, while the mobile phase is typically a liquid (Hammood et al., 2023).

UV-VIS Spectroscopy, on the other hand, measures the absorbances of colourless compounds using monochromatic light in the near-ultraviolet region of the spectrum, specifically between 200 and 400 nm. According to the Beer-Lambert law, absorbance is directly correlated with the concentration of the absorbing species and the path length of the light (Verma & Mishra, 2018). Together, these techniques provide a robust framework for analyzing phenolic compounds in winemaking, enabling more precise assessments of fining agent effectiveness.

CHAPTER 2

MATERIALS and METHODS

2.1 Materials

Polyvinylpyrrolidone (PVPP) was purchased from Sigma Aldrich. Additionally, six alternative fining agents were tested, including graphene nanoplatelets (G) (Sigma Aldrich), activated carbon (AC) (NOIR active max), and various functionalized carbon nanotubes (CNTs) from Nanografi: OH-functionalized CNTs (OH-CNTs), COOH-functionalized CNTs (COOH-CNTs), and NH_2-functionalized CNTs. All fining agents were used at five different dosages: 200 mg/L, 400 mg/L, 800 mg/L, 1000 mg/L, and 2000 mg/L. Two white wines were used as the baseline for the fining experiments.

Table 2.1 Physicochemical properties of PVPP and six alternative fining agents based on supplier information

Fining agent	Purity %	Colour	Outer diameter (nm)	Inner diameter (nm)	Length or particle size (μm)
PVPP	100	White	-	-	110
G	-	black	-	-	<2
AC	-	black	-	-	-
MWCNTs	> 95	black	30-50	5-10	10-25
OH-CNTs	> 96	black	28-48	5-15	10-25
COOH-MWCNTs	> 96	black	28-48	5-15	10-25
NH_2-CNTs	> 95	Black	8-14	2-5	60

2.1.1 Wine Samples and Treatment with Fining Agents

Two different unfined white wines, Riesling (RIE) and Chardonnay (CHA), with different protein and phenolic concentrations, were used in this study. Both wines were produced by normal commercial winemaking procedures and donated by Accolade Wines, Reynella, South Australia. The wines were stored below 10 °C before the experiment. The contact time of each fining agent with the wine was 30 minutes, during which the wines were mixed using a rotary mixer. After treatment, the wine samples were centrifuged at 3750 rpm for 5 minutes and at 15

°C. The resulting supernatant was filtered through a 0.45 µm membrane filter (Millipore) to remove any remaining particles.

2.1.2 Scanning Electron Microscopy (SEM) Analysis

The size and morphology of the PVPP and its alternative fining agents were analysed using scanning electron microscopy (SEM) (Inspect F50, Thermo Fisher Scientific, UK) at the Flinders University SEM facility. Seven samples were prepared for imaging: PVPP, G, AC, CNTs, OH-CNTs, COOH-CNTs, and NH_2-CNTs.

First, a thin layer of each sample was spread on a silicon wafer, and it was carefully mounted onto an SEM holder using a spatula to ensure optimal positioning and to obtain the highest possible image quality. To secure the samples to the SEM holder, double-sided adhesive tape was used. PVPP, graphene nanoplatelets, and activated carbon were platinum-coated prior to analysis to achieve better image resolution. The other samples (all CNT variants) were analysed without platinum coating (Vladár, 2015). After sample preparation, the SEM holders were carefully placed inside the vacuum chamber of the Inspect F50 SEM to capture the images. The samples were arranged to maximise electron beam interaction and enhance image clarity. Appropriate imaging parameters were selected to obtain high-resolution images. After optimizing the instrument parameters, SEM images were acquired to analyse the morphology, size, and surface characteristics of the samples. The instrumental software was used to collect the SEM images (Oginni et al., 2019)

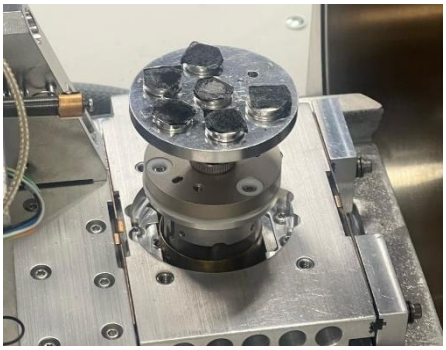

Figure 2.1. An SEM holder displaying a thin layer of each sample, which was then placed into the SEM vacuum chamber for imaging analysis.

2.1.3 Nanoparticle Tracking Analysis (NTA)

Nanoparticle tracking analysis (NTA) was performed using a NanoSight NS300 (Malvern Instruments Ltd., UK) equipped with a 405 nm laser and a syringe pump. A total of eight samples were prepared, including a control white wine sample and wines treated with PVPP, AC, G, CNTs, OH-CNTs, COOH-CNTs and NH_2-CNTs at 400 mg/L. These samples were injected into the sample chamber using a sterilized 1 ml syringe. The NanoSight NS300 2.3 NTA software was used to record 60-second video clips of each sample, automatically analysing 10 video clips per sample to capture natural Brownian motion. A syringe pump was used during the experiments to create a continuous flow of the sample through the flow cell at a flow rate of 10 µm/min while maintaining a room temperature. Samples were measured with manual shutter and gain settings. After optimizing the NTA post-acquisition parameters for the samples, each video was analysed to obtain the average particle size, median particle size, and concentration of particles in solution (Mierczynska-Vasilev et al., 2017).

Figure 2.2 Injection of samples into the NanoSight NS300 chamber using a sterile 1 mL syringe.

2.1.4 Zeta Potential Analysis

The zeta potential of the fining agents, both before and after treatment, was measured using the Zetasizer Nano (Malvern Instruments, UK) with a 633 nm red laser. The samples were injected into a folded capillary cell (DTS1060) with a volume of 1 mL to fully cover the electrodes of the cell. The samples were injected slowly to avoid the formation of air bubbles, and the analysis was only continued once no air bubbles were observed. After verification, the cell was placed in the Zetasizer and allowed to equilibrate at room temperature before measurement. The instrument uses laser Doppler electrophoresis to quantify the net velocity of the samples

under the influence of an applied electric field. The electrophoretic mobility of the particles is the primary measurement, which is then converted to zeta potential using Henry's approximation field (Tantra et al., 2010). All samples were run in triplicate. The data obtained were exported to Excel, where the replicate measurements were averaged to calculate the means and standard deviations. The results were presented as mean values with error bars corresponding to one standard deviation.

2.2 Evaluation of the Effectiveness of Fining Agents

The effectiveness of PVPP and six alternative fining agents, G, AC, CNTs, OH-CNTs, COOH-CNTs, and NH_2-CNTs, was evaluated at five different dosages: 200 mg/L, 400 mg/L, 800 mg/L, 1000 mg/L and 2000 mg/L. All wine samples were prepared according to the method

Preparation of 10 % (w/v) PVPP stock solution

The reason for preparing a 10% (w/v) stock solution of PVPP is that it achieves the best possible relationship of effective hydration, ease of handling, compliance with industry standards, and ensures uniform distribution in the treatment wine (Mélodie et al., 2017). To prepare a 10 % (w/v) stock solution of PVPP, approximately 10 mL of ethanol was added to 80 mL of distilled water. Next, approximately 10 g of PVPP was added to the mixture and stirred thoroughly to form a uniform slurry. The volume was then adjusted to 100 mL with Milli-Q water in a 100 mL volumetric flask and mixed well to ensure uniform distribution. According to AWRI's calculation, the addition of 1 mL of this stock solution to 100 mL of wine sample corresponds to the treatment concentration of 1000 mg/L of PVPP (AWRI, 2011). Five different concentrations of PVPP and carbon-based fining agents were used to treat 100 mL of wine samples. The specific quantities applied are detailed in Table 2.2.

Table 2.2 Required volume of PVPP stock solution and quantities of carbon-based finning agents for the preparation of 100 mL treated wine.

Concentration (mg/L)	Volume of the PVPP stock solution (mL)	Weight of Carbon-based finning agents (mg)
200	0.2	20
400	0.4	40
800	0.8	80
1000	1.0	100
2000	2.0	200

2.2.1 Ultraviolet-Visible (UV-Vis) Spectroscopy Analysis

The total phenolic content (TPC) of REI and CHA was measured before and after treatment with finning agents using a Cary 60 UV-Vis spectrophotometer (Agilent Technology). To quantify TPC, an absorbance wavelength of 280 nm was selected, as phenolic compounds typically absorb UV light in this range due to the phenolic ring structure. This method offers a straightforward and effective way to visualise TCP. For the analysis, two concentrations of each fining agent — 400 mg/L and 800 mg/L — were used.

Sample preparation

Control wines and wines treated with fining agents were diluted at a 1:3 ratio with Milli-Q water (one part wine to three parts water) using calibrated micropipettes. This dilution was performed to ensure absorbance values remained within the optical range for analysis. The 1:3 dilution factor was determined experimentally to avoid absorbance readings above 3, which can cause deviations from the Beer-Lambert law that underpins this method (Harbertson & Spayd, 2006).

Sample measurement and data analysis

Spectroscopic analysis was performed using 10 mm path length quartz cuvettes to achieve maximum transmission in the UV range. Approximately 3 mL of each diluted sample was filled into the quartz cuvettes and placed in the spectrophotometer. The absorption range was set from 250 nm to 400 nm in the Cary 60 software, with a specific focus on the absorbance at 280 nm, which represents the characteristic peak of TPC (Aleixandre-Tudo & Du Toit, 2019). Absorbance data at concentrations of 400 mg/L and 800 mg/L are presented in Appendix 02.

Results were displayed as bar charts showing absorbance at 280 nm. Each bar represents the mean TPC value, and error bars indicate the standard deviation from triplicate measurements (n=3). Statistical analysis was performed using one-way ANOVA, followed by Tukey's post hoc test to determine significant differences among treatments ($p < 0.05$).

2.2.2 Determination of the Effectiveness of Fining Agents on Wine Proteins Using HPLC

Proteins in wine, particularly thaumatin-like proteins (TLPs) and chitinases (Chit), are key contributors to haze formation, making their removal a vital step in the winemaking process. The aggregation of these TLPs and Chit is accelerated by interactions with phenolic compounds. When wine proteins become denatured, their hydrophobic regions bind to the hydroxyl groups on phenolic compounds, resulting in the formation of insoluble complexes (Benucci et al., 2022). This analysis aimed to assess the effectiveness of various fining agents in reducing protein content, with a particular focus on quantifying TLPs and Chit using high-performance liquid chromatography (HPLC).

Materials and regents

Milli-Q grade water, acetonitrile (ACN, Merck), trifluoroacetic acid (TFA, Sigma-Aldrich), and the thaumatin standard (Sigma-Aldrich) were used. Wine samples were treated with low, medium, and high concentrations (200 mg/L, 400 mg/L, and 2000 mg/L) of PVPP, as well as six alternative fining agents (G, AC, CNTs, OH-CNTs, COOH-CNTs, and NH_2-CNTs). Protein content in wines before and after treatment was measured using an Agilent 1260 HPLC system (Sigma Australia) equipped with a diode array detector and Vydac Prozap C18 column (2.1 x 10mm, 1.5µm, 500A), maintained at 35 °C.

Mobile phase preparation

Solution A (0.1% TFA in water) was prepared by adding 1 mL of TFA to approximately 500 mL of Mili-Q water in a 1000 mL volumetric flask, then diluting to the mark with Mili-Q water. The solution was transferred to a labelled Schott bottle. Solution B (0.1% TFA in acetonitrile) was prepared by adding 1 mL of TFA to 500 mL of acetonitrile in a 1000 mL volumetric flask, then bringing the volume to the mark with acetonitrile. The solution was transferred to a labelled Schott bottle.

Protein standard preparation

5 mg of thaumatin was weighed and dissolved in a 5 mL volumetric flask. The flask was then filled to the mark with Milli-Q water to prepare a 1000 mg/L thaumatin stock solution. This stock solution was subsequently used to prepare calibration standards as outlined below.

Table 2.3 Preparation of thaumatin calibration standards

Standard concentration (mg/L)	Amount of Milli-Q water (µL)	Amount of 1000 mg/L stock solution (µL)
10	990	10
25	975	25
50	950	50
100	900	100
250	750	250
500	500	500

Instrument and sample preparation

For the analysis of wine proteins, only Chardonnay wine was treated with fining agents at low, medium, and high concentrations (200 mg/L, 400 mg/L, and 2000 mg/L), as the protein content in Riesling wine was very low (below the detection limit). All samples were centrifuged and filtered before injection into the HPLC, following the sample preparation method outlined in Section 2.1.1. An aliquot of 1 mL of Chardonnay wine was pipetted into a 2 mL HPLC vial, labelled, sealed with screw caps, and placed in the autosampler tray for analysis. The mobile phase consisted of solvent A and solvent B, with a flow rate of 1.2 mL/min. A 15 µL injection

volume was used to achieve optimal separation, with detection performed at 210 nm to measure proteins. The HPLC system utilized "PROZAP_CURRENT" for analysis and "PROZAP_WASH" for column washing as described by (Mierczynska-Vasilev et al., 2017).

Protein quantification and data analysis

Wine proteins were identified by comparing the sample peak retention times to those of the thaumatin standards, utilizing the spectra library. Quantification was performed by comparing the peak area to the thaumatin standard curve (Appendix 1). The protein concentration of treated samples (mg/L) was calculated using a thaumatin-based calibration curve ($y = mx + c$). All fining agent-treated samples were analysed in triplicate ($n = 3$). Data are presented as bar graphs with standard deviation (SD) error bars. Significant differences ($p < 0.05$) between treatments were determined using one-way ANOVA, followed by Tukey's test, with different letters indicating significant differences in protein concentration.

2.2.3 Determination of the Effectiveness of Fining Agents on Wine Phenols Using HPLC

Materials and regents

Milli-Q grade water, acetonitrile (ACN, Merck), formic acid (Sigma-Aldrich), and phenolic standards (including gallic acid, tyrosol, GRP, caffeic acid, caftaric acid, ferulic acid, fertric acid, and Quercetin 3 B glucoside) were used in this study. To evaluate the removal of phenolic compounds, five different concentrations of PVPP and its potential alternatives, including graphene, activated carbon, and carbon nanotubes (CNTs, OH-CNTs, COOH-CNTs, and NH_2-CNTs), were tested at 200 mg/L, 400 mg/L, 800 mg/L, 1000 mg/L, and 2000 mg/L. Phenolic compounds were quantified using an Agilent 1260 HPLC system (Sigma Australia), equipped with a photodiode array detector and a Zorbax SB-C8 column (3.0 x 150mm). The column was maintained at a temperature of 45 ^{0}C during the analysis. The reason for selecting Zorbax SB-C8 column and 45^{0}C temperature was aligning with reversed-phase HPLC methods that are commonly optimized for separating phenolic compounds (Clarke et al., 2023).

Mobile phase preparation

Solution A (0.1% formic acid in water) was prepared by adding 1 mL of formic acid to approximately 500 mL of Mili-Q water in a 1000 mL volumetric flask. The solution was then diluted to the mark with Mili-Q water, thoroughly mixed and transferred to a labelled Schott bottle. Solution B (0.1% formic acid in acetonitrile) was prepared by mixing 1 mL of formic

acid with 500 mL of acetonitrile in a 1000 mL volumetric flask. The solution was brought up to the mark with acetonitrile, well mixed, and transferred to the labelled Schott bottle.

Standards preparation

Stock solutions of phenolic standards were prepared at a concentration of 1000 mg/L by dissolving 5 mg of each standard in 5 mL of appropriate solvent (Milli-Q water or methanol, depending on the solubility of the compounds). Working standard solutions were subsequently prepared according to the concentrations specified in Table 2.4.

Table 2.4 Preparation of phenolic calibration standards

Standard concentration (mg/L)	Amount of Milli-Q water (µL)	Amount of 1000 mg/L stock solution (µL)
10	990	10
25	975	25
50	950	50
100	900	100
250	750	250
500	500	500

Instrument and sample preparation

Detection of wine phenolics was performed at multiple wavelengths:

- 280 nm and 370nm for flavanols
- 320 nm for hydroxycinnamic acid.

The HPLC analysis was conducted using the "WWP_ Zorbax SB-C8_ Rapid1_2m" method.

White wine phenolics quantification and data analysis

White wine phenolics were identified by comparing the retention times of sample peaks to those of phenolic standards and by referencing the spectra library (Appendix 2). Quantification was performed by comparing the peak areas of the samples with the phenolic standard curves for each individual compound (Appendix 3). The white wine phenolic concentration (mg/L) in treated and untreated samples was calculated using a phenolic-based calibration curve ($y = mx + c$). All samples were analysed in triplicate ($n = 3$). The white wine phenolic compound

removal efficiency (RE) is presented as bar graphs with standard deviation (SD) error bars. A one-way ANOVA, followed by Tukey's post hoc test, was used to compare significant differences ($p < 0.05$) between treatments. Significant differences are indicated by different letters on the bar graphs.

The white wine phenolic compound removal efficiency (RE) was calculated using the following equation.

$$RE(\%) = \frac{C0 - C1}{C0} X100$$

Where C_0 is the initial phenolic compound concentration before fining treatment, and C_1 is the phenolic compound concentration after treatment (Río Segade et al., 2019).

For the analysis of white wine phenolics, Riesling and Chardonnay wines were treated with seven different fining agents at five concentrations: 200 mg/L, 400 mg/L, 800 mg/L, 1000 mg/L, and 2000 mg/L. All samples were centrifuged and filtered prior to injection, as described in Section 2.1.1. One millilitre of each centrifuged sample was transferred into a 2 mL HPLC vial, sealed with screw caps, labelled, and placed in the autosampler tray for analysis. The mobile phase consisted of solvent A and solvent B at a flow rate of 1.2 mL/min. An injection of 5 µL was used to achieve optimal separation.

2.3 Cost comparison Analysis of Finning Agents

The economic feasibility of the seven finning agents used in this work was assessed based on a comprehensive cost analysis. The agents evaluated included PVPP, G, AC, CNTs, OH-CNTs, COOH-CNTs, and NH_2-CNTs. Table 2.5 summarises the specifications, suppliers, and cost-related factors associated with each finning agent.

Table 2.5 Unit price comparison of PVPP and carbon-based finning agents used in wine treatment.

Product Description	**Supplier**	**Unit (g)**	**Price (A$)**	**Price /g (A$)**
Polyvinylpolypyrrolidone (PVPP) (77627-500g)	Sigma-Aldrich	500	697	2.22
Graphene nanoplatelets (G) (900407-250g)	Sigma-Aldrich	250	322.77	1.29
Activated carbon (AC) (242268-250G)	Sigma-Aldrich	250	115	0.46
Multi-walled carbon nanotubes (MWCNTs) (NG01MW0501)	Nanografi	1000	1254	1.25
Hydroxyl-functionalized multi-walled carbon nanotubes (OH-MWCNTs) (NG01MW0502)	Nanografi	500	1234.2	2.47
Carboxyl-functionalized multi-walled carbon nanotubes (COOH-MWCNTs) (NG01MW0503)	Nanografi	1000	1034.55	1.03
Amine-functionalized multi-walled carbon nanotubes (NH_2-MWCNTs)	Nanografi	5	1062.6	212.52

A PVPP stock solution (10% w/v) was prepared following the method described in Section 2.2. For cost estimation, the relationship between the stock solution volume and treatment concentration was established such that the addition of 1 mL of 10 % (w/v) PVPP stock solution to 100 mL of wine corresponded to a final concentration of 1000 mg/L.

The wine treatments at concentrations between 200 mg/L to 2000 mg/L were prepared according to Table 2.1, which listed the required volumes of PVPP stock solution and equivalent weight of carbon-based finning agents for the preparation of the respective treatment concentration. Economic calculations were made by multiplying each finning agent's required amount by the unit price (A$ per gram), with PVPP requiring an additional conversion step using a 10% (w/v) stock solution (0.1 g/mL).

The price per liter of wine treatment was determined for each fining agent as follows

- PVPP

For PVPP, each 1 mL of 10% (w/v) stock solution contains 0.1 g of PVPP, which was used to calculate the cost per litre of wine treatment.

Cost per treatment (A$) = Volume of stock solution × 0.1g/mL × cost/g (A$)

- Carbon-based finning agents

For carbon-based fining agents, the required weight for each treatment concentration was used directly in the cost calculation. A comprehensive cost comparison was then conducted, representing the cost per litre of wine treatments across five concentrations: 200 mg/L, 400 mg/L, 800 mg/L, 1000 mg/L, and 2000 mg/L.

Cost per treatment (A$) = Weight of finning agent × cost/g (A$)

2.3.1 Determination of Cost Implications for Commercial-scale Winery

Assuming a commercial winery treating 10,000 L of wine at 1000 mg/L, the cost implications for commercial-scale wine production were evaluated and are presented in Figure 2.3. The percentage cost reductions offered by carbon-based fining agents were calculated relative to PVPP. These values were plotted to illustrate the economic viability of each fining agent at a commercial scale.

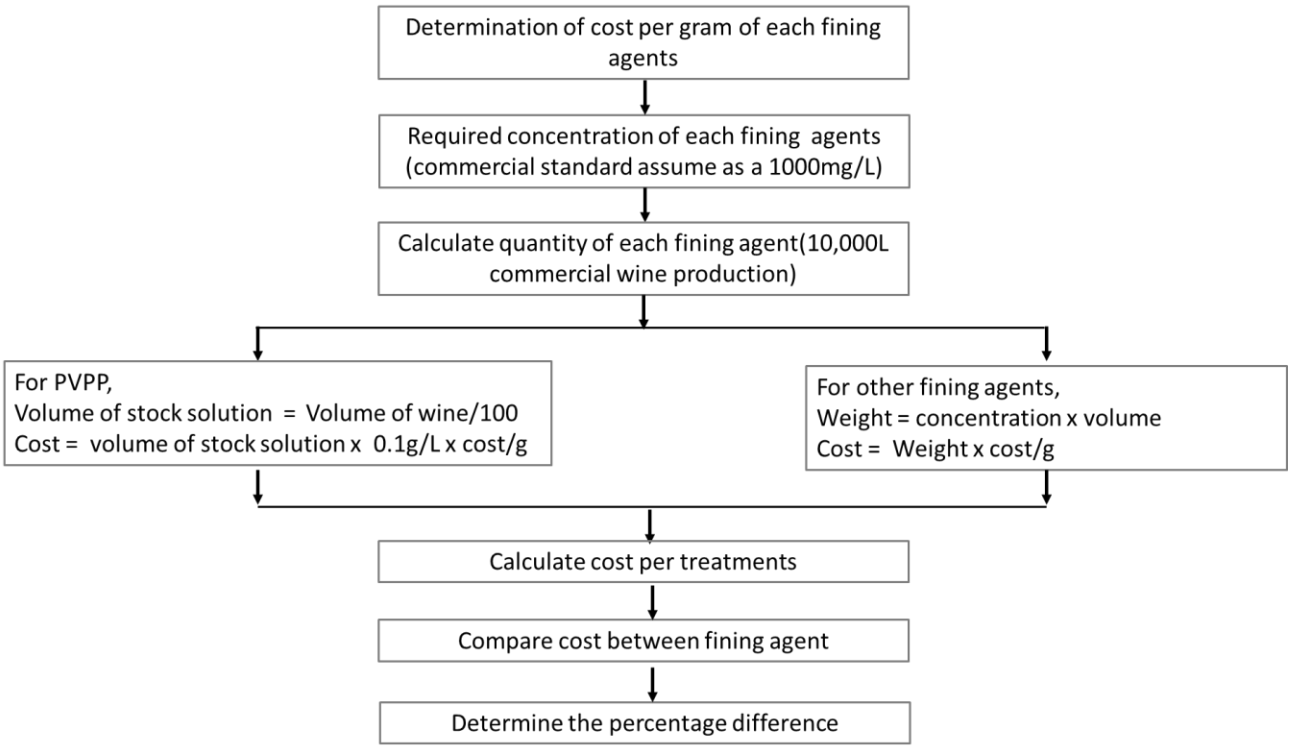

Figure 2.3 Cost analysis for wine treatments at a commercial scale comparing carbon-based fining agents to PVPP. The scenario assumes a winery treating 10,000 L of wine at a concentration of 1000 mg/L.

CHAPTER 3

RESULTS

3.1 Characterization of Fining Agents

3.1.1 Scanning Electron Microscopy (SEM) Analysis

Figure 3.1 shows the morphology, size, and shape of the fining agents examined using scanning electron microscopy. The analysed fining agents included polyvinylpolypyrrolidone (PVPP), graphene (G), activated carbon (AC), carbon nanotubes (CNTs), and functionalized CNTs (OH-CNTs, COOH-CNTs, and NH_2-CNTs).

The SEM image of polyvinylpolypyrrolidone exhibits an irregular, wrinkled, and porous surface with large voids and a sponge-like structure. These morphological features are commonly associated with materials that exhibit high surface areas. The flake-like texture indicates a heterogeneous particle structure. There is no clear lattice or repeating structure, suggesting a non-crystalline or amorphous morphology. According to SEM images, the largest particle size for PVPP was approximately 31 µm (Feret's diameter), analysed by Image J software (magnification 9.592x, horizontal field width 5.84 µm, voltage 5.00 kV). This result aligns with Gil et al. (Gil et al., 2017), who reported a rough, wrinkled, and highly porous structure of PVPP, with particle sizes ranging from 0.4- 300 µm, and confirms the porous structure's potential for high adsorption capacity.

The SEM image of activated carbon in Figure 3.1 reveals a flaky and fractured morphology with a rough surface, ranging in size from 2 - 10 µm (analysed by Image J software under magnification 51112x, horizontal field width 6.26 µm, voltage 5.00 kV). This rough morphology may contribute to its strong adsorption properties, which are critical in winemaking.

The SEM image of graphene reveals its crumpled, sheet-like structure. These wrinkles and folds are visual indicators of graphene's high surface area because the crumpling process increases the surface area by exposing more sites for interaction or adsorption. Guo et al. further highlight that graphene's high surface-to-volume ratio and thin-layer structure contribute to its theoretical surface area, which can reach up to 2,630 m^2/g. (Guo et al., 2014). This highly reactive surface could be particularly beneficial in applications requiring rapid adsorption or surface interactions.

The CNTs and their respective functionalized CNTs (COOH-CNTs and OH-CNTs) possess an entangled, fibrous, and flexible nature, with sizes ranging from approximately 10-15 µm (Feret's diameter), analysed by Image J software (magnification 47684x, horizontal field width 5.84 µm, voltage 5.00 kV). In contrast, NH_2-CNTs were observed to have a much greater length. Schütt et al. also observed these entangled, fibrous, and flexible morphologies, noting the significant impact of surface functionalization on the dimensional attributes of CNTs (Schütt et al., 2017). The functionalisation of materials with carboxyl (-COOH), hydroxyl (-OH), and amine (-NH_2) groups alters their surface chemistry and the morphology of the materials, enhancing their interactions with various substrates. As seen in the SEM images, these morphological differences highlight the distinct surface structures and features of these materials, which are crucial for their applications, particularly in terms of adsorption, filtration, and interaction with other compounds during winemaking processes.

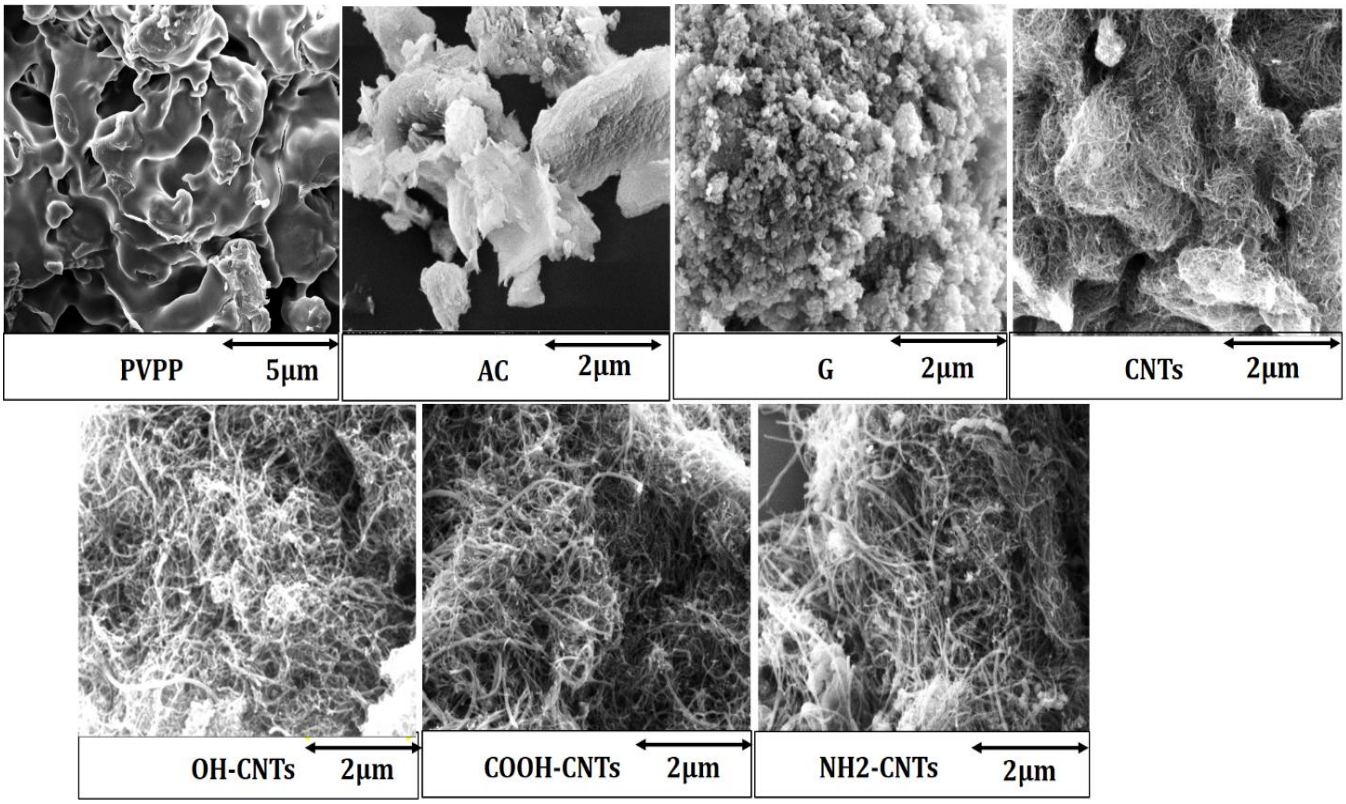

Figure 3.1 - High-resolution scanning electron microscopy images showing representative morphological characteristics of the seven materials investigated as fining wine agents: polyvinylpolypyrrolidone (PVPP), activated carbon (AC), graphene (G), carbon nanotubes (CNTs), and functionalized CNTs (OH-CNTs, COOH-CNTs, and NH_2-CNTs).

3.1.2 Measurement of Particle Size Distribution and Concentration in Wines Before and After Treatment with Fining Agents

The particle size distribution and concentration of Riesling wine (RIE) were measured before and after treatment with various fining agents to evaluate the effects of different treatments on particle characteristics. Results, including the particle size percentiles (D10, D50, D90), mean particle size, and particle concentration, are presented in Figure 3.2 and Table 3.1. The control sample (RIE control) exhibited a mean particle size of 131.0 nm and a particle concentration of 5.36 × 10^8 particles/mL, with a size distribution ranging from 80.4 nm (D10) to 209.9 nm (D90), indicating a moderate polydispersity. Treatment with PVPP increased both the size and concentration of the particles. The mean particle size increased to 155.0 nm and the concentration increased to 8.35×10^8 particles/mL. These results suggest that PVPP contributes to larger particle sizes and higher concentrations, which likely enhances its fining effect.

In contrast, activated carbon (AC) treatment resulted in a decrease in particle concentration to 3.43 × 10^8 particles/mL, while the mean particle size remained close to the control level of 129.7 nm. These results suggest that AC effectively reduces particle concentration without significantly altering the particle size distribution. This result is due to AC's unselective adsorption nature and high surface area (Velasco & Ania, 2011). Treatment with graphene (G) increased the mean particle size to 153.7 nm and moderately increased the particle concentration to 4.13 × 10^8 particles/mL. These results suggest that graphene enhances both particle size and concentration compared to the control and AC treatments.

Among the carbon nanotube-based treatments, bare carbon nanotubes (CNTs) produced the smallest mean particle size (95.1 nm), with a moderate concentration of 6.50 × 10^8 particles/mL. This suggests that CNTs generate smaller particles at relatively higher concentrations, which may be beneficial for specific fining objectives. In contrast, hydroxylated CNTs (OH-CNTs) caused a slight increase in mean particle size (107.0 nm) and a moderate increase in particle concentration (6.97 × 10^8 particles/mL), indicating that the hydroxylated CNTs lead to larger particles without significantly increasing the concentration.

Compared to the other CNT treatments, carboxylated CNTs (COOH-CNTs) resulted in a mean particle size of 118.5 nm and a decreased particle concentration of 3.33 × 10^8 particles/mL. This suggests that carboxylation may produce larger particles with a lower concentration, which could influence the overall effectiveness of the fining agent. Among the CNT treatments, amino-functionalized CNTs (NH_2-CNTs) had the largest mean particle size among the CNT treatments (130.8 nm) and the lowest particle concentration (1.28 × 10^8 particles/mL). This

suggests that amino functionalization increases particle size while reducing concentration, which may potentially impact stability and fining efficiency.

Overall, the results highlight the variability in particle size and concentration caused by different fining agents. Treatments with PVPP, AC, and graphene tend to increase both particle size and concentration. In contrast, CNT-based treatments exhibited distinct behaviours. Bare CNTs and OH-CNTs produced smaller particles at moderate concentrations. Carboxylated and amino-functionalized CNTs, however, modulated particle size and concentration differently. These findings provide valuable information for tailoring fining agents to achieve specific outcomes based on particle size and concentration, which influence the final quality of the treated wine.

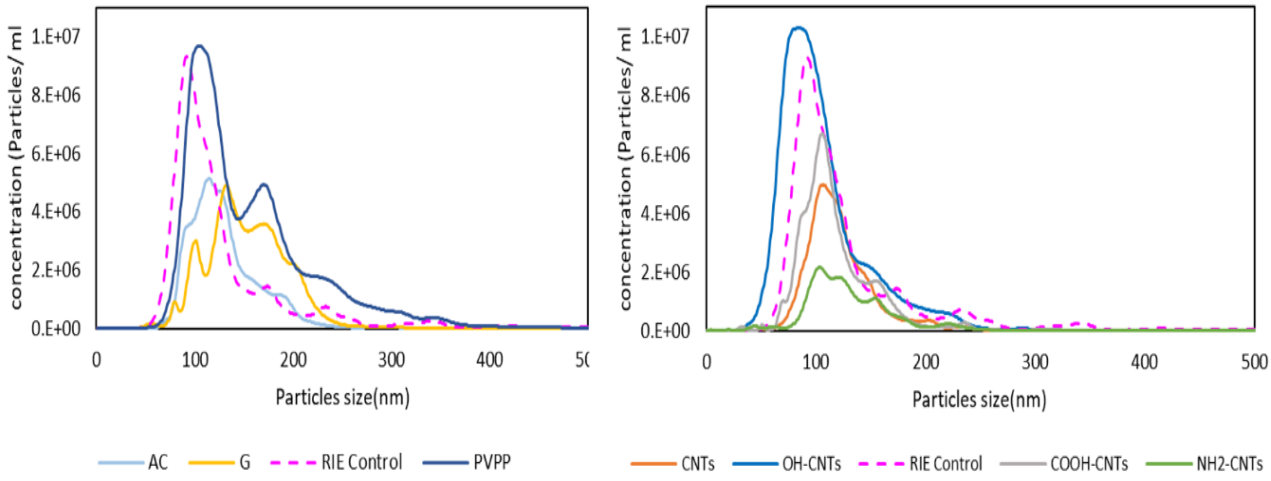

Figure 3.2 Particle size distribution profiles of Riesling wine in control and treated samples with various fining agents (400 mg/L), measured by NTA. Particle concentration (particles/mL) is shown as a function of particle size (nm) within the 0–500 nm range. The left figure compares RIE control with treatments using PVPP, activated carbon (AC), and graphene (G). The right figure compares RIE control with treatments using carbon nanotube-based fining agents: CNTs, OH-CNTs, COOH-CNTs, and NH_2-CNTs.

To assess the effects of various fining agents on the particle characteristics of Chardonnay wine (CHA), the particle size distribution and concentration of CHA before and after treatment were measured. Figure 3.3 and Table 3.1 present the results, including particle size percentiles (D10, D50 and D90), mean particle size, and particle concentration.

The CHA control sample had a mean particle size of 132.1 nm and a particle concentration of 3.52 × 10^8 particles/mL. Particle sizes ranged from 82.9 nm (D10) to 194.5 nm (D90),

indicating a moderate size distribution. Treatment with PVPP increased both the mean particle size to 145.6 nm and the concentration to 4.83 × 10^8 particles/mL. Particle sizes ranged from 91.8 nm (D10) to 217 nm (D90), suggesting that PVPP treatment increases both particle size and concentration. Activated carbon (AC) resulted in a mean particle size of 130.2 nm and a concentration of 4.47 × 10^8 particles/mL. Particle size distribution ranged from 85.3 nm (D10) to 189.0 nm (D90), indicating a minimal effect on particle size and concentration compared to the control. According to Wu's study, AC can absorb hydrophobic compounds without altering the colloidal structure (Wu & Pendleton, 2001). Graphene (G) treatment increased the mean particle size to 158.5 nm and the concentration to 4.78 × 10^8 particles/mL. Particle sizes ranged from 102.2 nm (D10) to 235.6 nm (D90). This suggests that graphene treatment produces larger particles and slightly higher concentration compared to the control.

For carbon nanotube-based (CNT) treatments, the bare CNTs resulted in a mean particle size of 113.8 nm and a concentration of 3.56 × 10^8 particles/mL. The particle size distribution ranged from 70.2 nm (D10) to 174.5 nm (D90). These results demonstrate that CNT treatment produces smaller particles at moderate concentrations. OH-CNTs increased the mean particle size to 124.4 nm, with a concentration of 3.66 × 10^8 particles/mL. The particle size distribution ranged from 78.7 nm (D10) to 191.7 nm (D90). This indicates that hydroxylation of CNTs slightly increases both particle size and concentration compared to plain CNTs. COOH-CNTs produced a mean particle size of 135.1 nm and a concentration of 2.64 × 10^8 particles/mL. Their particle size distribution ranged from 90.9 nm (D10) to 190.9 nm (D90). This suggests that carboxylation increases particle size, but results in a reduced particle concentration compared to other CNT treatments. NH_2-CNTs produced a mean particle size of 115.9 nm and a concentration of 2.94 × 10^8 particles/mL, with a particle size distribution ranging from 68.2 nm (D10) to 177.6 nm (D90). This treatment produced smaller particles, yet still resulted in a lower particle concentration than the other CNT treatments.

Overall, these findings reveal that different fining agents have varying effects on the particle size and concentration in Chardonnay wine. PVPP and graphene result in larger particles and higher concentrations. In contrast, CNT-based treatments, specifically NH_2-CNTs and COOH-CNTs, lead to smaller particles and lower concentrations.

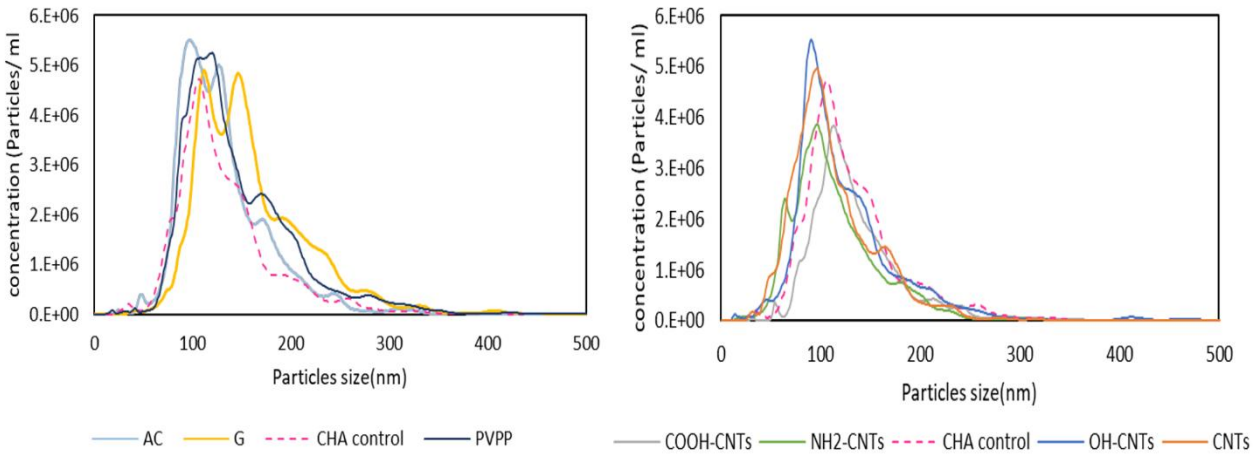

Figure 3.3 Particle size distribution profiles of Chardonnay wine in control and treated samples with various fining agents (400mg/L), measured by NTA. Particle concentration (particles/mL) is shown as a function of particle size (nm) in the 0–500 nm range. The left figure compares CHA control with treatments using PVPP, activated carbon (AC), and graphene (G), while the right figure compares CHA control with treatments using carbon nanotube-based fining agents: CNTs, OH-CNTs, COOH-CNTs, and NH_2-CNTs.

Untreated wines had a higher particle concentration after fining treatment. Overall, Riesling and Chardonnay wines exhibited similar trends in particle size and concentration after being treated with different fining agents. However, the magnitude of the changes varied between the two wines. Riesling generally showed a higher particle concentration than Chardonnay, particularly after PVPP and CNT treatments. Graphene treatments produced more significant increases in particle size and concentration in Chardonnay. These results demonstrate how the specific wine types and treatment methods can influence particle characteristics within wine.

Table 3.1 Particle size distribution percentiles (D10, D50, D90), mean particle size (nm), and particle concentration (particles/mL) in Riesling and Chardonnay wines before and after treatment with fining agents at 400 mg/L, as measured by NTA.

	Treatment	D10 (nm)	D50 (nm)	D90 (nm)	Mean (nm)	Concentration (particles/ml)
Riesling	RIE control	80.4±1.5	107.5±1.4	209.9±8.0	131.0±2.7	5.36e+08 ± 1.19e+07
	PVPP	93.7±1.3	137.2±2.6	244.9±3.9	155.0±1.6	8.35e+08 ± 5.85e+06
	AC	92.4±1.4	122.06±1.4	179.3±2.8	129.7±1.3	3.43e+08 ± 8.55e+06
	G	101.9±3.0	150.2±2.3	204.2±3.0	153.7±1.7	4.13e+08 ± 1.61e+07
	CNTs	56.2±1.4	86.8±1.1	142.0±1.1	95.1±1.0	6.50e+08 ± 8.17e+06
	OH-CNTs	67.6±1.4	96.4±1.1	165.1±5.2	107.0±1.9	6.97e+08 ± 1.28e+07
	COOH-CNTs	84.7±2.5	110.9±2.2	168.6±6.4	118.5±2.0	3.33e+08 ± 1.42e+07
	NH2-CNTs	92.0±1.6	122.7±2.8	186.4±7.5	130.8±2.4	1.28e+08 ± 1.70e+07
	Treatment	D10 (nm)	D50 (nm)	D90 (nm)	Mean (nm)	Concentration (particles/ml)
Chardonnay	CHA control	82.9±2.7	120.5±2.0	194.5±5.8	132.1±1.9	3.52e+08 ± 1.68e+07
	PVPP	91.8±1.9	129.8±2.7	217±6.1	145.6±2.7	4.83e+08 ± 3.87e+07
	AC	85.3±1.6	121.0±2.0	189.0±4.4	130.2±2.0	4.47e+08 ± 1.56e+07
	G	102.2±2.1	146.9±1.8	235.6±6.2	158.5±2.6	4.78e+08 ± 1.77e+07
	CNTs	70.2±2.2	104.6±1.5	174.5±2.7	113.8±1.9	3.56e+08 ± 9.38e+06
	OH-CNTs	78.7±2.3	110.2±3.2	191.7±5.8	124.4±3.5	3.66e+08 ± 1.98e+07
	COOH-CNTs	90.9±2.6	124.4±2.3	190.9±5.3	135.1±2.5	2.64e+08 ± 8.81e+06
	NH2-CNTs	68.2±2.8	105.8±2.4	177.6±4.7	115.9±2.7	2.94e+08 ± 1.26e+07

*Values represent the mean ± standard error of 10 measurements.

3.1.3 Determination of Zeta Potential in Wines Before and After Treatment with Fining Agents

The zeta potential of colloidal particles in Riesling (RIE) and Chardonnay (CHA) wines was measured to evaluate the effect of different fining agents on colloidal stability. The results are presented in Figure 3.4 and Table 3.2, with mean values reported as ± standard deviation (n = 3). Statistical analysis using one-way ANOVA confirmed significant differences among the treatments ($p < 0.001$).

In Riesling wines, the control sample exhibited a zeta potential of -3.04 ± 0.55 mV, and treatments such as activated carbon (AC, -3.48 ± 0.68 mV) and graphene (G, -3.44 ± 0.55 mV) resulted in similarly negative values. While these results suggest that the colloidal charge was maintained, it is important to note that such values are not strongly negative and therefore indicate only limited colloidal stability. In contrast, treatments with OH-functionalized CNTs (-0.63 ± 0.21 mV) and NH_2-functionalized CNTs (-0.70 ± 0.24 mV) reduced the magnitude of the zeta potential, indicating a shift toward colloidal destabilization and increased potential for particle aggregation.

In Chardonnay wines, however, the overall variation in zeta potential across treatments was much smaller, with values ranging narrowly between -0.05 and -0.70 mV. This indicates that fining agents induced only modest changes in colloidal charge in this matrix.

Zeta potential values in the range of -3 to -0.1 mV are considered only weakly negative and reflect systems with limited electrostatic stabilization. Literature commonly defines values below -30 mV or above +30 mV as thresholds for strong repulsive forces and high stability (Shah et al., 2014). As previously reported by (Mierczynska-Vasilev & Smith, 2015), zeta potentials approaching zero correspond to reduced electrostatic repulsion and are prone to aggregation and settling. Therefore, the values observed in this study suggest relatively mild electrostatic forces. This implies that, although some treatments caused statistically significant changes in zeta potential, they did not necessarily result in pronounced shifts in colloidal behaviour.

Furthermore, although both AC and graphene increased the negative charge and appeared to maintain colloidal stability, both agents demonstrated significant fining effectiveness. This suggests that their mechanisms of action may rely more on selective adsorption or interaction with specific wine components than on the broad destabilization of colloids. AC was shown to remove both desirable and undesirable macromolecules from wine (Cosme et al., 2021).

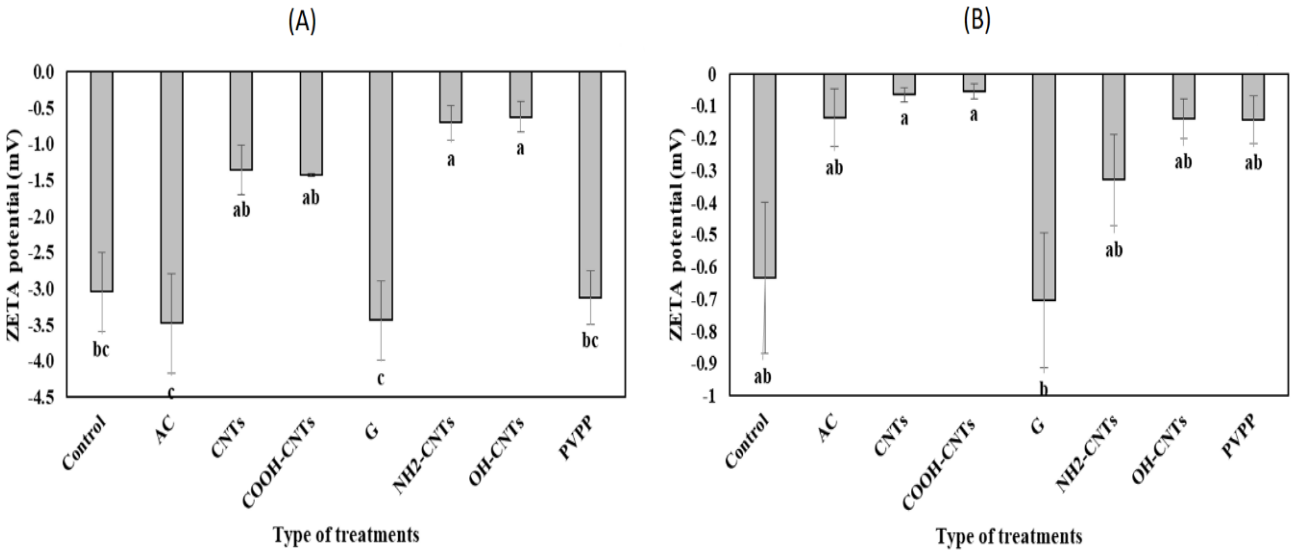

Figure 3.4 Zeta potential of Riesling (A) and Chardonnay (B) wines before and after treatment with fining agents, each applied at a concentration of 400 mg/L, measured using Zetasizer Nano. Different lowercase letters in the bar charts indicate statistically significant differences among treatments (Tukey's test, $p < 0.05$; $n = 3$).

Table 3.2 Zeta potential (mV) of Riesling and Chardonnay wines following treatment with fining agents at 400 mg/L.

Values that do not share a letter are significantly different. Data are presented as mean ± SD ($n = 3$).

Sample	Zeta potential (RIE) (mV)	Zeta potential (CHA) (mV)
Control	-3.04±0.55^{bc}	-0.64±0.23^{ab}
AC	-3.48±0.68^{c}	-0.14±0.09^{ab}
CNTs	-1.36±0.34^{ab}	-0.06±0.02^{a}
COOH-CNTs	-1.43±0.02^{ab}	-0.05±0.02^{a}
G	-3.44±0.55^{c}	-0.70±0.21^{b}
NH_2-CNTs	-0.70±0.24^{a}	-0.33±0.14^{ab}
OH-CNTs	-0.63±0.21^{a}	-0.14±0.06^{ab}
PVPP	-3.13±0.37^{bc}	-0.64±0.23^{ab}

3.2 Determination of the Effectiveness of Fining Agents

3.2.1 Total Phenolic Content (TPC) Assessment via 280 nm Absorbance in Wines Treated with Fining Agents

This section evaluates the effectiveness of various fining agents in reducing the total phenolic content (TPC) of Riesling (RIE) and Chardonnay (CHA) wines. TPC was quantified spectrophotometrically by measuring absorbance at 280 nm, a wavelength commonly associated with phenolic compounds. Treatments were applied at two concentrations (400 mg/L and 800 mg/L), and the extent of phenolic removal was determined by changes in absorbance values, with a decrease in absorbance indicating an effective reduction. Figure 3.1 compares the effectiveness of seven fining agents: polyvinylpolypyrrolidone (PVPP), graphene (G), activated carbon (AC), carbon nanotubes (CNTs), and functionalized CNTs (OH-CNTs, COOH-CNTs, and NH_2-CNTs), on RIE and CHA wines at concentrations of 200 mg/L and 800 mg/L. Untreated RIE and CHA wines served as controls representing baseline phenolic levels. Absorbance values at 280 nm were directly correlated with TPC, where higher absorbance indicated higher phenolic content and less reduction by the fining agents. This method provides a rapid quantitative analysis of the effectiveness of fining agents without the need for conversion to equivalent concentration units.

The main effect of the treatments on the absorbance of RIE and CHA wines was found to be significant (see Appendix 5; P-value = 0.000). This refers to the overall impact that that the different fining agents had on the total phenolic content (TPC) of the wines, as measured by absorbance at 280 nm. The control wines (RIE and CHA) displayed the highest absorbance values, indicating the highest levels of phenolic compounds. In contrast, the treated wines displayed significantly lower absorbance, reflecting effective phenolic reduction by the fining agents. There was no significant difference in the absorbance of RIE wines treated with PVPP, CNTs, NH_2-CNTs, or G, suggesting that these treatments had a similar effect on reducing total phenolic content (TPC). Similarly, no significant difference in absorbance was observed between CHA wines treated with PVPP, OH-CNTs, NH_2-CNTs, and COOH-CNTs (see Appendix 6 for RIE and Appendix C for CHA for the Tukey test).

Figure 3.5 shows that the absorbance of RIE and CHA wines treated with PVPP at a concentration of 400 mg/L was not significantly different from that of wines treated with CNTs at the same concentration. Similarly, the absorbance of RIE treated with PVPP at 400 mg/L was comparable to that of RIE treated with NH_2-CNTs at the same concentration. For CHA,

the absorbance after treatment with 800 mg/L of PVPP was not significantly different from the absorbance of CHA treated with 800 mg/L of OH-CNTs, NH_2-CNTs, and COOH-CNTs.

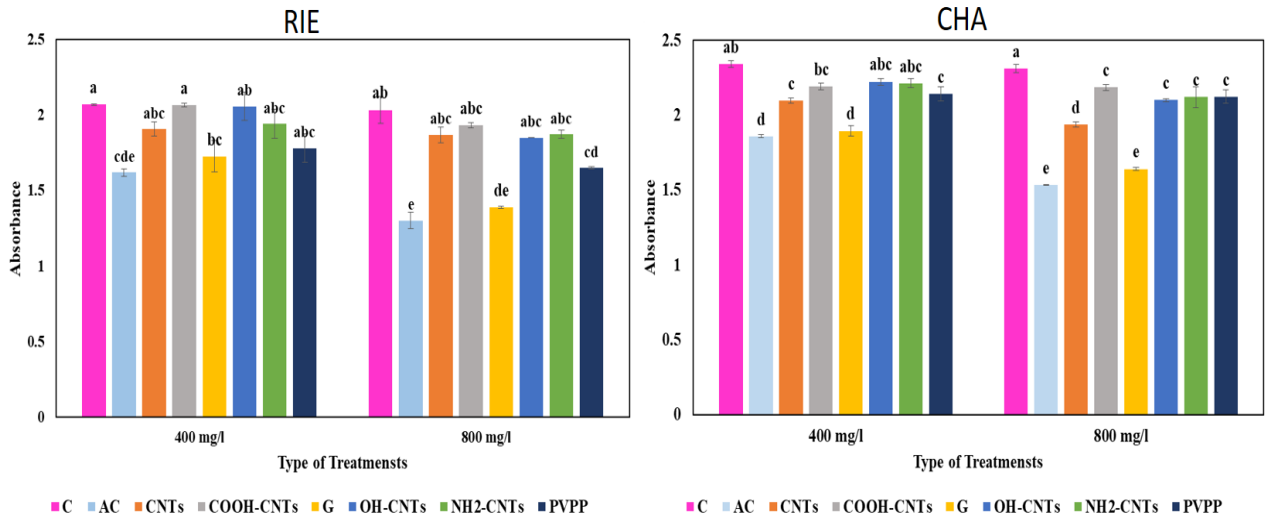

Figure 3.5 Absorbance values at 280 nm, indicating total phenolic content (TPC) in Riesling (left) and Chardonnay (right) wines, before and after treatments with different fining agents: polyvinylpolypyrrolidone (PVPP), graphene (G), activated carbon (AC), carbon nanotubes (CNTs), and functionalized CNTs (OH-CNTs, COOH-CNTs, and NH_2-CNTs), applied at concentrations of 400 mg/L and 800 mg/L. Absorbance at 280 nm is directly proportional to the TPC. Data represent mean ± standard deviation (n = 3). Statistical analysis was performed using two-way ANOVA followed by Tukey's post hoc test. Bars not sharing the same letter within each wine category indicate significant differences at the 0.05 significance level.

3.2.2 Impact of Fining Agents on Protein Concentration in Wine

Proteins in wine, particularly thaumatin-like proteins (TLPs) and chitinases, are crucial for its clarity, stability, and sensory profile (Liu et al., 2023). However, these proteins can also contribute to hazes and off-flavours. Thus, they are targeted during the fining process to improve wine quality (Marangon et al., 2013). Fining agents such as activated carbon, graphene, carbon nanotubes (CNTs), and functionalized CNTs are commonly used to remove unwanted compounds, including proteins (Sweetman et al., 2017). In contrast, polyvinylpolypyrrolidone (PVPP) is effective at reducing phenolic compounds while leaving protein concentrations largely unaffected, making it a useful baseline for comparison.

This study evaluates the effectiveness of various fining agents in reducing protein concentrations in Chardonnay wine, with a focus on TLPs and chitinases. Protein levels were quantified using a thaumatin calibration curve. The objective was to determine whether these fining agents affect protein concentrations in parallel with their impact on phenolic content.

The results revealed significant differences in protein reduction across treatments as shown in Table 3.3 and Figure 3.6. Control wines had the highest protein concentrations, ranging from 23.36 ± 0.21 mg/L to 24.22 ± 0.10 mg/L, establishing a baseline for comparison. In contrast, activated carbon showed considerable protein reduction, with concentrations of 21.10 ± 0.60 mg/L at 200 mg/L and 18.32 ± 0.08 mg/L at 400 mg/L. No data were available for the 2,000 mg/L for this treatment due to concentrations falling below the calibration curve, indicating near-complete protein removal at this dose.

At the lower concentration of 200 mg/L, the extent of protein removal was more moderate across treatments. Graphene achieved the lowest protein concentration at this level (16.46 ± 0.73 mg/L), indicating the greatest effectiveness. Similarly, CNTs, NH_2-CNTs and COOH-CNTs achieved concentrations of 17.91±0.23, 16.97 ± 0.31 mg/L and 18.94 ± 0.46 mg/L, respectively. Although reductions were evident, they were not as pronounced as those observed at higher fining levels, suggesting limited effectiveness at lower doses.

Notably, CNTs also demonstrated strong protein-binding capacity, with values falling below the calibration curve at 2,000 mg/L, consistent with complete protein removal. Among the functionalized CNTs, CNTs-OH achieved a protein concentration of 17.56 ± 0.38 mg/L at a concentration of 200 mg/L, indicating moderate efficacy. PVPP, on the other hand, had a minimal effect on protein concentrations. Samples treated with PVPP displayed protein levels similar to the controls, with values of 23.20 ± 0.38 mg/L at 200 mg/L, 22.42 ± 0.54 mg/L at 400 mg/L, and 23.87 ± 0.21 mg/L at 2000 mg/L, reaffirming its role as a phenolic-specific fining agent.

More pronounced reductions in protein concentrations were observed at higher treatment levels (400 mg/L and 2,000 mg/L), particularly in samples treated with graphene, CNTs, and activated carbon. These results demonstrate a dose-dependent effect, with higher concentrations leading to more effective protein removal. Several treatments approached or fell below the calibration curve limit, suggesting near-complete removal of TLPs and chitinases.

In conclusion, this study shows that fining agents such as AC, graphene, and CNTs, including functionalised derivatives, are highly effective at reducing protein content in Chardonnay wine.

These agents offer a promising alternative for improving wine clarity and stability by targeting haze-forming proteins. In contrast, PVPP does not significantly affect protein levels and remains suitable for phenolic-specific fining applications. Importantly, the findings highlight that higher fining agent concentrations are required for optimal protein removal.

Table 3.3 Protein concentration (mg/L) in Chardonnay wine before and after treatment with various fining agents at concentrations of 200, 400, and 2000 mg/L, as determined by HPLC. Values sharing the same letter are not significantly different, according to Tukey's test at the 0.05 significance level ($P < 0.05$).

	Concentration (mg/L)		
Treatment	**200**	**400**	**2000**
Control	23.36 ± 0.21^{ab}	23.40 ± 0.31^{ab}	24.22 ± 0.10^{a}
AC	21.10 ± 0.60^{c}	18.32 ± 0.08^{de}	Below the calibration curve
CNTs	17.91 ± 0.23^{def}	Below the calibration curve	
CNTs-COOH	18.94 ± 0.46^{d}		
G	16.46 ± 0.73^{f}		
CNTs-OH	17.56 ± 0.38^{def}		
$CNTs-NH_2$	16.97 ± 0.31^{ef}		
PVPP	23.20 ± 0.38^{ab}	22.42 ± 0.54^{bc}	23.87 ± 0.21^{ab}

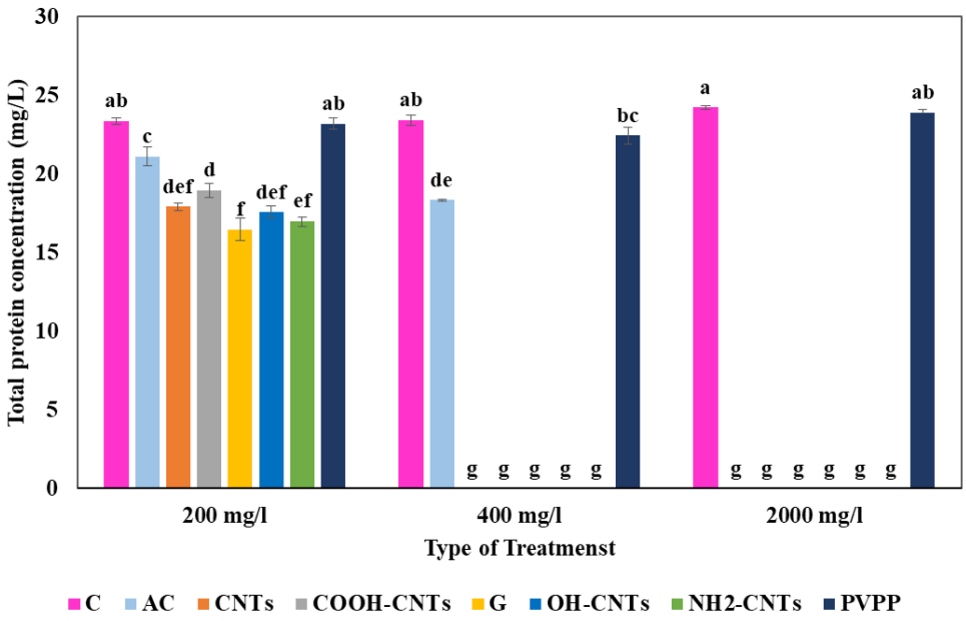

Figure 3.6 Effect of various fining agents on protein concentration (mg/L) in Chardonnay wine at treatment levels of 200 mg/L, 800 mg/L, and 2000 mg/L. The figure compares protein concentrations before and after treatment to evaluate the impact of each fining agent. Data are represented as mean ± SD (n = 3). Statistical analysis was performed using two-way ANOVA followed by Tukey's test. Bars not sharing the same letter are significantly different at the 0.05 significance level ($P < 0.05$).

3.2.3 Effectiveness of Fining Agents on Wine Phenolic Composition, Including Gallic Acid, Tyrosol, Hydroxycinnamic Acids, and Flavonol Derivatives

This study investigated the effect of seven fining agents: PVPP, graphene, activated carbon, and both bare and functionalised carbon nanotubes (CNTs, OH-CNTs, COOH-CNTs, and NH_2-CNTs) on the phenolic composition of Riesling and Chardonnay wines. Treatments were applied at five concentration levels (200, 400, 800, 1000, 2000 mg/L), and changes in phenolic content were measured using HPLC. Six phenolic compounds were identified in both wines: tyrosol, caftaric acid, coeluting GRP, caffeic acid, ferteric acid, and quercetin 3 glucoside. Additionally, gallic and ferulic acid were detected in Riesling only. Initial concentrations of each phenolic compound prior to treatment are presented in Table 3.4. To ensure robust comparisons, each fining agent was evaluated against its corresponding control sample. For example, Control 1 was used for PVPP treatment, Control 2 for graphene, and so on. This approach ensured that treatment effects were evaluated relative to matched baselines.

The percentage reduction of each phenolic compound relative to its respective control is illustrated in Figures 3.7 to 3.12. Complete data sets detailing these percentage changes for both Riesling and Chardonnay wines are provided in Appendices 9 to 11. Statistical analysis was conducted using two-way ANOVA to evaluate the effect of the fining agents and concentration, followed by pairwise comparisons using the Tukey test. Full statistical results are provided in Appendices 12 to 32.

Table 3.4 Initial phenolic concentration (mg/L) in Riesling and Chardonnay wines prior to treatment with each fining agent. Each fining treatment (PVPP, graphene, activated carbon, CNTs, OH-CNTs, COOH-CNTs, and NH_2-CNTs) was associated with its own corresponding untreated control. For instance, *Control 1* represents the untreated RIE and CHA wines for comparison with PVPP treatment, *Control 2* is the baseline for graphene, and so forth. This design ensures that each treatment effect is evaluated relative to a directly matched control, accounting for any variability in the base wine prior to treatment.

	Phenolic concentration in Riesling before treatment (mg/L)								**Phenolic concentration in Chardonnay before treatment (mg/L)**					
Control	Gallic	Tyrosol	Caftaric	Coel. GRP	Caffeic	Fertaric	Ferulic	Que.3 glucoside	Tyrosol	Caftaric	Coel. GRP	Caffeic	Fertaric	Que.3 glucodie.
1 (PVPP)	2.30	6.1	72.03	37.62	1.85	8.26	1.53	6.33	3.28	4.81	27.5	1.09	1.88	9.97
2 (G)	2.65	5.03	71.35	38.26	1.65	8.66	1.54	6.08	3.73	4.75	26.94	1.15	1.78	10.7
3 (AC)	2.62	5.34	71.98	39.37	1.64	8.62	1.54	5.69	3.53	4.75	27.63	1.11	1.91	11.03
4 (CNTs)	2.66	5.57	72.46	39.25	1.93	8.67	1.63	5.76	3.65	5.8	30.27	1.22	2.02	11.53
5OH-CNTs	2.56	4.68	71.85	38.16	1.93	8.65	1.62	5.80	4.05	5.24	29.24	1.15	1.88	11.5
6 COOH- CNTs	2.56	5.16	73.1	37.79	1.76	8.51	1.55	5.57	3.7	5.02	27.51	1.14	1.86	11.33
7 NH_2-CNTs	2.54	6.02	74.77	38.27	1.67	8.35	1.54	6.17	3.83	4.9	27.82	1.15	1.92	11.24

3.2.3.1 Comparison of the Percentage Reduction of Tyrosol in Wines Treated with Various Fining Agents at Different Concentrations

The interaction between treatment type and concentration on the tyrosol reduction percentages of RIE and CHA wines was significant at a 0.05 significance level of significance (Appendix 12: General linear model, p value = 0.000). The highest tyrosol reduction percentages of RIE and CHA were achieved with AC treatment at 2,000 mg/L, at 50.46±6.81% and 43.67±2.92%, respectively (Appendices 9 and 11). In contrast, the lowest tyrosol reduction percentage of RIE was observed with OH-CNTs at 400 mg/L (2.67±3.29%), which was not significantly different from OH-CNTs at 200 mg/L. Additionally, the tyrosol reduction percentage of CHA did not significantly differ among all treatments at 200 mg/L and 400 mg/L, except with G (Figure 3.7). Considering the range from 200 to 800 mg/L, the most significant reduction of tyrosol was observed with PVPP in RIE and with G in CHA (Figure 3.7). Although AC was capable of yielding high tyrosol reduction at high dosage levels (1,000-2,000 mg/L), low efficiency was observed at low concentrations. AC's non-selective adsorption removes a wide range of compounds indiscriminately. Therefore, its applicability is generally restricted to situations of extreme contamination (e.g., extreme smoke taint) with low concentrations (Wang et al., 2016). PVPP's selectivity is a result of specific hydrogen bonding interactions between its carbonyl functional groups and the phenolic hydroxyl of tyrosol. These interactions facilitate the specific binding and subsequent removal of tyrosol by PVPP (Durán-Lara et al., 2015).

The average effect of the treatment across all concentrations, as well as the tyrosol reduction percentages of RIE with PVPP, and CHA with G, were significantly highest (Appendix 13 and 14: Tukey test). In contrast, the tyrosol reduction percentage in RIE with OH-CNTs was significantly the lowest, and CHA treated with COOH-CNTs was the second lowest. However, there was no significant difference in the tyrosol reduction percentage between CHA treated with COOH-CNTs, PVPP, and bare CNTs. Specifically, the reduction percentage of PVPP was very close to that of bare CNTs, OH-CNTs, and NH_2-CNTs.

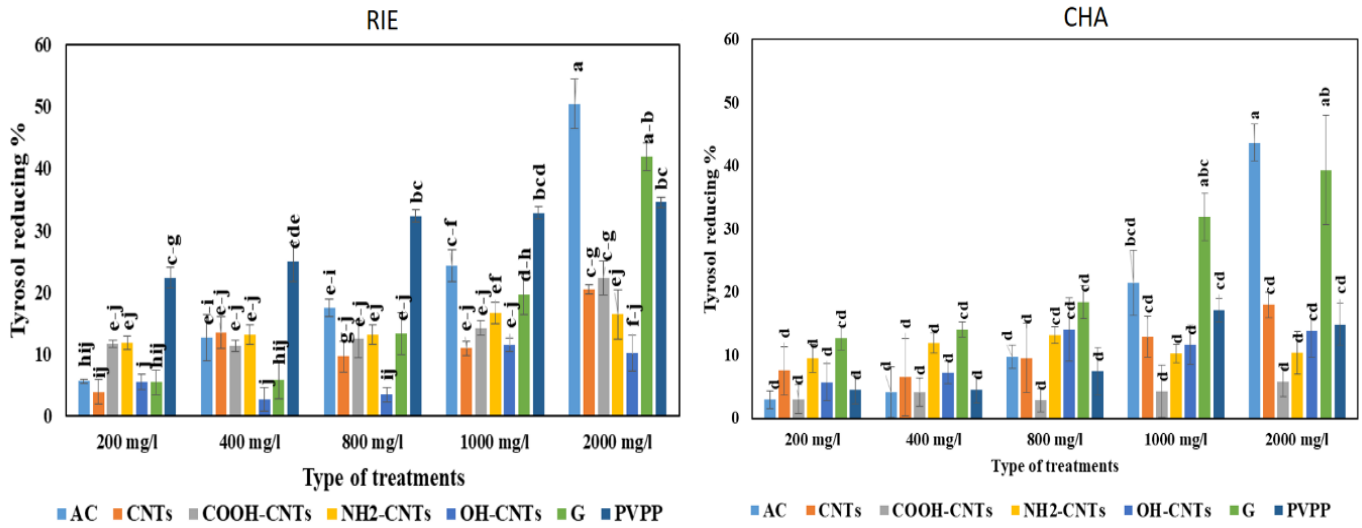

Figure 3.7 Percentage reduction of tyrosol in RIE (left) and CHA (right) wines treated with seven different fining agents (PVPP, G, AC, CNTs, OH-CNTs, COOH-CNTs, and NH2-CNTs) at five concentrations (200, 400, 800, 1000, 2000 mg/L). The data demonstrate the effects of each fining agent and its concentration on the efficiency of reducing tyrosol. Values are represented as mean ± SD (n=3). Data were analysed using two-way ANOVA followed by a Tukey's test. Bars not sharing the same letter indicate significant differences among treatments within each wine type at the 0.05 significance level.

3.2.3.2 Comparison of the Percentage Reduction of Caftaric Acid in Wines Treated with Various Fining Agents at Different Concentrations

The interaction between treatment type and concentration on the percentage reduction of caftaric acid in RIE and CHA wines was significant at a 0.05 level (Appendix 15: General linear model, p value = 0.000). According to the Tukey test, the highest caftaric acid reduction percentages in REI and CHA were achieved with AC at 2,000 mg/L, with values of 73.95 ± 2.68% and 63.00 ± 0.41%, respectively (Appendices 9 and 11). In contrast, the lowest reductions were observed in RIE treated with OH-CNTs and CHA treated with NH_2-CNTs at 200 mg/L, with values 1.17±0.05% and 1.15±0.15%, respectively. Among the 200 mg/L treatments, the most significant reductions of caftaric acid were observed in RIE treated with PVPP and in CHA treated with graphene. (Figure 3.8).

On average, the lowest caftaric acid reduction was observed with COOH-CNTs in both RIE and CHA treatments, whereas the highest reduction was achieved with AC in both wines (Appendix 16 for RIE, Appendix 17 for CHA: Tukey test). However, some treatments in CHA did not significantly differ in their effects on caftaric acid reduction. For instance, the reduction

achieved with COOH-CNTs was not significantly different from that of NH_2-CNTs. The same was true for PVPP and OH-CNTs. Additionally, there was no significant difference in the caftaric acid percentage reduction of RIE between NH_2-CNTs and OH-CNTs.

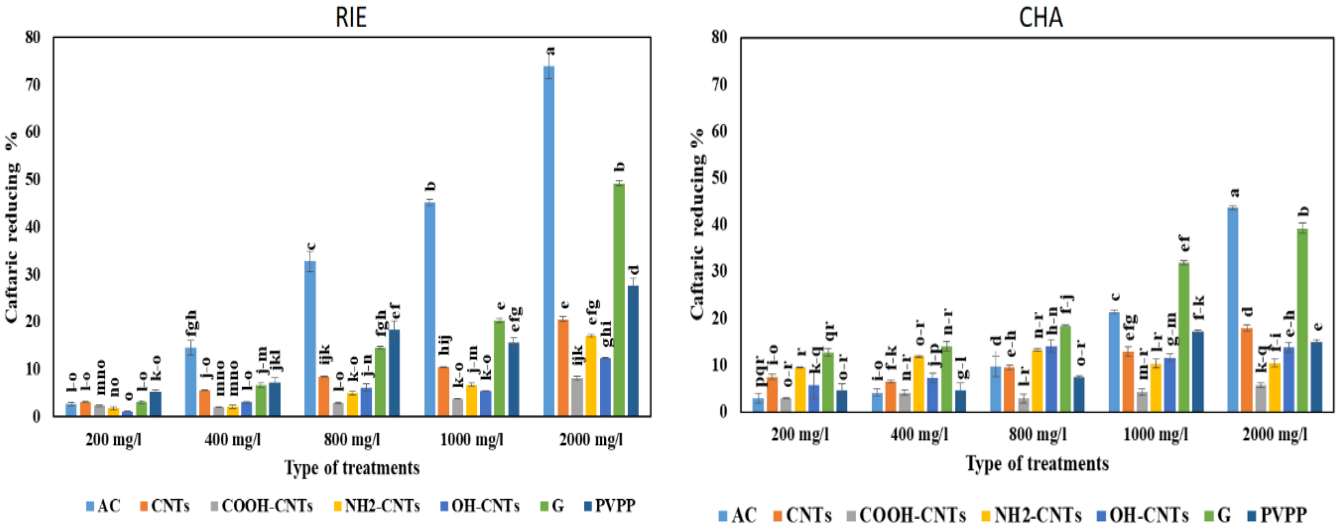

Figure 3.8 Percentage reduction of caftaric acid in RIE (left) and CHA (right) wines treated with seven different fining agents (PVPP, G, AC, CNTs, OH-CNTs, COOH-CNTs, and NH2-CNTs) at five concentrations (200, 400, 800, 1000, 2000 mg/L). The data demonstrate the effects of each fining agent and concentration on the reduction efficiency of caftaric acid. Values are represented as mean ± SD (n=3). Data were analysed using two-way ANOVA followed by Tukey's test. Bars not sharing the same letter indicate significant differences among treatments within each wine type at the 0.05 significance level.

3.2.3.3 Comparison of the Percentage Reduction of Coeluting GRP in Wines Treated with Various Fining Agents at Different Concentrations

HPLC easily detects GRP with absorbance at 320nm under standard conditions on C18 columns, GRP elutes at approximately an 11.7 retention time in the chromatogram. But numerous other wine phenolics, including caffeic, p-coumaric, and ferulic, absorb at 310-330nm like GRP, and regularly elute close to one another on the columns of C18. Due to poor chromatographic separation, GRP's peak is overlapped by these compounds, and GRP is mentioned as a coeluting GRP (Makris et al., 2003). The interaction between treatment type and concentration significantly affected the reduction percentage of coeluting GRP in RIE and CHA wines at a 0.05 significance level (Appendix 18: General linear model, p value = 0.000). Similar to the trend observed for the other phenolic compounds, the highest coeluting GRP reduction percentages in REI and CHA were achieved with AC at 2,000 mg/L, with values of

43.47±0.71% and 60.41±0.32%, respectively (Appendices 9 and 11). In contrast, the lowest reductions were observed in RIE treated with NH_2-CNTs and in CHA treated with PVPP at 200 mg/L, with values of 0.47±0.36% and 0.26±0.26%, respectively. However, the reduction with PVPP in CHA was not significantly different from that of COOH-CNTs at 200 mg/L (0.36±0.19). Considering the range from 200 to 800 mg/L, the most significant reductions in coeluting GRP were observed in Riesling and Chardonnay wines treated with AC (Figure 3.9).

When considering the average effect across all concentrations, the lowest coeluting GRP reduction percentage was observed in RIE-treated samples with NH2-CNTs and in CHA-treated samples with PVPP, while the highest reduction in both wines was achieved with AC treatment. In Riesling wine, there was no significant difference in the coeluting GRP reduction among treatments with PVPP, NH_2-CNTs, and COOH-CNTs (Appendices 19 and 20: Tukey test).

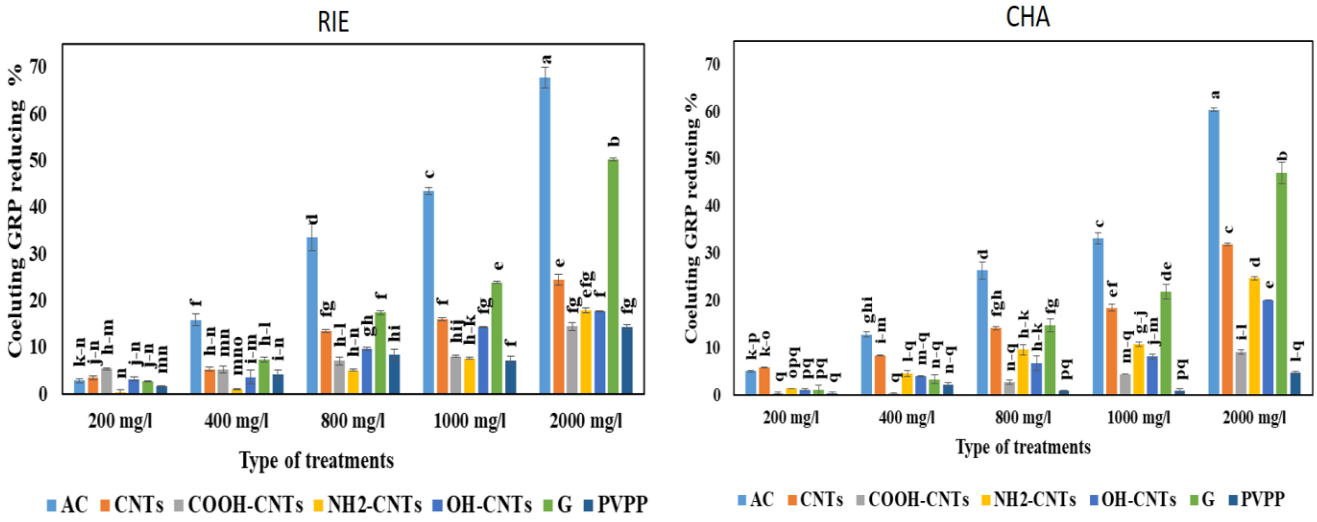

Figure 3.9 Percentage reduction of coeluting GRP in RIE (left) and CHA (right) wines treated with seven different fining agents (PVPP, G, AC, CNTs, OH-CNTs, COOH-CNTs, and NH2-CNTs) at five concentrations (200, 400, 800, 1000, 2000 mg/L). The data demonstrate the effects of each fining agent and concentration on coeluting GRP reduction efficiency. Values are represented as mean ± SD (n=3). Data were analysed using two-way ANOVA followed by Tukey's test. Bars that do not share the same letter show significant differences among treatments within each wine type at the 0.05 significance level.

3.2.3.4 Comparison of the Percentage Reduction of Caffeic Acid in Wines Treated with Various Fining Agents at Different Concentrations

The interaction between treatment type and concentration significantly affected the percentage reduction of caffeic acid in RIE and CHA at a 0.05 significance level (Appendix 21: General linear model, p-value = 0.000). In Riesling wine, caffeic acid reduction reached 100 % after treatment with activated acid and graphene at 2,000 mg/L, while in Chardonnay wine, the highest reduction was 78.21±0.85% with graphene at 2,000 mg/L. In contrast, the lowest reductions were observed in Riesling with NH_2-CNTs and in Chardonnay with PVPP at 200 mg/L, with values of 4.52±0.21% and 4.96±0.26%, respectively (Appendices 10 and 11). At the 200 mg/L concentration, the most significant reduction of caftaric acid was achieved with activated carbon treatment in Riesling and with graphene treatment in Chardonnay (Figure 3.10). Considering the average effect across all concentrations, the highest reduction percentage of caffeic acid was achieved in REI treated with AC, and it was not significantly different with G.In CHA the highest reduction percentage of caffeic acid was achieved with G. In contrast, the lowest reduction percentages were observed in RIE treated with NH_2-CNTs and in CHA treated with PVPP. Notably, there was no significant difference in caffeic acid reduction between CHA treated with PVPP and COOH-CNTs. (Appendix: 22 for RIE, Appendix: 23 for CHA: Tukey test).

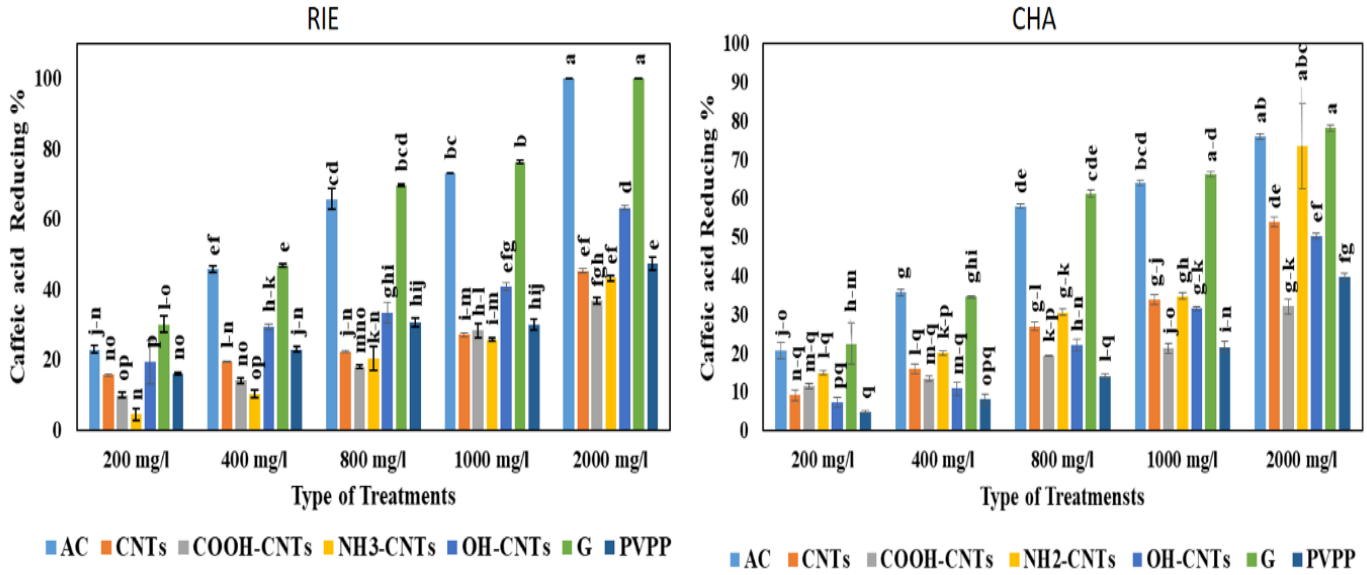

Figure 3.10 Percentage reduction of caffeic acid in RIE (left) and CHA (right) wines with seven different fining agents (PVPP, G, AC, CNTs, OH-CNTs, COOH-CNTs, and NH2-CNTs) at five concentrations (200, 400, 800, 1000, 2000 mg/L). The data demonstrate the effects of each fining agent and the concentration on the reduction efficiency of caffeic acid. Values are represented as mean ± SD (n=3). Data were analysed using two-way ANOVA followed by Tukey's test. Bars not sharing the same letter indicate significant differences among treatments within each wine type at the 0.05 significance level.

3.2.3.5 Comparison of the Percentage Reduction of Ferteric acid in Wines Treated with Various Fining Agents at Different Concentrations

The interaction between treatment type and concentration on ferteric acid reduction percentage of RIE and CHA was significant at a 0.05 significance level (Appendix 24: General linear model, p value = 0.000). ferteric acid reduction percentages in RIE and CHA-treated wines with AC at 2,000 mg/L were significantly the highest, with values of 98.00±2.00% and 100%, respectively (Appendices 10 and 11). In contrast, the lowest ferteric acid reduction percentages were observed in RIE-treated samples, with values of 1.78±0.69% and 0.90±0.39%, respectively. Considering the 200mg/L mg/L concentration, the most significant reduction (%) of caftaric acid was observed with AC in RIE and with G in CHA, similar to caftaric acid (Figure 3.11). Considering the average across all concentrations, ferteric acid reduction was lowest in RIE-treated samples with COOH-CNTs and in CHA-treated samples with PVPP. In contrast, treatment with AC resulted in significantly higher reduction percentages in both wines (Appendices 25 and 26: Tukey test). However, there was no significant difference between ferteric acid reduction percentage in CHA treated with PVPP and COOH-CNTs. Additionally, no significant difference was found between ferteric acid reduction percentages in Riesling treated with PVPP and NH_2-CNTs.

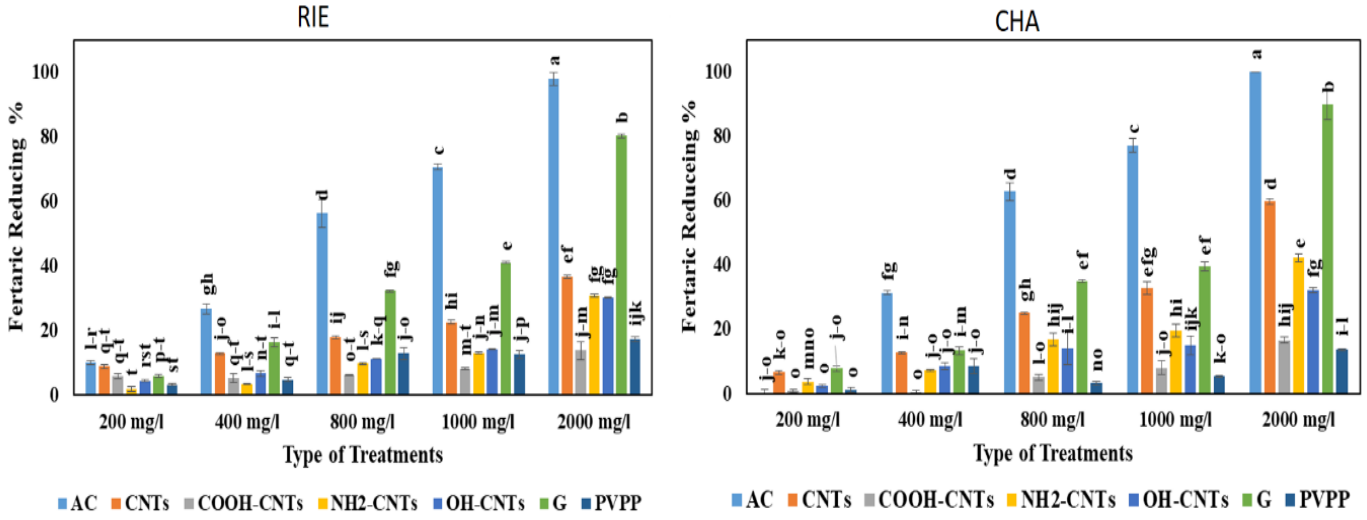

Figure 3.11 Percentage reduction of ferteric acid in RIE (left) and CHA (right) wines treated with seven different fining agents (PVPP, G, AC, CNTs, OH-CNTs, COOH-CNTs, and NH2-CNTs) at five concentrations (200, 400,800, 1000, 2000 mg/L). The data demonstrate the effects of each fining agent and concentration on ferteric acid reduction efficiency. Values are represented as mean ± SD (n=3). Data were analysed using two-way ANOVA followed by

Tukey's test. Bars that do not share the same letter show significant differences among treatments within each wine type at the 0.05 significance level.

3.2.3.6 Comparison of the Percentage Reduction of Quercetin 3-Glucoside in Wines Treated with Various Fining Agents at Different Concentrations

The interaction between treatment type and concentration on the reduction percentage of quercetin 3-glucoside in RIE and CHA was significant at a 0.05 level of significance (Appendix 16: General linear model, p value = 0.000).

A 100 % reduction of quercetin 3-glucoside was observed in RIE with AC and G at concentrations of 800 mg/L or higher. Similarly, a complete removal of quercetin 3-glucoside was observed in RIE with OH-CNTs at concentrations of 100 mg/L or higher. All other fining agents, except PVPP, resulted in a 100 % reduction of quercetin 3-glucoside at 2,000 mg/L.
On the other hand, 100 % reduction of Quercetin 3-glucoside was observed in CHA with all fining agents except PVPP and COOH-CNTs. The lowest reduction percentage of Quercetin 3-glucoside was observed in RIE and CHA with PVPP at 200 mg/L, with respective values of 25.88% ± 1.43% and 13.00% ± 1.56% (Appendices 10 and 11).
No significant difference was observed in RIE treated with bare CNTs at 200 mg/L compared to PVPP at 1,000 mg/L within the 200 to 1,000 mg/L concentration range. In CHA, treatments with CNTs, OH-CNTs, and COOH-CNTs at 200 mg/L showed no significant difference compared to PVPP at 800 mg/L(Figure 3.12). The average effect of the treatment on the percentage reduction of quercetin 3-glucoside in RIE and CHA-treated wines with PVPP was lowest across all concentrations. The highest quercetin 3-glucoside reduction percentage was observed in RIE and CHA after treatment with G (Appendices 17 and 18: Tukey test).

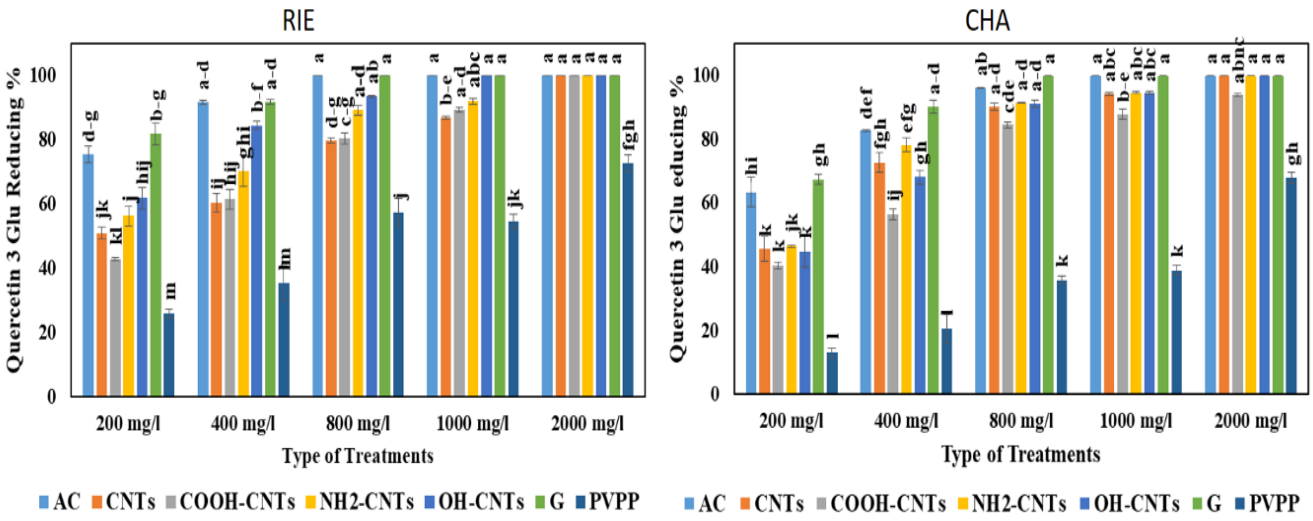

Figure 3.12 Percentage reduction of quercetin 3-glucoside in RIE (left) and CHA (right) wines treated with seven different fining agents (PVPP, G, AC, CNTs, OH-CNTs, COOH-CNTs, and NH2-CNTs) at five concentrations (200, 400, 800, 1000, 2000 mg/L). The data demonstrate the effects of each fining agent and concentration effects on quercetin 3-glucoside reduction efficiency. Values are represented as mean ± SD (n=3). Data were analysed using two-way ANOVA followed by Tukey's test. Bars that do not share the same letter show significant differences among treatments within each wine type at the 0.05 significance level.

3.2.3.7 Comparison of the Percentage Reduction of Gallic Acid and Ferulic Acid in Wines Treated with Various Fining Agents at Different Concentrations

Reduction percentages of gallic and ferulic acids in Chardonnay wine were not determined due to the low concentration of these compounds in Chardonnay control wine, which was below the calibration curve. The interaction between treatment and concentration on reduction percentages of gallic and ferulic acids in Riesling was significant at the 0.05 significance level (Appendix 19: General linear model, p value = 0.000).

The highest gallic acid reduction in RIE was observed with AC at 2,000 mg/L, with a value of 48.60% ± 3.12% (Appendix 9). At the concentration of 200 mg/L, no reduction of gallic acid was observed with CNTs and OH-CNTs, which was not significantly different from G at the same concentration (Figure 3.13). For ferulic acid, a 100% reduction was observed in RIE-treated samples with AC and G at 2,000 mg/L, whereas the lowest reduction was seen in PVPP treatment at 200 mg/L, with a value of 1.55% ± 0.35% (Appendix 10).

On average, the highest percentage of gallic acid reduction was observed in the AC treatment, while the lowest percentage was observed in the OH-CNTs treatment (Appendix 20: Tukey

test). The gallic acid reduction percentage for PVPP was not significantly different from the percentage for treatment with NH_2-CNTs. The highest ferulic acid reduction percentage was observed in the G treatment (Appendix: 21: Tukey test). In contrast, the lowest ferulic acid reduction percentage was observed in RIE treated with PVPP.

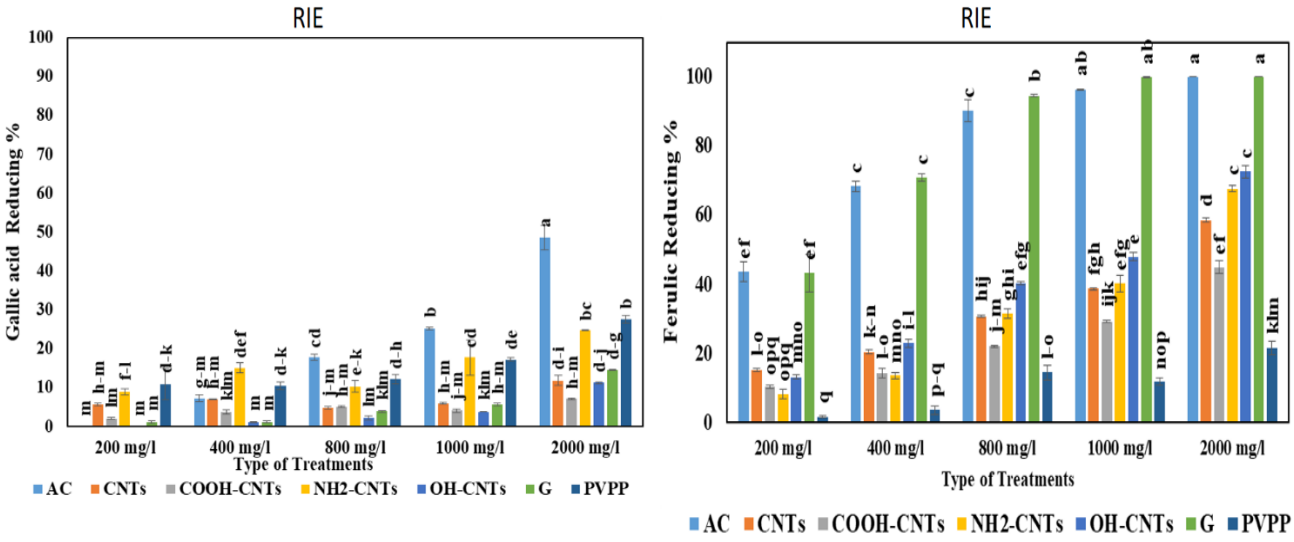

Figure 3.13 Percentage reduction of gallic acid (left) and ferulic acid (right) in RIE wines after treatment with seven different fining agents (PVPP, G, AC, CNTs, OH-CNTs, COOH-CNTs, and NH2-CNTs) at five concentrations (200, 400,800, 1000, 2000 mg/L). The data demonstrate the effects of each fining agent and the concentration effects on the reduction efficiency of gallic and ferulic acid. Values are represented as mean ± SD (n=3). Data were analysed using two-way ANOVA followed by Tukey's test. Bars that do not share the same letter show significant differences among treatments within each wine type at the 0.05 significance level.

3.3 Cost Comparison of Carbon-Based Fining Agents and PVPP

3.3.1 Laboratory-Scale Cost Comparison

First, the cost of the fining agents was compared at the laboratory scale. The cost viability of seven different fining agents at various treatment levels was examined. The overall cost of treating 1L of wine at concentrations of 200 mg/L, 400 mg/L, 800 mg/L, 1,000 mg/L, and 2,000 mg/L is listed in Table 3.5. COOH-CNTs showed the greatest cost-effectiveness across all treatment levels, ranging from A$ 0.0206 for 200 mg/L to A$ 0.2060 for 2,000 mg/L. PVPP showed moderate costs (A$ 0.0444 to A$ 0.444), whereas NH_2-CNTs were extremely costly (A$ 4.2504 to A$ 42.504). The cost analysis revealed that four of the seven fining agents examined (AC, G, CNTs, and COOH-CNTs) were more cost-effective than PVPP, saving between 41.36% (G) and 78.18% (AC). Only OH-CNTs and NH_2-CNTs had a higher treatment price than PVPP. OH-CNTs were 11.3% more expensive, while NH_2-CNTs were approximately 96 times more expensive.

Table 3.5 Cost comparison (A$) of fining agents for treating 1 L of wine at various concentrations.

Concentration (mg/L)	PVPP (A$)	AC (A$)	G (A$)	CNTs (A$)	OH-CNTs (A$)	COOH-CNTs (A$)	NH_2-CNTs (A$)
200	0.444	0.096	0.258	0.25	0.494	0.206	42.504
400	0.888	0.192	0.516	0.5	0.988	0.412	85.008
800	1.776	0.384	1.032	1.0	1.976	0.824	170.016
1000	2.22	0.48	1.29	1.25	2.47	1.03	212.52
2000	4.44	0.96	2.58	2.5	4.94	2.06	425.04

3.3.2 Commercial-Scale Cost Comparison

Figure 3.14 presents the cost comparison of fining agents against PVPP (standardized at 100%) for the treatment of 10,000 L of wine at a concentration of 1,000 mg/L. Based on this analysis, the most significant cost reduction was achieved by using activated carbon, which resulted in a 78.18% decrease in treatment costs.

Using COOH-functionalized carbon nanotubes also resulted in substantial savings, reducing treatment costs by A$ 11,700 per cycle (A$ 10,300 vs. A$ 22,000), representing a 53.18% cost reduction. Similarly, bare carbon nanotubes and graphene offered notable savings of A$ 9,500 (43.18%) and A$ 9,100 (41.36%), respectively.

In contrast, the use of OH-functionalised carbon nanotubes would increase treatment costs by A$ 2,700 (12.27%). NH_2-functionalised carbon nanotubes were found to be economically unviable, with projected treatment cost exceeding A$ 2.1 million, making it impractical for commercial use.

Additionally, the reusability potential of carbon-based finning agents and the potential for reduced prices through bulk purchasing could further enhance the cost-effectiveness of these alternatives.

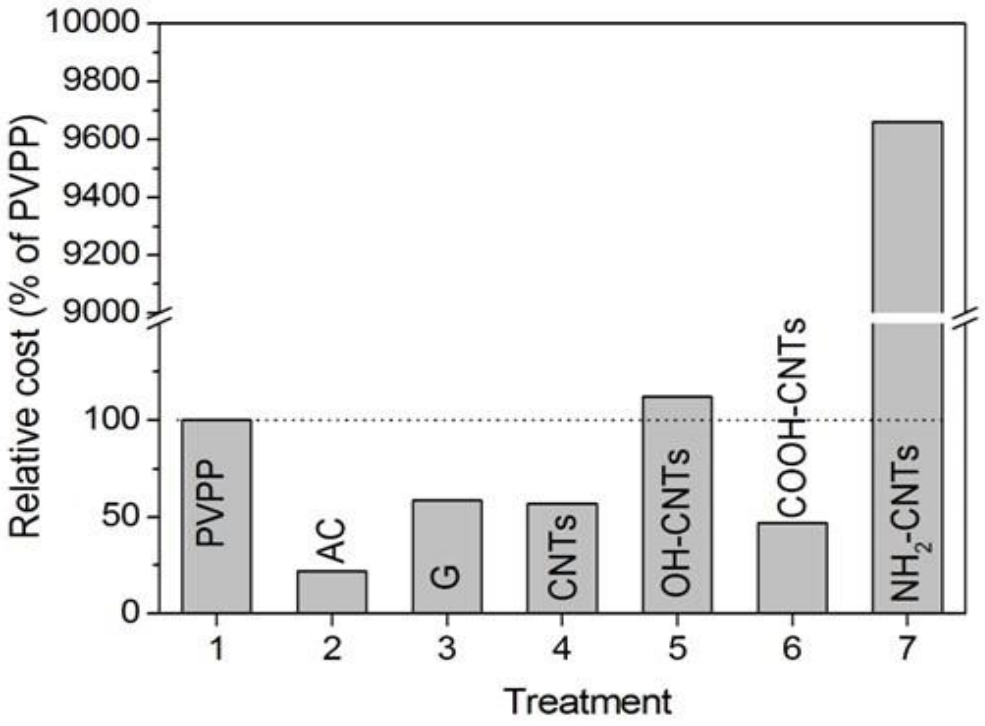

Figure 3.14 Relative cost comparison of fining agents compared to PVPP (set at 100%) for treating 10,000 L of wine at 1,000 mg/L concentration.

CHAPTER 4

DISCUSSION AND CONCLUSION

4.1 Research Significance

In 2014, white wine accounted for 32 % of global wine production, with an output of approximately 270 million hectolitres (Aurand, 2015). Based on typical dosages, this would require around 1,037 tons of PVPP would be required for fining purposes. However, PVPP is difficult to degrade and contributes to environmental challenges due to its persistence in waste streams (Ferreira et al., 2018).

With the growing awareness of sustainable development, research focused on environmentally friendly practices has increased. Over the past decade, topics such as cleaner production, pollution prevention, resource efficiency, and eco-design have received considerable attention (Glavič & Lukman, 2007). In this context, graphene, carbon nanotubes, and functionalized carbon nanotubes have emerged as promising green alternatives. These carbon-based materials can effectively remove phenolic compounds from wine and be regenerated and reused, which significantly reduces the environmental footprint of wine production processes without compromising efficacy. This shift toward sustainable practices aligns with broader efforts to promote ecological responsibility and innovation within the industry. This research aimed to evaluate these alternative fining agents by examining their morphological characteristics, phenolic removal efficiency, colloidal impact, protein absorption ability, and overall cost effectiveness.

4.2 Overview of the Main Findings and Interpretation of Results

4.2.1 Morphological Characteristics and Absorption Mechanism of Fining Agents

This study revealed significant differences in the morphology and functional behaviour of carbon-based alternative fining agents to PVPP, providing insights into their mechanisms of action in wine treatment. SEM analysis revealed unique morphological distinctions among the fining agents. These variations help explain the differing abilities of each fining agent to capture wine components, such as proteins and phenolic compounds. PVPP was observed to have a wrinkled and highly porous structure, which aligns with previous studies, and provides PVPP with a high surface area and numerous sites for binding phenolic compounds. Its uneven surface increases its surface area, enabling it to trap these compounds through hydrogen

bonding and hydrophobic interactions. Additionally, the porous structure offers extensive binding sites via surface micro-pockets to capture large polyphenols and internal cavities (2-5 nm) to retain smaller phenolic compounds, such as monomeric flavanols (Mohammad Alwi et al., 2021). AC was observed to have a flaky, fractured nature, with microspores and mesopores. Together, they contribute to a high surface area of 500-1500 m^2/g, which allows for the absorption of phenolic compounds of various sizes (Velasco & Ania, 2011).

Graphene was observed to be crumpled nanosheets with a high surface area and a diameter below 2 μm. This provides an extremely high surface area for binding phenolic-like compounds (Guo et al., 2014). Graphene has multiple interaction mechanisms, including π-π stacking with phenolic rings. This aligns with previous research involving graphene-based absorbance (Catherine et al., 2018).

CNTs and functionalised-CNTs were observed as an entangled, fibrous network of interlaced fragments, forming a network with many binding sites that can capture large particles, thereby reducing the presence of proteins and other compounds (Saifuddin et al., 2013). The longer, fibrous morphology of NH_2-CNTs may enable the formation of a distinctive structural network that absorbs particles differently from unfunctionalized-CNTs (Yaghoubi & Ramazani, 2018). In addition, the functionalised-CNTs exhibit varying degrees of binding structure depending on the attached chemical groups, impacting stability and dispersion in wine. Functional groups such as hydroxyl (-OH) and carboxyl (-COOH) increase the polarity of the surface, enhancing its interaction with polar binding sides and potentially improving the absorption of phenolic compounds in wine (Liu et al., 2018).

The NTA data reveal the colloidal properties of Riesling and Chardonnay wines treated with PVPP and carbon-based fining agents. Comparable particle size distributions were observed in the untreated RIE and CHA, with mean particle sizes of 131 nm and 132 nm, respectively. Earlier studies found that the untreated white wine has colloidal particles ranging from 20 to 200 nm due to combination of proteins, polysaccharides, and phenolic complexes (Bindon et al., 2016). Treatments with PVPP increased the mean particle size and concentration of particles in both RIE (from 131 to 155 nm) and CHA (from 132 to 146 nm), indicating that PVPP binds to the phenolic hydroxyl groups, resulting in the flocculation of large complexes (Sims et al., 1995) (Bindon et al., 2016). AC was observed to have only limited and minor effects on mean particle size changes in both wines, consistent with its unselective adsorption nature (Velasco & Ania, 2011). CNTs significantly decreased the mean particle size (RIE: from

131 to 95 nm and CHA: from 132 to 114 nm). The fibrous and 3D structure of CNTs increases the absorbance of complex substances (John et al., 2021). NH_2-CNTs had the lowest particle concentration (RIE: 1.28e+08, CHA: 2.94e+08 particles/mL), likely due to electrostatic attraction favouring sedimentation (Mierczynska-Vasilev & Smith, 2016).

Zeta potential measurements supported these findings, with untreated RIE and CHA wines exhibiting moderately negative zeta potential values (-3.1 and -1.1 mV), consistent with unstable colloidal suspensions in wine (Seidel et al., 2023). PVPP had minimal impact on zeta potential, indicating selective removal of targeted phenolics without destabilising protein-based colloids (Gil et al., 2017). In contrast, NH_2-CNTs resulted in higher (less negative or even positive) zeta potential values, likely due to their inherently positive surface charge and enhanced attraction to negatively charged wine compounds such as polysaccharides (Mierczynska-Vasilev & Smith, 2016).

4.2.2 Performance of Carbon-Based Fining Agents in Wine Fining

The efficiency of a fining agent depends on how it interacts with the wine constituents such as phenolics, proteins, and polysaccharides. Mechanisms such as hydrogen bonding, hydrophobic interactions, π-π stacking, and electrostatic attraction all contribute to these interactions (Toledo et al., 2017). The high rate of tyrosol reduction by PVPP (an average reduction of 29.40 %) supports its known mode of action. Additionally, a significant reduction in caftaric acid and gallic acid was observed at 200 mg/L with PVPP compared to other fining agents in Riesling wine. As Rihak et al 2022 explained, this observation is justified. PVPP acts mainly through a hydrogen bond interaction between its carbonyl groups (C=O) and the phenolic hydroxyl groups (-OH) of the target compounds. The molecular-level details of this interaction are provided by (Rihak et al., 2022). Tyrosol, caftaric acid, and gallic acid have phenolic hydroxyl groups that are ideally located to form hydrogen bonds with PVPP's pyrrolidone rings. Quantum chemical analysis confirms this interaction, with PVPP acting as a nucleophile and phenolic compounds as electrophiles (Durán-Lara et al., 2015). PVPP had minimal effect on protein levels, consistent with its neutral charge and lack of electrostatic interaction with proteins.

The high effectiveness of graphene in adsorbing caffeic acid (64.65% RIE, 52.62% CHA) and quercetin 3-glucoside (over 90% in both wines) can be attributed to its unique structural features and multi-mechanism adsorption. Recent studies have discovered three different

methods of adsorption within graphene-based materials including, the sp^2-hybridized carbon framework of the basal planes in graphene allows for strong π-π interactions with the aromatic rings of phenolic compounds (Wang et al., 2014). This interaction is most effective with planar flavonoids, such as quercetin 3-glucoside, which could account for its nearly complete removal. The next binding mechanism is hydrogen bonds. Edge functional groups on graphene oxide (GO) surfaces can form hydrogen bonds with phenolic -OH groups, but with a lower binding energy than π-π stacking (Kim et al., 2010). The third binding mechanism of graphene is the hydrophobic interaction. The less polar areas on the surface of graphene interact most readily with the less polar phenolic compound, which accounts for its superior performance in Chardonnay wine with respect to tyrosol (23.30% reduction) compared to PVPP (9.76 %). According to J. Wang's study, π-π stacking, hydrogen bonding, and hydrophobic interactions were responsible for the absorption of aromatic compounds in water (Wang et al., 2014).
Additionally, graphene has been found to be highly efficient in removing proteins. This is a significant advantage over PVPP. Its crumpled nanosheet shape, multi-mechanism adsorption, and high surface area are responsible for its high removal of thaumatin-like proteins (TLPs) and chitinases. These proteins are key contributors to haze formation in white wine (Albuquerque et al., 2021).
AC was observed to exhibit high, but non-selective, phenolic reduction at a concentration of 2,000 mg/L. This findings aligns with the known mode of action described in Wang et al. study (Wang et al., 2016). AC has a flaky, fractured microstructure with a rough surface, producing numerous adsorption sites that can hold a broad array of compounds. Its high surface area allows for extensive physical adsorption through van der Waals forces, accounting for its ability to reduce wine components more effectively (Jeirani et al., 2017).

The differing behaviours of CNTs and functionalized CNTs with various phenolic compounds highlight how surface chemical modification can alter adsorption selectivity. For example, OH-functionalized CNTs show limited reduction of tyrosol (6.65% RIE), but exhibited superior removal of quercetin 3-glucoside (88.00% RIE), emphasising the importance of aligning the physicochemical properties of fining agents with those of target compounds.

The adsorption behaviour of CNTs in wine mirrors that of graphene for several phenolic compounds. The pristine CNT surface, composed of graphitic carbon and inherently non-polar, facilitates π-π stacking and hydrophobic interactions with aromatic or non-polar moieties (Lin & Xing, 2008). Moreover, functionalized CNTs, such as NH_2-CNTs, interact with phenolic compounds through a hydrogen bonding and electrostatic interaction. Similarly, their

effectiveness in reducing protein levels can be attributed to electrostatic interactions between the cationic amine groups on the CNT and anionic nature of wine proteins (Garrido et al., 2020).

4.2.3 Cost Analysis

Four of the seven fining agents under investigation – AC, G, CNTs, and COOH-CNTs – were found to be more cost-effective than PVPP. The cost reductions ranged from 41.36% (G) to 78.18 % (AC). At a commercial scale of 10,000 L at 1000 mg/L, COOH-CNTs could save A$11,700 per treatment cycle compared to PVPP, representing a 53.18 % reduction in treatment costs. Bare CNTs could save A$9,500 per treatment cycle compared to PVPP, representing a 43.18 % reduction in treatment cost.

4.2.4 Matrix Effects and Environmental Factors Influencing Fining Agent Efficiency

The differential efficiency of the fining agents for RIE and CHA wines reflects the effect of wine composition on fining performance. In CHA, higher protein levels most likely competed with phenolics for binding sites on the fining agents, thereby altering their effectiveness relative to RIE. This matrix-dependent behaviour highlights the need for composition-specific fining treatments rather than standardised treatments.

For example, PVPP was more effective at reducing tyrosol in RIE than in CHA, whereas graphene was more effective at reducing tyrosol in CHA. This observation aligns with the findings by Mierczynska-Vasilev and Smith, who observed that protein-phenolic interactions can significantly influence the activity of fining agents (Mierczynska-Vasilev & Smith, 2016). On the other hand, optimum pH conditions and ionic strength depend on absorption efficiency. According to previous studies, maximum absorption is achieved in mildly acidic conditions (pH 3-4) through the protonation of the phenolic -OH group, which facilitates strong hydrogen bonding. However, high salt concentrations lower adsorption by 15-20 % due to the formation of ion pairs (Wu et al., 2024).

4.2.5 Practical Implications for Winemaking

Activated carbon demonstrated the highest overall reduction of phenolics. However, it is non-selective and removes both desirable and undesirable components in wine. This was supported by Wang' study. Activated carbon should only be used for wines with major contamination, such as smoke taint (Wang et al., 2016). Moreover, AC's limited effectiveness is a major drawback due to its variable behaviour at low concentrations (200-800 mg/L) compared to high

concentrations. Graphene was the most balanced option for fining phenolic compounds, especially caffeic acid and quercetin 3-glucoside, as well as for satisfactory protein removal. However, its exceptional effectiveness for certain phenolic compounds limited its overall efficiency. This may allow it to target specific wine quality issues more effectively than other fining materials.

4.3 Sustainable Wine Industry and Innovation

4.3.1 Environmental Impact and Sustainability

The eco-friendly nature of carbon-based nanomaterials aligns well with the growing consumer preference for sustainable products. As wineries adopt greener practices, they can potentially attract a more environmentally conscious customer base, enhancing their market appeal and increasing sales because the purchasing decisions of consumers based on sustainability concerns are increased in now a days and they are willing to pay a premium for environmentally responsible products (Schäufele & Hamm, 2017). Aligning with sustainability helps companies not only meet regulatory requirements but also positions them favourably in an increasingly competitive market focused on ecological responsibility.

4.3.2 Concept of Innovation

The potential applications of nanotechnology in the wine industry are vast and encompass everything from cultivation and winemaking to packaging. Innovations in this field can significantly improve wine stabilization and intensify flavours, opening new avenues for quality improvement (Dumitriu et al., 2018). During adsorption, phenolic compounds attach to the surface of CNTs via van der Waals forces, π-π interactions, and hydrogen bonding. This process is essential for removing of unwanted phenolic compounds that can negatively affect wine quality. Research has shown that CNTs can function as artificial flocculants, enhancing the flocculation of wine and contributing to improved wine clarity and stability (Luchian et al., 2024). The ability to refine wines effectively, without the disadvantages associated with traditional agents like PVPP, provides winemakers with a valuable tool for enhancing quality. Embracing these innovative materials not only promises to elevate wine quality but also aligns the wine industry with broader commitments to sustainability and ecological responsibility.

4.3.3 Economic Benefits

For white wine fining, PVPP consumption was approximately 147 tons in Portugal in 2016, with global usage projected to reach 10,000-12,000 tons annually by 2025 (Cosme et al., 2019).

The global cost per kilogram of PVPP ranges from USD 30-150, depending on the supplier and purity. Considerable costs are estimated to be spent on the fining process. In recent years, nanotechnology has gained significant traction in the wine industry, with carbon-based materials emerging as a preferred choice for various applications (Malik et al., 2023).

One of the primary economic benefits comes from the exceptional structural properties of these materials. Their high surface area and reactivity allow for the effective adsorption of phenolic compounds, which improves wine quality and reduces the need for traditional fining agents, as well as minimising waste management expenses. PVPP generates considerable waste that requires careful disposal, often involving additional costs. In contrast, the renewable properties of CNTs and graphene make them a popular choice in adsorption-based water purification (Kotia et al., 2020). Their regenerative properties would allow wineries to significantly reduce the frequency of fining agent use, drastically cutting waste management costs.

4.4. Limitations and Future Research Directions

4.4.1 Limitations of the Current Study

This research was limited to white wines, which makes it difficult to generalise the findings to red wines that present different phenolic compositions. Moreover, laboratory-scale trials cannot accurately reflect the conditions under which most commercial winemaking operations take place, such as tank geometry, temperature during cycling, and volume, all of which can impact the efficiency of the fining agent (Casalta et al., 2010). Sensory analysis, which is important for understanding consumer acceptance of wines fined using the mentioned substitutes (Lesschaeve & Noble, 2022), was not carried out in the study. While phenolic reduction was measured, the effects on wine aroma, taste, and mouthfeel remain unclear.

Additionally, PVPP is commonly used to fine white wines, but it is used less frequently for red wines because phenolic compounds, such as tannins and anthocyanins, are important for red wine color and mouthfeel. Since PVPP can bind phenolic compounds, it has the potential to remove desirable ones. Therefore, its use in red wines is generally limited to specific purposes, such as reducing bitterness or stabilizing color, rather than routine fining. Therefore, further investigation is needed to determine the applicability of the findings to red wine fining with PVPP or alternative agents.

4.4.2 Future Research Direction

Based on the findings of this research, several conclusions are valuable for future investigations into the use of carbon-based fining agents in winemaking for commercial applications. One major priority is the overall sensory analysis of wine fining with graphene and functionalized carbon nanotubes (CNTs), particularly with regard to their effects on volatile flavour and mouthfeel characteristics. According to previous research, sensory characteristics are sensitive to carbon-based substances (Luchian et al., 2024). Another valuable line of research would be to extend these investigations to red wines, which have a high phenolic load and complicated tannin matrices. To achieve efficient performance on a commercial scale, it is necessary to overcome scalability issues by analyzing key process parameters, including contact time, agitation processes, and separation methods. Another important direction for future research is to investigate the reusability of carbon-based nanomaterials to reduce costs. Ultimately, investigating combined systems that feature multiple carbon-based fining agents with distinct functionalities may enhance performance through their complementary absorption processes. Previous research on composite nanomaterials for site-selective separation of molecules supports this idea (Luchian et al., 2024). Together, these lines of research suggest the possibility of creating an economically and environmentally friendly alternative to PVPP that preserves or improves the wine quality.

4.5 Conclusion

This study demonstrates that carbon-based fining agents, such as graphene and carbon nanotubes (CNTs), as well as carboxylated carbon nanotubes (COOH-CNTs), can serve as suitable alternatives to polyvinylpolypyrrolidone (PVPP) in wine fining applications. These materials efficiently reduce phenolics and offer additional advantages, such as protein removal properties and potential cost effectiveness. The specific morphological properties and chemical characteristics of each fining agent directly affect its absorption mechanism and pattern, providing wine producers with a new solution for addressing quality issues in the wine. The variation in results also highlights the importance of selecting a fining agent that is suitable for the specific winemaking objectives. This includes determining if the selective removal of phenolic compounds or proteins is necessary, and if the removal of desired constituents is feasible and affordable.

Although activated carbon demonstrated the highest phenolic reduction, its lack of selectivity limits its practical application. This research addresses growing environmental concerns related to PVPP, confirming its efficacy and exploring more sustainable alternatives. By aligning laboratory findings with industry needs, the study supports the wine sector's efforts to enhance sustainability without compromising product quality.

REFERENCES

Abu-Nada, A., Abdala, A., & McKay, G. (2021). Removal of phenols and dyes from aqueous solutions using graphene and graphene composite adsorption: a review. *Journal of Environmental Chemical Engineering*, *9*(5), 105858. https://doi.org/https://doi.org/10.1016/j.jece.2021.105858

Albuquerque, W., Seidel, L., Zorn, H., Will, F., & Gand, M. (2021). Haze formation and the challenges for peptidases in wine protein fining. *Journal of Agricultural and Food Chemistry*, *69*(48), 14402-14414. https://doi.org/https://doi.org/10.1021/acs.jafc.1c05427

Aleixandre-Tudo, J. L., & Du Toit, W. (2019). Spectroscopy for Phenolic Compounds Quantification in. *Frontiers and new trends in the science of fermented food and beverages*, 25.

Anderson, K. (2018). Australian wine industry competitiveness: why so slow to emerge? *Australian Journal of Agricultural and Resource Economics*, *62*(4), 507-526. https://doi.org/ https://doi.org/10.1111/1467-8489.12276

Apul, O. G., Wang, Q., Zhou, Y., & Karanfil, T. (2013). Adsorption of aromatic organic contaminants by graphene nanosheets: Comparison with carbon nanotubes and activated carbon. *Water research*, *47*(4), 1648-1654. https://doi.org/http://dx.doi.org/10.1016/j.watres.2012.12.031

Aurand, J.-M. (2015, 06/07/2015)). 38th World Congress of Vine and Wine. *OIV report on the world vitivinicultural situation*.

Benucci, I., Lombardelli, C., Muganu, M., Mazzocchi, C., & Esti, M. (2022). A minimally invasive approach for preventing white wine protein haze by early enzymatic treatment. *Foods*, *11*(15), 2246. https://doi.org/https://doi.org/10.3390/foods11152246

Bhattacharjee, S. (2016). DLS and zeta potential–what they are and what they are not? *Journal of controlled release*, *235*, 337-351. https://doi.org/https://doi.org/10.1016/j.jconrel.2016.06.017

Bindon, K. A., Carew, A. L., Mierczynska-Vasilev, A., Kassara, S., Kerslake, F., & Smith, P. A. (2016). Characterization of macromolecular complexes in red wine: Composition, molecular mass distribution and particle size. *Food chemistry*, *199*, 838-846. https://doi.org/https://doi.org/10.1016/j.foodchem.2015.12.079

[Record #204 is using a reference type undefined in this output style.]

Boulton, R. B., Singleton, V. L., Bisson, L. F., & Kunkee, R. E. (2013). *Principles and practices of winemaking*. Springer Science & Business Media.

Burin, V. M., Arcari, S. G., Bordignon-Luiz, T, M., & Costa, L. L. F. (2011). Determination of some phenolic compounds in red wine by RP-HPLC: method development and validation. *Journalof chromatographic science*, *49*(8), 647-651.

Casalta, E., Aguera, E., Picou, C., Rodriguez-Bencomo, J.-J., Salmon, J.-M., & Sablayrolles, J.-M. (2010). A comparison of laboratory and pilot-scale fermentations in winemaking conditions. *Applied microbiology and biotechnology*, *87*(5), 1665-1673.

Castillo-Sánchez, J., García-Falcón, M., Garrido, J., Martínez-Carballo, E., Martins-Dias, L., & Mejuto,X. (2008). Phenolic compounds and colour stability of Vinhao wines: Influence of wine-making protocol and fining agents. *Food chemistry*, *106*(1), 18-26.

Catherine, H. N., Ou, M.-H., Manu, B., & Shih, Y.-h. (2018). Adsorption mechanism of emerging and conventional phenolic compounds on graphene oxide nanoflakes in water. *ScienceoftheTotal Environment*, *635*, 629-638. https://doi.org/https://doi.org/10.1016/j.scitotenv.2018.03.389

Chidawanyika, W., & Nyokong, T. (2010). Characterization of amine-functionalized single-walled carbon nanotube-low symmetry phthalocyanine conjugates. *Carbon*, *48*(10), 2831-2838. https://doi.org/https://doi.org/10.1016/j.carbon.2010.04.015

Chira, K., Jourdes, M., & Teissedre, P.-L. (2012). Cabernet sauvignon red wine astringency quality control by tannin characterization and polymerization during storage. *European Food Research and Technology*, *234*, 253-261.

Clarke, S., Bosman, G., du Toit, W., & Aleixandre-Tudo, J. L. (2023). White wine phenolics: current methods of analysis. *Journal of the Science of Food and Agriculture*, *103*(1), 7-25. https://doi.org/https://doi.org/10.1002/jsfa.12120

Cosme, F., Capão, I., Filipe-Ribeiro, L., Bennett, R., & Mendes-Faia, A. (2012). Evaluating potential alternatives to potassium caseinate for white wine fining: Effects on physicochemical and sensory characteristics. *LWT-Food Science and Technology*, *46*(2), 382-387. https://doi.org/https://doi.org/10.1016/j.lwt.2011.12.016

Cosme, F., Ferreira, S., Alves, A., Filipe-Ribeiro, L., & Nunes, F. (2019). Recycling of PVPP used in the wine industry: An opportunity for obtaining reusable PVPP and bioactive phenolic compounds. BIO web of conferences,

Cosme, F., Inês, A., Silva, D., Filipe-Ribeiro, L., Abrunhosa, L., & Nunes, F. M. (2021). Elimination of ochratoxin A from white and red wines: Critical characteristics of activated carbonsandimpact on wine quality. *LWT*, *140*, 110838. https://doi.org/https://doi.org/10.1016/j.lwt.2020.110838

Dumitriu, G.-D., de Lerma, N. L., Luchian, C. E., Cotea, V. V., & Peinado, R. A. (2018). Study of the potential use of mesoporous nanomaterials as fining agent to prevent protein haze in white wines and its impact in major volatile aroma compounds and polyols. *Food chemistry*, *240*, 751-758. https://doi.org/https://doi.org/10.1016/j.foodchem.2017.07.163

Durán-Lara, E. F., López-Cortés, X. A., Castro, R. I., Avila-Salas, F., González-Nilo, F. D., Laurie, V. F., & Santos, L. S. (2015). Experimental and theoretical binding affinity between polyvinylpolypyrrolidone and selected phenolic compounds from food matrices. *Food chemistry*, *168*, 464-470. https://doi.org/https://doi.org/10.1016/j.foodchem.2014.07.048

Ferreira, R. B., Piçarra-Pereira, M. A., Monteiro, S., Loureiro, V. l. B., & Teixeira, A. R. (2001). The wine proteins. *Trends in food science & technology*, *12*(7), 230-239. https://doi.org/https://doi.org/10.1016/S0924-2244(01)00080-2

Ferreira, S. S., Alves, A. J., Filipe-Ribeiro, L., Cosme, F., & Nunes, F. M. (2018). Holistic and sustainable approach for recycling and valorization of Polyvinylpolypyrrolidone used in wine fining. *ACS Sustainable Chemistry & Engineering*, *6*(11), 14599-14606. https://doi.org/https://doi.org/10.1021/acssuschemeng.8b03208

Garrido, M., Gualandi, L., Di Noja, S., Filippini, G., Bosi, S., & Prato, M. (2020). Synthesis and applications of amino-functionalized carbon nanomaterials. *Chemical Communications*, *56*(84), 12698-12716. https://doi.org/https://doi.org/10.1039/D0CC05316C

Geană, E.-I., Ciucure, C. T., Apetrei, C., & Artem, V. (2019). Application of spectroscopic UV-Vis andFT-IR screening techniques coupled with multivariate statistical analysis for red wine authentication: Varietal and vintage year discrimination. *Molecules*, *24*(22), 4166. https://doi.org/doi:10.3390/molecules24224166

Ghanem, C., Taillandier, P., Rizk, M., Rizk, Z., Nehme, N., Souchard, J.-P., & El Rayess, Y. (2017).Analysis of the impact of fining agents types, oenological tannins and mannoproteins and their concentrations on the phenolic composition of red wine. *LWT-Food Science and Technology*, *83*, 101-109. https://doi.org/http://dx.doi.org/10.1016/j.lwt.2017.05.009

Gil, M., Louazil, P., Iturmendi, N., Moine, V., Cheynier, V., & Saucier, C. (2019). Effect of polyvinylpolypyrrolidone treatment on rosés wines during fermentation: Impact on color, polyphenols and thiol aromas. *Food chemistry*, *295*, 493-498. https://doi.org/https://doi.org/10.1016/j.foodchem.2019.05.125

Gil, M. l., Avila-Salas, F., Santos, L. S., Iturmendi, N., Moine, V., Cheynier, V., & Saucier, C. d. (2017). Rosé wine fining using polyvinylpolypyrrolidone: Colorimetry, targeted polyphenomics,and molecular dynamics simulations. *Journal of Agricultural and Food Chemistry*, *65*(48), 10591-10597. https://doi.org/10.1021/acs.jafc.7b04461

Glavič, P., & Lukman, R. (2007). Review of sustainability terms and their definitions. *Journal of cleaner production*, *15*(18), 1875-1885.

Guo, F., Creighton, M., Chen, Y., Hurt, R., & Külaots, I. (2014). Porous structures in stacked, crumpled and pillared graphene-based 3D materials. *Carbon*, *66*, 476-484. https://doi.org/https://doi.org/10.1016/j.carbon.2013.09.024

Hammood, R. R. K., Hammood, A. J., Abdulrasool, W. A., & Hussein, S. S. (2023). High-Performance Liquid Chromatography (HPLC): Primary Mechanism and Popular Applications. *Al-Nahrain Journal of Science*, *26*(4), 1-12.

Harbertson, J. F., & Spayd, S. (2006). Measuring phenolics in the winery. *American Journal of Enology and Viticulture*, *57*(3), 280-288.

Iijima, S. (1991). Helical microtubules of graphitic carbon. *nature*, *354*(6348), 56-58. https://doi.org/doi: 10.1038/354056a0

Jeirani, Z., Niu, C. H., & Soltan, J. (2017). Adsorption of emerging pollutants on activated carbon. *Reviews in Chemical Engineering*, *33*(5), 491-522.

John, J. P., TE, M. N., & TK, B. S. (2021). A comprehensive review on the environmental applications of graphene–carbon nanotube hybrids: recent progress, challenges and prospects. *Materials Advances*, *2*(21), 6816-6838. https://doi.org/10.1039/D1MA00324K

Jordão, A. M., Vilela, A., & Cosme, F. (2015). From sugar of grape to alcohol of wine: Sensorial impact of alcohol in wine. *Beverages*, *1*(4), 292-310. https://doi.org/https://doi.org/10.3390/beverages1040292

Kim, J., Cote, L. J., Kim, F., Yuan, W., Shull, K. R., & Huang, J. (2010). Graphene oxide sheets at interfaces. *Journal of the American Chemical Society*, *132*(23), 8180-8186. https://doi.org/https://doi.org/10.1021/ja102777p

Kong, Q., Shi, X., Ma, W., Zhang, F., Yu, T., Zhao, F., Zhao, D., & Wei, C. (2021). Strategies to improve the adsorption properties of graphene-based adsorbent towards heavy metal ions and their compound pollutants: A review. *Journal of Hazardous Materials*, *415*, 125690. https://doi.org/https://doi.org/10.1016/j.jhazmat.2021.125690

Kotia, A., Yadav, A., Rohit Raj, T., Gertrud Keischgens, M., Rathore, H., & Sarris, I. E. (2020). Carbon nanoparticles as sources for a cost-effective water purification method: A comprehensive review. *Fluids*, *5*(4), 230. https://doi.org/https://doi.org/10.3390/fluids5040230

Lesschaeve, I., & Noble, A. C. (2022). Sensory analysis of wine. *Managing wine quality*, 243-277. https://doi.org/https://doi.org/10.1016/B978-0-08-102067-8.00010-5

Li, H., Guo, A., & Wang, H. (2008). Mechanisms of oxidative browning of wine. *Food chemistry*, *108*(1), 1-13. https://doi.org/doi:10.1016/j.foodchem.2007.10.065

Lin, D., & Xing, B. (2008). Adsorption of phenolic compounds by carbon nanotubes: role of aromaticity and substitution of hydroxyl groups. *Environmental science & technology*, *42*(19), 7254-7259. https://doi.org/https://doi.org/10.1021/es801297u

Liu, H., Wang, J., Wang, J., & Cui, S. (2018). Sulfonitric treatment of multiwalled carbon nanotubes and their dispersibility in water. *Materials*, *11*(12), 2442. https://doi.org/doi: 10.3390/ma11122442

Liu, W.-W., Chai, S.-P., Mohamed, A. R., & Hashim, U. (2014). Synthesis and characterization of graphene and carbon nanotubes: A review on the past and recent developments. *Journal of Industrial and Engineering Chemistry*, *20*(4), 1171-1185. https://doi.org/http://dx.doi.org/10.1016/j.jiec.2013.08.028

Liu, Z., Xu, L., Wang, J., Duan, C., Sun, Y., Kong, Q., & He, F. (2023). Research progress of protein haze in white wines. *Food Science and Human Wellness*, *12*(5), 1427-1438. https://doi.org/https://doi.org/10.1016/j.fshw.2023.02.004

Lozada-Ramírez, J. D., Ortega-Regules, A. E., Hernández, L. R., & Anaya de Parrodi, C. (2021). Spectroscopic and spectrometric applications for the identification of bioactive compounds from vegetal Extracts. *Applied Sciences*, *11*(7), 3039. https://doi.org/https://doi.org/10.3390/app11073039

Luchian, C., Niculaua, M., Cotea, V. v., Bilba, N., Vasile, A., & Copcia, V. (2011). Phenolic stabilization of wines using mesoporous silica SBA-15 molecular sieve. *Mitteilungen Klosterneuburg*, *61*(2), 91-100.

Luchian, C. E., Codreanu, M., Scutarașu, E. C., Colibaba, L. C., & Cotea, V. (2024). Impact of Nanomaterials on Wine Quality: A Focus of Siliceous, Aluminosiliceous, and Carbon-Based Nanomaterials on the Phenolic Fraction of Wine. https://doi.org/DOI: 10.5772/intechopen.1005268

Majewski, P., Barbalet, A., & Waters, E. (2011). $1 billion hidden cost of bentonite fining. *Australian and New Zealand grapegrower and winemaker*(569), 58-62.

Makris, D. P., Psarra, E., Kallithraka, S., & Kefalas, P. (2003). The effect of polyphenolic composition as related to antioxidant capacity in white wines. *Food Research International*, *36*(8), 805-814. https://doi.org/https://doi.org/10.1016/S0963-9969(03)00075-9

Malik, S., Muhammad, K., & Waheed, Y. (2023). Nanotechnology: A revolution in modern industry. *Molecules*, *28*(2), 661. https://doi.org/https://doi.org/10.3390/molecules28020661

Mamvura, T. A., Iyuke, S. E., Sibanda, V., & Yah, C. S. (2012). Immobilisation of yeast cells on carbon nanotubes. *South African Journal of Science*, *108*(7), 1-7. https://doi.org/http://dx.doi.org/10.4102/sajs. v108i7/8.768

Mansfield, E. D., Sillence, K., Hole, P., Williams, A. C., & Khutoryanskiy, V. V. (2015). POZylation:anew approach to enhance nanoparticle diffusion through mucosal barriers. *Nanoscale*, *7*(32), 13671-13679. https://doi.org/10.1039/C5NR03178H

Marangon, M., Stockdale, V. J., Munro, P., Trethewey, T., Schulkin, A., Holt, H. E., & Smith, P. A. (2013). Addition of carrageenan at different stages of winemaking for white wine protein stabilization. *Journal of Agricultural and Food Chemistry*, *61*(26), 6516-6524. https://doi.org/https://doi.org/10.1021/jf401712d

Mélodie, G., Fabian, A.-S., Nerea, I., Virginie, M., Véronique, C., & Cédric, S. (2017). Rosé Wine Fining Using Polyvinylpolypyrrolidone: Colorimetry, Targeted Polyphenomics, and Molecular Dynamics Simulations. https://doi.org/https://doi.org/10.1021/acs.jafc.7b04461

Merkytė, V., Longo, E., Windisch, G., & Boselli, E. (2020). Phenolic compounds as markers of wine quality and authenticity. *Foods*, *9*(12), 1785. https://doi.org/doi:10.3390/foods9121785

Mierczynska-Vasilev, A., Boyer, P., Vasilev, K., & Smith, P. A. (2017). A novel technology for the rapid, selective, magnetic removal of pathogenesis-related proteins from wines. *Food chemistry*, *232*, 508-514. https://doi.org/https://doi.org/10.1016/j.foodchem.2017.04.050

Mierczynska-Vasilev, A., Mierczynski, P., Maniukiewicz, W., Visalakshan, R. M., Vasilev, K., & Smith, P. A. (2019). Magnetic separation technology: Functional group efficiency in the removal of haze-forming proteins from wines. *Food chemistry*, *275*, 154-160. https://doi.org/https://doi.org/10.1016/j.foodchem.2018.09.046

Mierczynska-Vasilev, A., & Smith, P. A. (2016). Surface modification influencing adsorption of red wine constituents: The role of functional groups. *Applied Surface Science*, *386*, 14-23. https://doi.org/https://doi.org/10.1016/j.apsusc.2016.06.016

Mierczynska-Vasilev, A., & Smith, P. (2015). Current state of knowledge and challenges in wine clarification. *Australian Journal of Grape and Wine Research*, *21*, 615-626. https://doi.org/https://doi.org/10.1111/ajgw.12198

Mills, D. A., Phister, T., Neeley, E., & Johannsen, E. (2008). Wine fermentation. *Molecular techniques in the microbial ecology of fermented foods*, 162-192.

Mocke, B. B. (2023, June 30,). The beginning of the end of PVPP in winemaking. *Laffort*.

Mohammad Alwi, M. A., Normaya, E., Ismail, H., Iqbal, A., Mat Piah, B., Abu Samah, M. A., & Ahmad, M. N. (2021). Two-dimensional infrared correlation spectroscopy, conductor-like screening model for real solvents, and density functional theory study on the adsorption mechanism of polyvinylpolypyrrolidone for effective phenol removal in an aqueous medium. *ACS omega*, *6*(39), 25179-25192. https://doi.org/https://doi.org/10.1021/acsomega.1c02699

Mukherjee, S., Kumar, S., Misra, A. K., & Fan, M. (2007). Removal of phenols from water environment by activated carbon, bagasse ash and wood charcoal. *Chemical Engineering Journal*, *129*(1-3), 133-142. https://doi.org/https://doi.org/10.1016/j.cej.2006.10.030

Muñoz-Bernal, Ó. A., Vazquez-Flores, A. A., de la Rosa, L. A., Rodrigo-García, J., Martínez-Ruiz, N. R.,& Alvarez-Parrilla, E. (2023). Enriched red wine: phenolic profile, sensory evaluation andinvitro bioaccessibility of phenolic compounds. *Foods*, *12*(6), 1194. https://doi.org/; https://doi.org/10.3390/foods12061194

Niyogi, S., Hamon, M., Hu, H., Zhao, B., Bhowmik, P., Sen, R., Itkis, M., & Haddon, R. (2002). Chemistry of single-walled carbon nanotubes. *Accounts of Chemical Research*, *35*(12), 1105-1113. https://doi.org/https://doi.org/10.1021/ar010155r

Novoselov, K. S., Geim, A. K., Morozov, S. V., Jiang, D.-e., Zhang, Y., Dubonos, S. V., Grigorieva, I. V., & Firsov, A. A. (2004). Electric field effect in atomically thin carbon films. *science*, *306*(5696), 666-669.

Oginni, O., Singh, K., Oporto, G., Dawson-Andoh, B., McDonald, L., & Sabolsky, E. (2019). Effect ofone-step and two-step H3PO4 activation on activated carbon characteristics. *Bioresource Technology Reports*, *8*, 100307. https://doi.org/https://doi.org/10.1016/j.biteb.2019.100307

Pereira, A. C., Reis, M. S., Saraiva, P. M., & Marques, J. C. (2010). Analysis and assessment of Madeira wine ageing over an extended time period through GC–MS and chemometric analysis. *Analytica Chimica Acta*, *660*(1-2), 8-21.

Rihak, Z., Prusova, B., Prokes, K., & Baron, M. (2022). The effect of different fining treatments on phenolic and aroma composition of grape musts and wines. *Fermentation*, *8*(12), 737. https://doi.org/ https://doi.org/10.3390/fermentation8120737

Río Segade, S., Paissoni, M. A., Vilanova, M., Gerbi, V., Rolle, L., & Giacosa, S. (2019). Phenolic composition influences the effectiveness of fining agents in vegan-friendly red wine production. *Molecules*, *25*(1), 120. https://doi.org/ https://doi.org/10.3390/molecules25010120

Rossi, J. A., & Singleton, V. L. (1966). Flavor effects and adsorptive properties of purified fractions of grape-seed phenols. *American Journal of Enology and Viticulture*, *17*(4), 240-246. https://doi.org/ 10.5344/ajev.1966.17.4.240

Saifuddin, N., Raziah, A., & Junizah, A. (2013). Carbon nanotubes: a review on structure and their interaction with proteins. *Journal of Chemistry*, *2013*(1), 676815. https://doi.org/https://doi.org/10.1155/2013/676815

Sanborn, M., Edwards, C. G., & Ross, C. F. (2010). Impact of fining on chemical and sensory properties of Washington State Chardonnay and Gewürztraminer wines. *American Journal of Enology and Viticulture*, *61*(1), 31-41. https://doi.org/10.5344/ajev.2010.61.1.31

Schäufele, I., & Hamm, U. (2017). Consumers' perceptions, preferences and willingness-to-pay for wine with sustainability characteristics: A review. *Journal of cleaner production*, *147*, 379-394. https://doi.org/https://doi.org/10.1016/j.jclepro.2017.01.118

Schütt, F., Signetti, S., Krüger, H., Röder, S., Smazna, D., Kaps, S., Gorb, S. N., Mishra, Y. K., Pugno, N. M., & Adelung, R. (2017). Hierarchical self-entangled carbon nanotube tube networks. *Nature communications*, *8*(1), 1215.

Seabrook, A., & van der Westhuizen, T. (2018). Fining during fermentation: Focus on white and rose: Advantages of fining in must rather than wine on aroma and colour. *Wine & Viticulture journal*, *33*(1), 30-33.

Seidel, L., Albuquerque, W., Happel, K., Ghezellou, P., Gand, M., Spengler, B., Zorn, H., Will, F., & Schweiggert, R. (2023). Composition, ζ potential, and molar mass distribution of 20 must and wine colloids from five different cultivars obtained during four consecutive vintages. *Journal of Agricultural and Food Chemistry*, *72*(4), 1938-1948. https://doi.org/https://doi.org/10.1021/acs.jafc.2c09048

Shah, R., Eldridge, D., Palombo, E., & Harding, I. (2014). Optimisation and stability assessment of solid lipid nanoparticles using particle size and zeta potential. *Journal of physical science*, *25*(1).

Sharma, S. K., Verma, D. S., Khan, L. U., Kumar, S., & Khan, S. B. (2018). *Handbook of materials characterization*. Springer.

Sims, C. A., Eastridge, J. S., & Bates, R. P. (1995). Changes in phenols, color, and sensory characteristics of muscadine wines by pre-and post-fermentation additions of PVPP, casein, and gelatin. *American Journal of Enology and Viticulture*, *46*(2), 155-158. https://doi.org/10.5344/ajev.1995.46.2.155

Sing, K. S. (2013). Adsorption by active carbons. *Rouquerol, F., Rouquerol, J., Sing, KSW, Llewellyn, P., and Maurin, G., Academic Press*, 321-391.

Skouroumounis, G. K., Kwiatkowski, M., Francis, I., Oakey, H., Capone, D., Peng, Z., Duncan, B., Sefton, M., & Waters, E. (2005). The influence of ascorbic acid on the composition, colour and flavour properties of a Riesling and a wooded Chardonnay wine during five years' storage. *Australian Journal of Grape and Wine Research*, *11*(3), 355-368.

Sweetman, M. J., May, S., Mebberson, N., Pendleton, P., Vasilev, K., Plush, S. E., & Hayball, J. D.(2017). Activated carbon, carbon nanotubes and graphene: materials and composites for advanced water purification. *C*, *3*(2), 18. https://doi.org/https://doi.org/10.3390/c3020018

Tantra, R., Schulze, P., & Quincey, P. (2010). Effect of nanoparticle concentration on zeta-potential measurement results and reproducibility. *Particuology*, *8*(3), 279-285. https://doi.org/doi:10.1016/j.partic.2010.01.003

Toledo, L., Salazar, F., & Aquino, A. (2017). A theoretical approach for understanding the haze phenomenon in bottled white wines at molecular level. *South African Journal of Enology and Viticulture*, *38*(1), 64-71.

Van Buiten, C. B., & Elias, R. J. (2024). Impact of pre-and post-fermentation fining with polyvinylpolypyrrolidone on the chemical stability and aromatic profile of Viognier wine. *Journal of Food Science*, *89*(7), 4286-4297. https://doi.org/ https://doi.org/10.1111/1750-3841.17141

Van Sluyter, S. C., McRae, J. M., Falconer, R. J., Smith, P. A., Bacic, A., Waters, E. J., & Marangon, M. (2015). Wine protein haze: Mechanisms of formation and advances in prevention. *Journal of Agricultural and Food Chemistry*, *63*(16), 4020-4030. https://doi.org/https://doi.org/10.1021/acs.jafc.5b00047

Vanharova, L., Julinova, M., & Slavik, R. (2017). PVP based materials: biodegradation in different environments. *Ecological Chemistry and Engineering S*, *24*(2), 299-309. https://doi.org/ 10.1515/eces-2017-0021

Velasco, L. F., & Ania, C. O. (2011). Understanding phenol adsorption mechanisms on activated carbons. *Adsorption*, *17*, 247-254. https://doi.org/DOI 10.1007/s10450-011-9322-x

Verma, G., & Mishra, M. (2018). Development and optimization of UV-Vis spectroscopy-a review. *World J. Pharm. Res*, *7*(11), 1170-1180. https://doi.org/10.20959/wjpr201811-12333

Vincenzi, S., Polesani, M., & Curioni, A. (2005). Removal of specific protein components by chitin enhances protein stability in a white wine. *American Journal of Enology and Viticulture*, *56*(3), 246-254.

Visioli, F., Panaite, S.-A., & Tomé-Carneiro, J. (2020). Wine's phenolic compounds and health: A pythagorean view. *Molecules*, *25*(18), 4105. https://doi.org/https://doi.org/10.3390/molecules25184105

Vladár, A. E. (2015). Strategies for scanning electron microscopy sample preparation and characterization of multiwall carbon nanotube polymer composites. *NIST Special Publication*, *1200*, 17.

Wang, J., Chen, Z., & Chen, B. (2014). Adsorption of polycyclic aromatic hydrocarbons by graphene and graphene oxide nanosheets. *Environmental science & technology*, *48*(9), 4817-4825. https://doi.org/https://doi.org/10.1021/es405227u

Wang, W., Gong, Q., Chen, Z., Wang, W. D., Huang, Q., Song, S., Chen, J., & Wang, X. (2019). Adsorption and competition investigation of phenolic compounds on the solid-liquid interface of three-

dimensional foam-like graphene oxide. *Chemical Engineering Journal*, *378*, 122085. https://doi.org/https://doi.org/10.1016/j.cej.2019.122085

Wang, Z., Zhuang, J., Wang, X., Li, Z., Fu, Y., & Qin, M. (2016). Limited adsorption selectivity of active carbon toward non-saccharide compounds in lignocellulose hydrolysate. *Bioresource technology*, *208*, 195-199. https://doi.org/https://doi.org/10.1016/j.biortech.2016.02.072

Waterhouse, A. L. (2002). Wine phenolics. *Annals of the New York Academy of Sciences*, *957*(1), 21-36. https://doi.org/https://doi.org/10.1111/j.1749-6632.2002.tb02903.x

Waterhouse, A. L., Sacks, G. L., & Jeffery, D. W. (2024). *Understanding wine chemistry*. John Wiley & Sons.

Waters, E. J., Alexander, G., Muhlack, R., Pocock, K., Colby, C., O'neill, B., Høj, P., & Jones, P. (2005). Preventing protein haze in bottled white wine. *Australian Journal of Grape and Wine Research*, *11*(2), 215-225. https://doi.org/https://doi.org/10.1111/j.1755-0238.2005.tb00289.x

Wu, S. H., & Pendleton, P. (2001). Adsorption of anionic surfactant by activated carbon: effect of surface chemistry, ionic strength, and hydrophobicity. *Journal of colloid and interface science*, *243*(2), 306-315. https://doi.org/https://doi.org/10.1006/jcis.2001.7905

Wu, Y., Zhang, X., Liu, C., Tian, L., Zhang, Y., Zhu, M., Qiao, W., Wu, J., Yan, S., & Zhang, H. (2024). Adsorption behaviors and mechanism of phenol and catechol in wastewater by magnetic graphene oxides: A comprehensive study based on adsorption experiments, mathematical models, and molecular simulations. *ACS omega*, *9*(13), 15101-15113. https://doi.org/https://doi.org/10.1021/acsomega.3c09346

Yaghoubi, A., & Ramazani, A. (2018). Synthesis of amino-functionalized carbon nanotubes and their applications. *Current Organic Chemistry*, *22*(15), 1505-1522. https://doi.org/https://doi.org/10.2174/1385272822666180731143454

Zhao, X., Duan, C.-Q., Li, S.-Y., Zhang, X.-K., Zhai, H.-Y., He, F., & Zhao, Y.-P. (2023). Non-enzymatic browning of wine induced by monomeric flavan-3-ols: A review. *Food chemistry*, *425*, 136420. https://doi.org/https://doi.org/10.1016/j.foodchem.2023.136420

APPENDICES

Appendix 1: Thaumatin standard curve plotted with peak area against thaumatin concentration (mg/L). This standard curve equation was used to determine each protein concentration (mg/L) in CHA, before and after treatments.

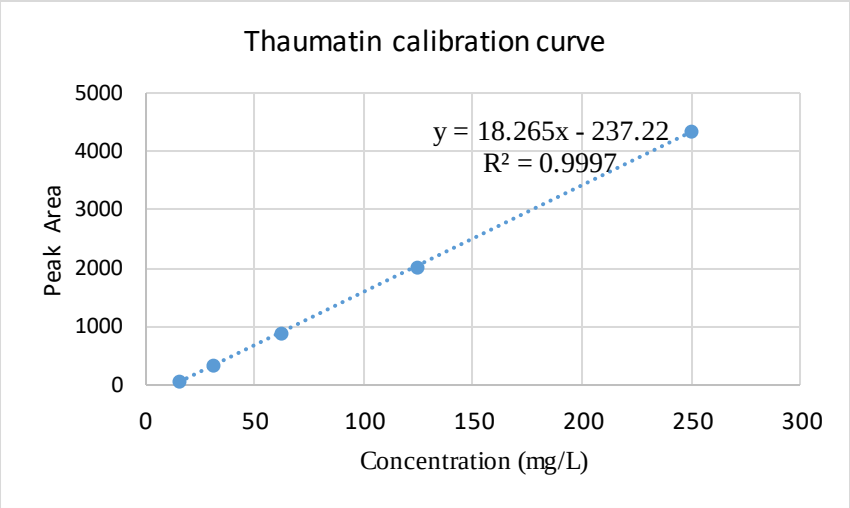

Appendix 2: Retention time and detection wavelength (nm) of phenolic compounds identified in REI and CHA.

Phenolic Compound	wavelength (nm)	Retention time
Gallic acid	280	2.1
Tyrosol	280	10.2
Coeluting GRP	320	11.7
Caftaric acid	320	8.4
Caffeic acid	320	16
Fertaric acid	320	19.2
Ferulic acid	320	24.8
Quercetin 3 glucoside	370	24.95

Appendix 3: Phenolic compounds standard curves plotted with peak area (PA) against concentration (mg/L). This standard curve equation was used to determine each phenolic concentration (mg/L) in REI and CHA, before and after treatments.

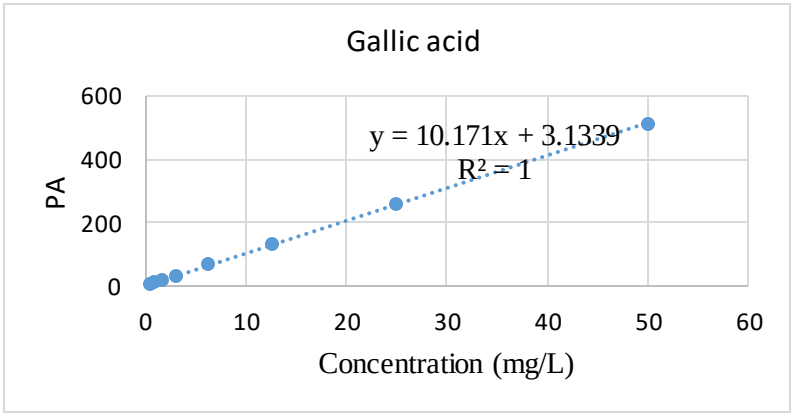

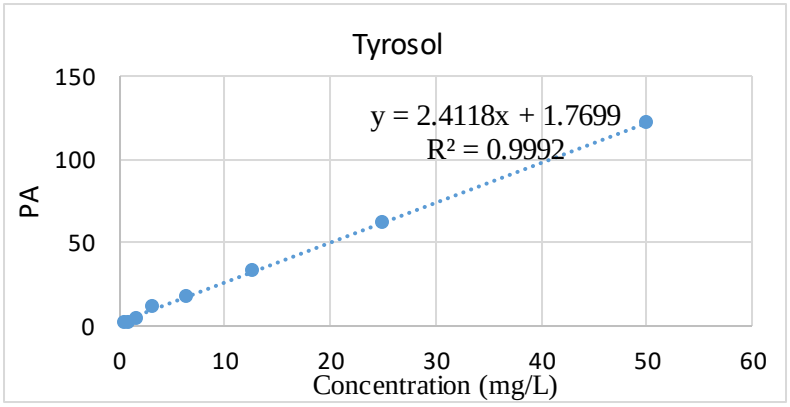

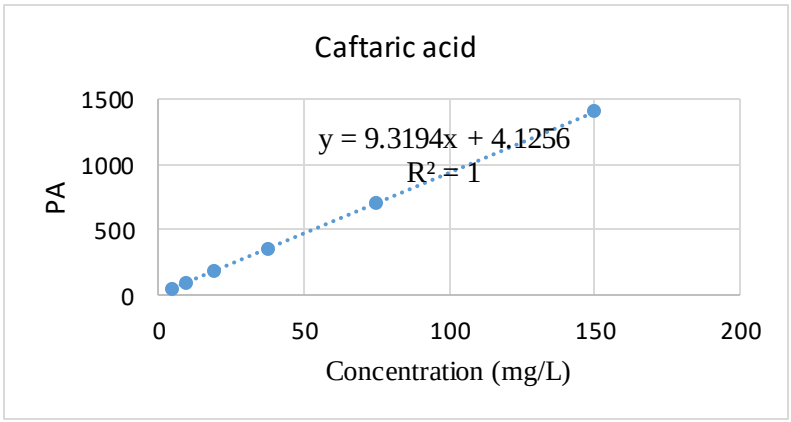

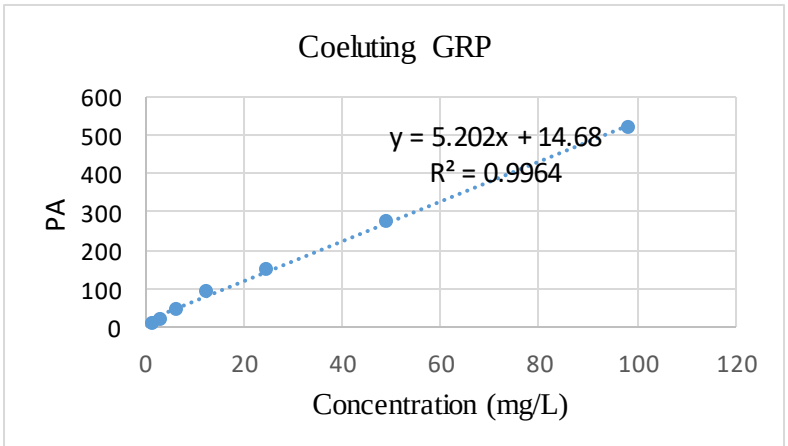

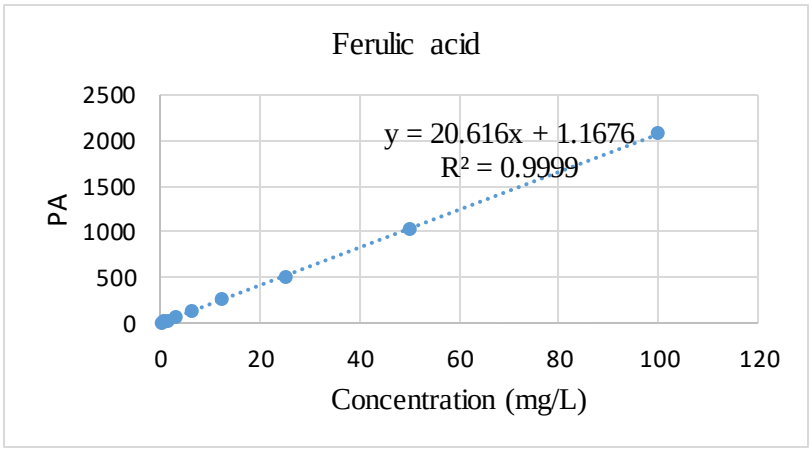
Ferulic acid
y = 20.616x + 1.1676
R² = 0.9999
PA
Concentration (mg/L)
2500
2000
1500
1000
500
0
0
20
40
60
80
100
120

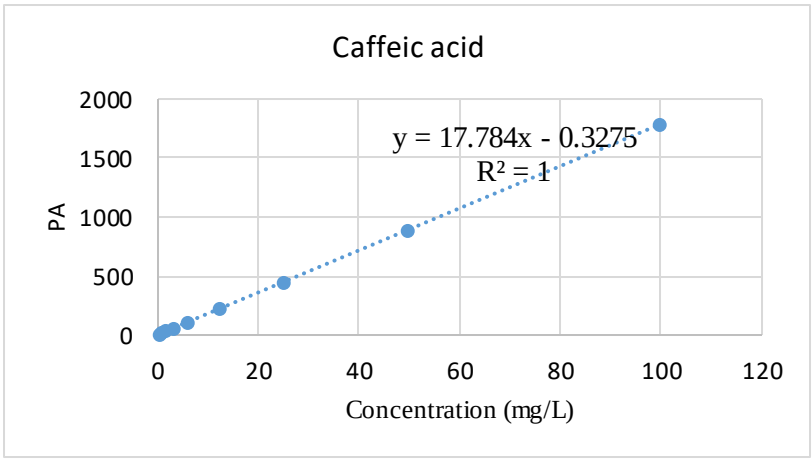
Caffeic acid
y = 17.784x - 0.3275
R² = 1
PA
Concentration (mg/L)
2000
1500
1000
500
0
0
20
40
60
80
100
120

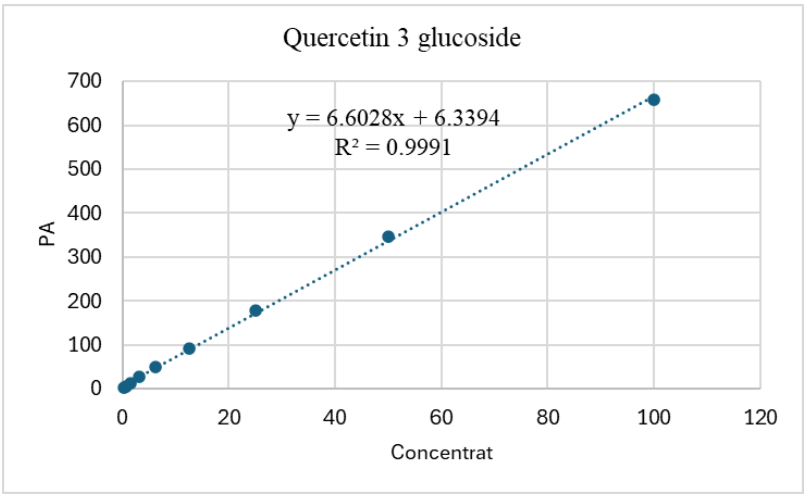
Quercetin 3 glucoside
y = 6.6028x + 6.3394
R² = 0.9991
PA
Concentrat
700
600
500
400
300
200
100
0
0
20
40
60
80
100
120

Appendix 4: HPLC Determination of the Phenolic Compounds in Riesling Wine Treated with Various Fining Agents

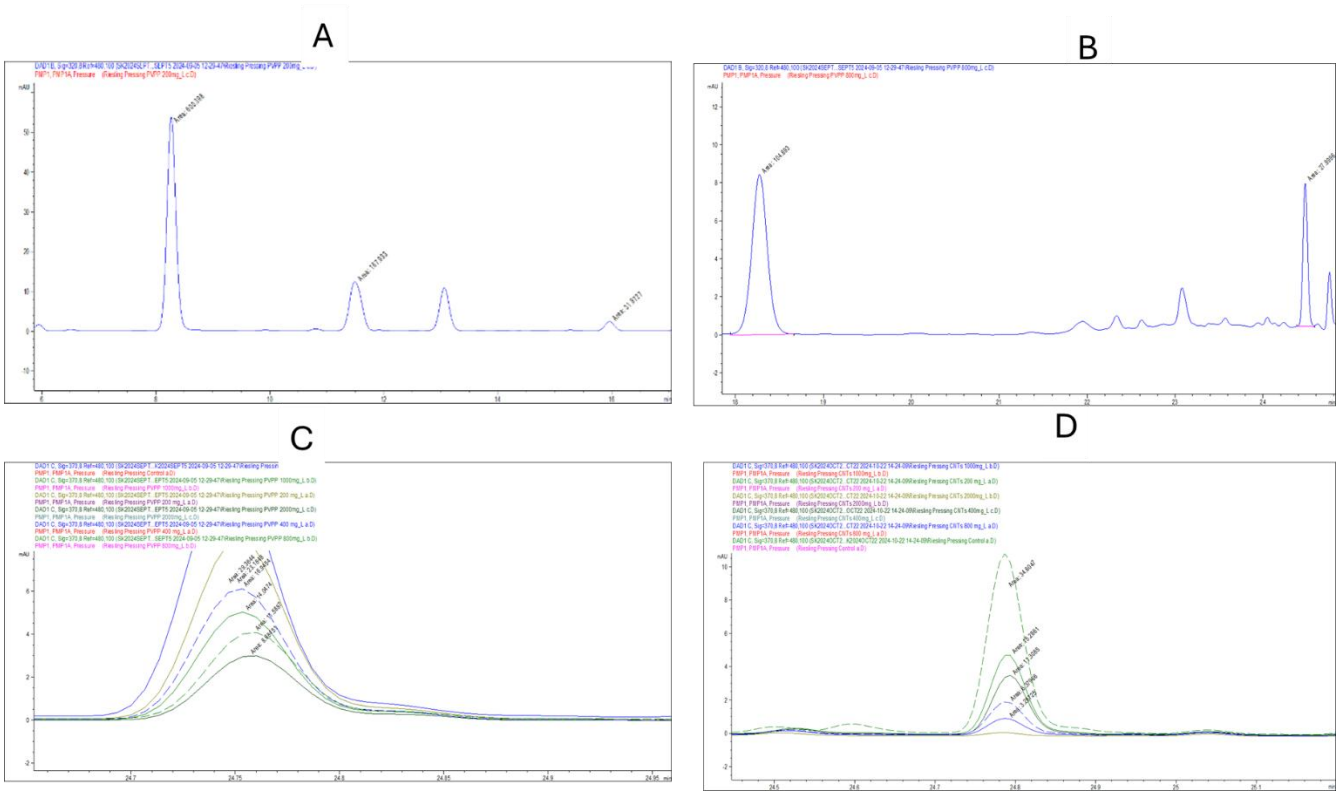

A- HPLC chromatogram of Riesling wine treated with 200 mg/L PVPP, indicating the separation of phenolic acids at the wavelength of 320 nm. Major peaks are identified as caftaric acid (retention time, 8.4 min), GRP (retention time, 11.7 min), and caffeic acid (retention time, 16 min). B- HPLC chromatogram of Riesling wine treated with 800 mg/L PVPP, analyzed at a wavelength of 320 nm, indicating fertaric acid (retention time, 18.5 min) and ferulic acid (retention time, 24.5 min) peaks. C - Overlay of HPLC chromatograms indicating the effect of five different concentrations of PVPP on quercetin-3-glucoside peak area detected with a wavelength of 370 nm. D - Overlay of HPLC chromatograms indicating the effect of five different concentrations of carbon nanotube (CNTs) on quercetin-3-glucoside peak area detected with a wavelength of 370 nm.

Appendix 5: The comparison of the interaction of treatment and concentration on Absorbance of RIE and CHA

General Linear Model: Absorbance_of RIE versus Concentration_Rie, Treatment_Rie

```
Method

Factor coding  (-1, 0, +1)


Factor Information

Factor             Type   Levels  Values
Concentration_Rie  Fixed       2  400, 800
Treatment_Rie      Fixed       8  AC, CNTs, Control, COOH-CNTs, G, NH2-CNTs, OH-CNTs,
PVPP


Analysis of Variance

Source                              DF   Adj SS    Adj MS  F-Value  P-Value
  Concentration_Rie                  1  0.20130  0.201297    28.89    0.000
  Treatment_Rie                      7  1.29741  0.185345    26.60    0.000
  Concentration_Rie*Treatment_Rie    7  0.09913  0.014161     2.03    0.114
Error                               16  0.11148  0.006968
Total                               31  1.70932


Model Summary

        S    R-sq  R-sq(adj)  R-sq(pred)
0.0834720  93.48%     87.36%      73.91%
```

General Linear Model: Absorbance_CHA versus Concentrationcha, Treatment_cha

```
Method

Factor coding  (-1, 0, +1)


Factor Information

Factor            Type   Levels  Values
Concentrationcha  Fixed       2  400, 800
Treatment_cha     Fixed       8  AC, CNTs, Control, COOH-CNTs, G, NH2-CNTs, OH-CNTs,
PVPP


Analysis of Variance

Source                              DF   Adj SS    Adj MS  F-Value  P-Value
  Concentrationcha                   1  0.19180  0.191798   103.25    0.000
  Treatment_cha                      7  1.99885  0.285551   153.71    0.000
  Concentrationcha*Treatment_cha     7  0.14005  0.020007    10.77    0.000
Error                               32  0.05945  0.001858
Total                               47  2.39015


Model Summary

        S    R-sq  R-sq(adj)  R-sq(pred)
0.0431007  97.51%     96.35%      94.40%
```

Appendix 6: Comparisons of the Absorbance of RIE

Tukey Pairwise Comparisons: Response = Absorbance_Rie, Term = Treatment_Rie

```
Grouping Information Using the Tukey Method and 95% Confidence

Treatment_Rie  N     Mean   Grouping
Control        4  2.05178  A
COOH-CNTs      4  1.99998  A
OH-CNTs        4  1.95481  A
NH2-CNTs       4  1.90727  A  B
CNTs           4  1.88873  A  B
PVPP           4  1.71588     B  C
G              4  1.55875        C  D
AC             4  1.46126           D

Means that do not share a letter are significantly different.
```

Appendix 7: Comparisons of the Absorbance of CHA

Tukey Pairwise Comparisons: Response = Absorbance_CHA, Term = Treatment_CHA

```
Grouping Information Using the Tukey Method and 95% Confidence

Treatment_cha  N     Mean   Grouping
Control        6  2.32605  A
COOH-CNTs      6  2.18918     B
NH2-CNTs       6  2.16653     B
OH-CNTs        6  2.16265     B
PVPP           6  2.13292     B
CNTs           6  2.01797        C
G              6  1.76839           D
AC             6  1.69708           D

Means that do not share a letter are significantly different.
```

Appendix 8: Comparisons of the Total protein concentrate (mg/L), of CHA

Tukey Pairwise Comparisons: Response = Protein concentrate (mg/l), Term = Tretment

```
Grouping Information Using the Tukey Method and 95% Confidence

Tretment     N     Mean   Grouping
control      9  23.6619  A
PVPP         9  23.1636  A
AC           9  13.1399     B
COOH- CNTs   9   6.3124        C
CNTs         9   5.9711        C  D
OH-CNTs      9   5.8519        C  D
NH2 CNTs     9   5.6565        C  D
G            9   5.4883           D

Means that do not share a letter are significantly different.
```

Appendix 9: Percentages of phenolic compounds reduced in Riesling wine treated with PVPP, graphene, activated carbon, CNTs, OH-CNTs, COOH-CNTs, and NH_2-CNTs with different concentration

Reduction percentage of phenols of Riesling

Concenatrete (mg/L)	Treatment (%)	Gallic acid (%)	Tyrosol (%)	Caftaric (%)	Coeluting GRP (%)
200	AC	0.00±0.00	5.62±0.30	2.69±0.36	2.87±0.37
	CNTs	5.67±0.40	3.89±1.96	3.16±0.25	3.52±0.45
	COOH-CNTs	2.07±0.15	11.67±0.61	2.28±0.22	5.39±0.26
	NH2-CNTs	8.88±0.75	11.83±1.12	1.76±0.42	0.47±0.36
	OH-CNTs	0.00±0.0	5.53±1.25	1.17±0.05	3.24±0.41
	G	1.13±0.34	5.46±2.02	3.01±0.27	2.72±0.20
	PVPP	10.93±4.03	22.37±1.62	5.29±0.36	1.67±0.12
400	AC	7.23±0.86	12.64±3.73	14.54±1.54	15.84±1.27
	CNTs	6.96±0.18	13.41±2.58	5.63±0.11	5.35±0.37
	COOH-CNTs	3.74±0.57	11.34±0.94	2.03±0.11	5.23±0.73
	NH2-CNTs	15.08±1.33	13.14±1.62	2.16±0.36	0.99±0.16
	OH-CNTs	1.17±0.04	2.67±1.90	3.06±0.16	3.67±1.54
	G	1.24±0.27	5.88±3.09	6.73±0.47	7.38±0.46
	PVPP	10.43±1.00	24.94±3.14	7.19±1.06	4.22±0.84
800	AC	17.75±0.73	17.50±1.45	32.79±2.20	33.59±2.88
	CNTs	4.89±0.35	9.62±2.49	8.44±0.15	13.59±0.32
	COOH-CNTs	5.10±0.19	12.41±2.97	2.90±0.11	7.08±0.83
	NH2-CNTs	10.34±1.53	13.14±1.62	5.01±0.37	5.15±0.22
	OH-CNTs	2.18±0.49	3.46±1.16	6.09±0.80	9.62±0.32
	G	3.87±0.20	13.37±3.38	14.52±0.23	17.43±0.42
	PVPP	12.27±1.19	32.33±0.94	18.40±1.86	8.43±1.15
1000	AC	25.22±0.28	24.29±2.58	45.24±0.62	43.47±0.71
	CNTs	5.96±0.22	10.96±1.16	10.44±0.05	16.11±0.31
	COOH-CNTs	4.11±0.39	14.21±1.17	3.80±0.03	8.08±0.16
	NH2-CNTs	17.77±4.54	16.68±1.73	6.74±0.37	7.64±0.22
	OH-CNTs	3.83±0.02	11.47±1.08	5.46±0.05	14.34±0.03
	G	5.64±0.37	19.68±3.34	20.32±0.51	23.90±0.24
	PVPP	17.28±0.45	32.82±1.02	15.70±0.87	7.22±0.83
2000	AC	48.60±3.12	50.46±3.93	73.95±2.68	67.85±2.25
	CNTs	11.80±1.27	20.40±0.75	20.52±0.56	24.40±1.17
	COOH-CNTs	7.11±0.15	22.30±2.67	8.15±0.44	14.49±0.89
	NH2-CNTs	24.68±0.11	16.42±3.97	17.16±0.28	17.91±0.49
	OH-CNTs	11.26±0.22	10.11±2.88	12.38±0.18	17.72±0.07
	G	14.50±0.09	41.88±2.29	49.25±0.54	50.31±0.27
	PVPP	27.55±0.92	34.53±0.81	27.58±1.57	14.37±0.59

Results are expressed as mean ± standard deviation

Appendix 10: Percentages of phenolic compounds reduction in Riesling wine treated with PVPP, graphene, activated carbon, CNTs, OH-CNTs, COOH-CNTs, and NH_2-CNTs with different concentration.

Reduction the percentage of phenols of Riesling

Con. (mg/L)	Treatment (%)	Caffeic acid (%)	Fertaric (%)	Ferulic (%)	Quercetin 3 glu. (%)
200	AC	22.98±0.21	10.03±0.55	43.62±2.91	75.41±2.6
	CNTs	15.69±0.26	8.88±0.59	15.18±0.44	50.99±1.74
	COOH-CNTs	10.08±0.15	5.80±0.82	10.17±0.43	42.92±0.54
	NH2-CNTs	4.52±0.21	1.78±0.69	8.13±1.36	56.30±2.98
	OH-CNTs	19.43±0.24	4.32±0.34	13.07±0.65	61.86±3.42
	G	30.22±0.11	5.86±0.48	43.17±5.42	81.85±3.37
	PVPP	16.05±0.07	3.15±0.40	1.55±0.35	25.88±1.43
400	AC	45.89±0.74	26.71±1.57	68.3±1.55	91.71±0.55
	CNTs	19.46±0.22	12.76±0.19	20.39±0.66	60.39±2.92
	COOH-CNTs	14.15±0.42	5.10±1.39	14.23±1.28	61.56±3.11
	NH2-CNTs	10.34±0.09	3.26±0.14	13.45±1.01	70.29±4.94
	OH-CNTs	29.44±0.89	6.65±0.90	22.84±1.08	84.57±1.21
	G	46.88±0.27	16.33±1.30	70.76±0.98	91.83±0.74
	PVPP	23.02±0.48	4.62±0.61	3.55±1.17	35.34±5.61
800	AC	65.77±1.66	56.24±4.24	90.18±3.23	100.0±0.0
	CNTs	22.43±0.19	17.90±0.50	30.58±0.30	79.80±0.84
	COOH-CNTs	18.09±0.48	6.21±0.12	21.94±0.17	80.35±1.66
	NH2-CNTs	20.49±0.13	9.72±0.23	31.44±1.43	89.24±1.44
	OH-CNTs	33.51±0.19	11.18±0.04	40.32±0.49	93.58±0.27
	G	69.78±0.24	32.21±0.27	94.49±0.28	100.0±0.0
	PVPP	30.72±0.66	12.77±1.94	14.38±2.14	57.35±4.56
1000	AC	73.13±0.41	70.63±1.01	96.34±0.10	100.0±0.0
	CNTs	27.15±0.18	22.51±0.63	38.62±0.20	87.01±0.43
	COOH-CNTs	28.45±0.09	8.04±0.26	29.18±0.22	89.34±0.67
	NH2-CNTs	25.83±0.13	13.05±0.19	40.18±2.41	92.10±0.9
	OH-CNTs	41.00±0.02	14.15±0.11	47.89±1.28	100.0±0.0
	G	76.35±0.14	41.05±0.33	99.91±0.09	100.0±0.0
	PVPP	30.04±0.48	12.47±1.18	11.73±1.08	54.47±2.32
2000	AC	100.00±1.30	98.00±2.00	100.0±0.0	100.0±0.0
	CNTs	45.40±0.67	36.61±0.57	58.54±0.48	100.0±0.0
	COOH-CNTs	36.97±0.51	13.78±2.73	44.83±1.84	100.0±0.0
	NH2-CNTs	43.34±0.28	30.66±0.44	67.63±0.89	100.0±0.0
	OH-CNTs	63.32±0.04	30.09±0.18	72.53±1.82	100.0±0.0
	G	100.00±0.16	80.20±0.72	100.00±0.0	100.0±0.0
	PVPP	47.41±0.34	17.33±0.75	21.43±2.05	72.70±2.55

Results are expressed as mean ± standard deviation

Appendix 11- Percentages of phenolic compounds reduction in Chardonnay wine treated with PVPP, graphene, activated carbon, CNTs, OH-CNTs, COOH-CNTs, and NH_2-CNTs with different concentration

Reduction percentage of phenols of Chardonnay

Con. (mg/L)	Treatment	Tyrosol (%)	Caftaric (%)	Co.GRP (%)	Caffeic (%)	Fertaric (%)	Querc. 3 glu (%)
200	AC	2.97±1.38	2.80±0.96	5.00±0.23	20.85±2.19	9.50±1.31	63.41±4.70
	CNTs	7.54±3.80	9.27±0.56	5.76±0.12	9.25±1.49	6.57±0.64	45.52±3.88
	COOH-CNTs	3.05±2.31	4.12±0.10	0.36±0.19	11.59±0.71	0.90±0.39	40.54±1.09
	NH2-CNTs	9.53±2.24	1.15±0.15	1.33±0.09	15.02±0.62	3.69±0.86	46.54±0.34
	OH-CNTs	5.75±2.94	6.86±2.80	1.11±0.14	7.34±1.28	2.39±0.37	44.78±4.73
	G	12.74±1.87	1.46±0.78	1.07±1.07	22.62±5.22	7.86±0.93	67.49±1.46
	PVPP	4.59±2.21	4.38±1.40	0.26±0.26	4.96±0.26	1.23±0.85	13.00±1.56
400	AC	4.14±4.05	8.74±0.77	12.82±0.48	35.79±0.75	31.38±0.55	82.70±0.31
	CNTs	6.54±6.13	12.17±0.28	8.43±0.08	15.93±1.24	12.70±0.23	72.75±3.18
	COOH-CNTs	4.15±2.21	4.69±0.57	0.28±0.19	13.58±0.65	0.58±0.53	56.46±1.74
	NH2-CNTs	11.93±1.63	3.96±0.15	4.59±0.65	20.13±0.55	7.20±0.26	78.29±2.26
	OH-CNTs	7.24±1.77	7.28±1.01	4.01±0.12	10.94±1.70	8.51±1.18	68.21±2.12
	G	14.06±1.18	5.52±1.09	3.31±0.86	34.66±0.32	13.34±1.29	90.18±2.07
	PVPP	4.59±2.10	3.22±1.62	2.16±0.39	8.33±1.24	8.55±2.39	20.57±4.40
800	AC	9.75±1.84	25.16±2.17	26.33±1.84	58.09±0.59	62.81±2.76	96.15±0.14
	CNTs	9.55±5.48	14.79±0.50	14.12±0.33	27.08±1.18	25.03±0.22	90.23±1.02
	COOH-CNTs	2.89±1.83	6.14±0.95	2.67±0.42	19.41±0.25	5.07±0.97	84.60±0.94
	NH2-CNTs	13.21±1.36	5.41±0.28	9.54±1.08	30.72±0.80	16.75±2.00	91.55±0.08
	OH-CNTs	14.10±5.07	9.89±1.30	6.68±1.52	22.25±1.55	14.17±5.20	91.17±1.01
	G	18.45±2.61	12.45±0.15	14.75±1.33	61.30±1.00	34.88±0.41	100.00±0.0
	PVPP	7.49±3.75	11.43±0.27	0.83±0.15	14.18±0.59	3.20±0.73	35.87±1.26
1000	AC	21.46±5.17	34.31±0.38	33.11±1.22	64.05±0.68	77.15±2.08	100.00±0.0
	CNTs	12.91±3.27	16.23±1.02	18.42±0.76	33.91±1.16	32.83±2.07	94.36±0.51
	COOH-CNTs	4.34±4.12	5.75±0.67	4.43±0.08	21.37±1.34	8.06±2.14	87.93±1.46
	NH2-CNTs	10.31±1.46	6.46±0.93	10.72±0.51	34.83±0.87	19.59±1.97	94.69±0.25
	OH-CNTs	11.70±3.13	11.12±0.69	8.08±0.56	31.68±0.57	14.97±2.88	94.65±0.47
	G	31.91±3.76	17.18±0.47	21.87±1.58	66.31±0.71	39.53±1.34	100.00±0.0
	PVPP	17.19±1.86	12.02±0.24	0.87±0.39	21.71±1.40	5.37±0.34	38.99±1.65
2000	AC	43.67±2.92	63.00±0.41	60.41±0.32	76.15±0.66	100.00±0.0	100.00±0.0
	CNTs	17.98±2.00	28.15±0.66	31.90±0.27	54.10±1.33	59.74±1.0	100.00±0.0
	COOH-CNTs	5.78±2.28	6.74±0.51	9.08±0.46	32.14±1.89	16.66±0.95	93.87±0.45
	NH2-CNTs	10.42±3.41	12.93±0.85	24.72±0.41	73.66±11.02	42.19±1.20	100.00±0.0
	OH-CNTs	13.82±4.07	14.77±1.01	20.11±0.08	50.50±0.70	32.15±0.83	100.00±0.0
	G	39.32±8.63	42.77±1.15	47.03±2.35	78.21±0.85	89.81±4.50	100.00±0.0
	PVPP	14.91±3.34	19.05±0.57	4.69±0.29	39.70±1.18	13.67±0.23	67.85±1.71

Appendix 12: The comparison of the interaction of treatment and concentration on Tyrosol reduction percentage of RIE and CHA

General Linear Model: Tyrosol reduced% of RIE versus Treatment, and Concentration mg/l

```
Method

Factor coding  (-1, 0, +1)


Factor Information

Factor              Type   Levels  Values
Treatment           Fixed       7  AC, CNTs, CNTs-COOH, CNTs-NH3, CNTs-OH, Graphene,
PVPP
Concentration mg/l  Fixed       5  200, 400, 800, 1000, 2000


Analysis of Variance

Source                            DF  Adj SS   Adj MS  F-Value  P-Value
  Treatment                        6    4925   820.85    41.77    0.000
  Concentration mg/l               4    4414  1103.61    56.16    0.000
  Treatment*Concentration mg/l    24    3122   130.07     6.62    0.000
Error                             70    1376    19.65
Total                            104   13837


Model Summary

      S    R-sq  R-sq(adj)  R-sq(pred)
4.43306  90.06%     85.23%      77.63%
```

General Linear Model: Tyrosol reduced% of CHA versus Treatment, Concentration mg/l

```
Method

Factor coding  (-1, 0, +1)


Factor Information

Factor              Type   Levels  Values
Treatment           Fixed       7  AC, CNTs, CNTs-COOH, CNTs-NH2, CNTs-OH, Graphene,
PVPP
Concentration mg/l  Fixed       5  200, 400, 800, 1000, 2000


Analysis of Variance

Source                            DF  Adj SS  Adj MS  F-Value  P-Value
  Treatment                        6    3285  547.50    15.16    0.000
  Concentration mg/l               4    2984  746.04    20.66    0.000
  Treatment*Concentration mg/l    24    2998  124.93     3.46    0.000
Error                             70    2528   36.11
Total                            104   11795


Model Summary

      S    R-sq  R-sq(adj)  R-sq(pred)
```

```
6.00930  78.57%     68.16%      51.78%
```

Appendix 13: Comparisons of the Tyrosol reduction percentage of RIE

Tukey Pairwise Comparisons: Response = Tyrosol Riesling, Term = Treatment

```
Grouping Information Using the Tukey Method and 95% Confidence

Treatment   N     Mean     Grouping
PVPP       15  29.3973  A
AC         15  22.1006     B
Graphene   15  17.2548     B  C
CNTs-COOH  15  14.3875        C  D
CNTs-NH3   15  14.2403        C  D
CNTs       15  11.6562           D
CNTs-OH    15   6.6493              E

Means that do not share a letter are significantly different.
```

Appendix 14: Comparisons of the Tyrosol reduction percentage of CHA

Tukey Pairwise Comparisons: Response = Tyrosol Reduced %, Term = Treatment

```
Grouping Information Using the Tukey Method and 95% Confidence

Treatment   N     Mean  Grouping
Graphene   15  23.2957  A
AC         15  16.3998     B
CNTs-NH3   15  11.0790     B
CNTs       15  10.9043     B
CNTs-OH    15  10.5218     B  C
PVPP       15   9.7573     B  C
CNTs-COOH  15   4.0404        C

Means that do not share a letter are significantly different.
```

Appendix 15: The comparison of the interaction of treatment and concentration on Caftaric reduction percentage of RIE and CHA

General Linear Model: Caftaric reduced% of RIE versus Treatment, Concentration mg/L

```
Method

Factor coding  (-1, 0, +1)


Factor Information

Factor              Type   Levels  Values
Treatment           Fixed       7  AC, CNTs, CNTs-COOH, CNTs-NH3, CNTs-OH, Graphene,
PVPP
Concentration mg/l  Fixed       5  200, 400, 800, 1000, 2000


Analysis of Variance

Source                          DF   Adj SS   Adj MS  F-Value  P-Value
  Treatment                      6   9922.2  1653.70   748.57    0.000
```

```
  Concentration mg/l              4   9336.4  2334.11  1056.56    0.000
  Treatment*Concentration mg/l   24   6215.7   258.99   117.23    0.000
Error                            70    154.6     2.21
Total                           104  25629.0
```

```
Model Summary

      S    R-sq  R-sq(adj)  R-sq(pred)
1.48632  99.40%     99.10%      98.64
```

General Linear Model: Caftaric reduced% of CHA versus Treatment, Concentration mg/L

```
Method

Factor coding  (-1, 0, +1)


Factor Information

Factor              Type   Levels  Values
Treatment           Fixed       7  AC, CNTs, CNTs-COOH, CNTs-NH3, CNTs-OH, Graphene,
PVPP
Concentration mg/l  Fixed       5  200, 400, 800, 1000, 2000


Analysis of Variance

Source                           DF   Adj SS   Adj MS  F-Value  P-Value
  Treatment                       6   4981.6   830.27   296.10    0.000
  Concentration mg/l              4   6535.8  1633.96   582.72    0.000
  Treatment*Concentration mg/l   24   4924.8   205.20    73.18    0.000
Error                            70    196.3     2.80
Total                           104  16638.5


Model Summary

      S    R-sq  R-sq(adj)  R-sq(pred)
1.67452  98.82%     98.25%      97.35%
```

Appendix 16: Comparisons of the Caftaric acid reduction percentage of RIE

Tukey Pairwise Comparisons: Response = Caftaric Reduced % of RIE, Term = Treatment

```
Grouping Information Using the Tukey Method and 95% Confidence

Treatment   N     Mean      Grouping
AC         15  33.8441  A
Graphene   15  18.7670     B
PVPP       15  14.8344        C
CNTs       15   9.6393           D
CNTs-NH2   15   6.5662              E
CNTs-OH    15   5.6323              E
CNTs-COOH  15   3.8320                 F

Means that do not share a letter are significantly different.
```

Appendix 17: Comparisons of the Caftaric acid reduction percentage of CHA

Tukey Pairwise Comparisons: Response = Caftaric acid Reduced %, of CHA Term = Treatment

```
Grouping Information Using the Tukey Method and 95% Confidence

Treatment   N     Mean   Grouping
AC         15  26.8020  A
CNTs       15  16.1218     B
Graphene   15  15.8766     B
PVPP       15  10.0209        C
CNTs-OH    15   9.9828        C
CNTs-NH2   15   5.9804           D
CNTs-COOH  15   5.4892           D

Means that do not share a letter are significantly different.
```

Appendix 18: The comparison of the interaction of treatment and concentration on Coeluting GRP reduction percentage of RIE and CHA

General Linear Model: Coeluting GRP Reduced % of RIE versus Treatment, Concentration mg/L

```
Method

Factor coding  (-1, 0, +1)


Factor Information

Factor              Type   Levels  Values
Treatment           Fixed       7  AC, CNTs, CNTs-COOH, CNTs-NH3, CNTs-OH, Graphene,
PVPP
Concentration mg/l  Fixed       5  200, 400, 800, 1000, 2000


Analysis of Variance

Source                           DF   Adj SS   Adj MS  F-Value  P-Value
  Treatment                       6   8251.9  1375.32   607.77    0.000
  Concentration mg/l              4   9248.4  2312.10  1021.75    0.000
  Treatment*Concentration mg/l   24   4928.9   205.37    90.76    0.000
Error                            70    158.4     2.26
Total                           104  22587.6


Model Summary

      S    R-sq  R-sq(adj)  R-sq(pred)
1.50429  99.30%     98.96%      98.42%
```

General Linear Model: Coeluting GRP Reduction % of CHA versus Treatment, Concentration mg/l

```
Method

Factor coding  (-1, 0, +1)


Factor Information

Factor              Type   Levels  Values
Treatment           Fixed       7  AC, CNTs, CNTs-COOH, CNTs-NH3, CNTs-OH, Graphene,
PVPP
Concentration mg/l  Fixed       5  200, 400, 800, 1000, 2000


Analysis of Variance

Source                           DF   Adj SS   Adj MS  F-Value  P-Value
  Treatment                       6   7278.0  1213.00   607.40    0.000
  Concentration mg/l              4   8728.2  2182.05  1092.64    0.000
  Treatment*Concentration mg/l   24   3962.4   165.10    82.67    0.000
Error                            70    139.8     2.00
Total                           104  20108.4


Model Summary

      S    R-sq  R-sq(adj)  R-sq(pred)
1.41317  99.30%     98.97%      98.44%
```

Appendix 19: Comparisons of the Coeluting GRP reduction percentage of RIE

Tukey Pairwise Comparisons: Response = Coeluting GRP Reduced %, RIE, Term = Treatment

```
Grouping Information Using the Tukey Method and 95% Confidence

Treatment   N     Mean     Grouping
AC         15  32.7226  A
Graphene   15  20.3473     B
CNTs       15  12.5929        C
CNTs-OH    15   9.7180           D
CNTs-COOH  15   8.0558           D  E
PVPP       15   7.1817              E
CNTs-NH3   15   6.4308              E

Means that do not share a letter are significantly different.
```

Appendix 20: Comparisons of the Coeluting GRP reducing percentage of CHA

Tukey Pairwise Comparisons: Response = Coeluting GRP reduction %, Term = Treatment

```
Grouping Information Using the Tukey Method and 95% Confidence

Treatment   N     Mean        Grouping
```

```
AC         15  27.5325  A
Graphene   15  17.6050     B
CNTs       15  15.7241        C
CNTs-NH2   15  10.1807           D
CNTs-OH    15   7.9998              E
CNTs-COOH  15   3.3634                 F
PVPP       15   1.7648                    G

Means that do not share a letter are significantly different.
```

Appendix 21: The comparison of the interaction of treatment and concentration on Caffeic acid reduction percentage of RIE and CHA

General Linear Model: Caffeic acid reduction % RIE versus Treatment, Concentration mg/l

```
Method

Factor coding  (-1, 0, +1)


Factor Information

Factor              Type   Levels  Values
Treatment           Fixed       7  AC, CNTs, CNTs-COOH, CNTs-NH3, CNTs-OH, Graphene,
PVPP
Concentration mg/l  Fixed       5  200, 400, 800, 1000, 2000


Analysis of Variance

Source                           DF   Adj SS   Adj MS  F-Value  P-Value
  Treatment                       6  30627.2  5104.54   601.95    0.000
  Concentration mg/l              4  24767.2  6191.80   730.17    0.000
  Treatment*Concentration mg/l   24   4753.9   198.08    23.36    0.000
Error                            70    593.6     8.48
Total                           104  60742.0


Model Summary

      S    R-sq  R-sq(adj)  R-sq(pred)
2.91204  99.02%     98.55%      97.80%
```

Appendix 22: Comparisons of the Caffeic acid reduction percentage of RIE

Tukey Pairwise Comparisons: Response = Caffeic acid reducing% of RIE, Term = Treatment

```
Grouping Information Using the Tukey Method and 95% Confidence

Treatment   N     Mean     Grouping
Graphene   15  64.6471  A
AC         15  61.5548  A
CNTs-OH    15  37.3407     B
```

```
PVPP       15  29.4485        C
CNTs       15  26.0256           D
CNTs-COOH  15  21.5479              E
CNTs-NH3   15  20.9053              E

Means that do not share a letter are significantly different.
```

Appendix 23: Comparisons of the Caffeic acid reduction percentage of CHA

Tukey Pairwise Comparisons: Response = Caffeic acid Reduced % of CHA, Tea Treatment

```
Grouping Information Using the Tukey Method and 95% Confidence

Treatment   N     Mean   Grouping
Graphene   15  52.6204  A
AC         15  50.9853  A
CNTs-NH3   15  34.8719     B
CNTs       15  28.0552        C
CNTs-OH    15  24.5409        C
CNTs-COOH  15  19.6197           D
PVPP       15  17.7759           D

Means that do not share a letter are significantly different.
```

Appendix 24: The comparison of the interaction of treatment and concentration on Fertaric acid reduction percentage of RIE and CHA

General Linear Model: : Fertaric Reduced % of RIE versus Treatment, Concentration mg/l

```
Method

Factor coding  (-1, 0, +1)


Factor Information

Factor              Type   Levels  Values
Treatment           Fixed       7  AC, CNTs, CNTs-COOH, CNTs-NH3, CNTs-OH, Graphene,
PVPP
Concentration mg/l  Fixed       5  200, 400, 800, 1000, 2000


Analysis of Variance

Source                            DF   Adj SS   Adj MS  F-Value  P-Value
  Treatment                        6  24319.5  4053.24   986.02    0.000
  Concentration mg/l               4  18546.4  4636.59  1127.93    0.000
  Treatment*Concentration mg/l    24  10757.8   448.24   109.04    0.000
Error                             70    287.8     4.11
Total                            104  53911.4


Model Summary

      S    R-sq  R-sq(adj)  R-sq(pred)
2.02749  99.47%     99.21%      98.80%
```

General Linear Model: Fertaric Reduced % of CHA versus Treatment, Concentration mg/l

```
Method

Factor coding  (-1, 0, +1)


Factor Information

Factor              Type   Levels  Values
Treatment           Fixed       7  AC, CNTs, CNTs-COOH, CNTs-NH3, CNTs-OH, Graphene,
PVPP
Concentration mg/l  Fixed       5  200, 400, 800, 1000, 2000


Analysis of Variance

Source                           DF   Adj SS   Adj MS  F-Value  P-Value
  Treatment                       6  29548.7  4924.79   541.04    0.000
  Concentration mg/l              4  26300.2  6575.06   722.34    0.000
  Treatment*Concentration mg/l   24  12136.0   505.67    55.55    0.000
Error                            70    637.2     9.10
Total                           104  68622.1


Model Summary

      S    R-sq  R-sq(adj)  R-sq(pred)
3.01702  99.07%     98.62%      97.91%
```

Appendix 25: Comparisons of the Fertaric acid reduction percentage of RIE

Tukey Pairwise Comparisons: Response = = Fertaric Reduced %, Term = Treatment

```
Grouping Information Using the Tukey Method and 95% Confidence

Treatment   N     Mean      Grouping
AC         15  52.3217  A
Graphene   15  35.1296     B
CNTs       15  19.7292        C
CNTs-OH    15  13.2761           D
CNTs-NH3   15  11.6962           D  E
PVPP       15  10.0713              E
CNTs-COOH  15   7.7853                 F

Means that do not share a letter are significantly different.
```

Appendix 26: Comparisons of the Fertaric acid reduction percentage of CHA

Tukey Pairwise Comparisons: Response = Fertaric Reduced %, Term = Treatment

```
Grouping Information Using the Tukey Method and 95% Confidence

Treatment   N     Mean      Grouping
AC         15  56.1681  A
Graphene   15  37.0854     B
```

```
CNTs       15  27.3738        C
CNTs-NH3   15  17.8858           D
CNTs-OH    15  14.4369              E
PVPP       15   6.4059                 F
CNTs-COOH  15   6.2533
Means that do not share a letter are significantly different.
```

Appendix 27: The comparison of the interaction of treatment and concentration on Fertaric acid reduction percentage of RIE and CHA

General Linear Model: Quercetin 3 glucoside Reduced % of RIE versus Treatment, Concentration mg/l

```
Method

Factor coding  (-1, 0, +1)


Factor Information

Factor              Type   Levels  Values
Treatment           Fixed       7  AC, CNTs, CNTs-COOH, CNTs-NH3, CNTs-OH, Graphene,
PVPP
Concentration mg/l  Fixed       5  200, 400, 800, 1000, 2000


Analysis of Variance

Source                           DF   Adj SS   Adj MS  F-Value  P-Value
  Treatment                       6  21907.3  3651.22   265.83    0.000
  Concentration mg/l              4  21232.5  5308.12   386.45    0.000
  Treatment*Concentration mg/l   24   2874.7   119.78     8.72    0.000
Error                            70    961.5    13.74
Total                           104  46975.9


Model Summary

      S    R-sq  R-sq(adj)  R-sq(pred)
3.70613  97.95%     96.96%      95.39%
```

General Linear Model: Quercetin 3 glucoside reduction% of CHA versus Treatment, Concentration mg/l

```
Method

Factor coding  (-1, 0, +1)


Factor Information

Factor              Type   Levels  Values
Treatment           Fixed       7  AC, CNTs, CNTs-COOH, CNTs-NH3, CNTs-OH, Graphene,
PVPP
Concentration mg/l  Fixed       5  200, 400, 800, 1000, 2000
```

```
Analysis of Variance

Source                            DF   Adj SS   Adj MS  F-Value  P-Value
  Treatment                        6  32110.5  5351.75   480.24    0.000
  Concentration mg/l               4  31998.7  7999.68   717.86    0.000
  Treatment*Concentration mg/l    24   2815.6   117.31    10.53    0.000
Error                             70    780.1    11.14
Total                            104  67704.8


Model Summary

      S    R-sq  R-sq(adj)  R-sq(pred)
3.33824  98.85%     98.29%      97.41%
```

Appendix 28: Comparisons of the Quercetin 3 glucoside reduction percentage of RIE

Tukey Pairwise Comparisons: Response = Quercetin 3 glucoside Riesling, Term = Treatment

```
Grouping Information Using the Tukey Method and 95% Confidence

Treatment   N     Mean     Grouping
Graphene   15  94.7367  A
AC         15  93.4232  A
CNTs-OH    15  88.0018     B
CNTs-NH3   15  81.5849        C
CNTs       15  75.6372           D
CNTs-COOH  15  74.8332           D
PVPP       15  49.1478              E

Means that do not share a letter are significantly different.
```

Appendix 29: Comparisons of the Quercetin 3 glucoside reduction percentage of CHA

Tukey Pairwise Comparisons: Response = Quercetin 3 glucoside reduction %, of CHA Term = Treatment

```
Grouping Information Using the Tukey Method and 95% Confidence

Treatment   N     Mean   Grouping
Graphene   15  91.5335  A
AC         15  88.4511  A
CNTs-NH3   15  82.2125     B
CNTs       15  80.5729     B
CNTs-OH    15  79.7618     B
CNTs-COOH  15  72.6800        C
PVPP       15  35.2565           D

Means that do not share a letter are significantly different.
```

Appendix 30: The comparison of the interaction of treatment and concentration on Gallic and Ferulic acids reduction percentage of RIE

General Linear Model: Gallic acid reduction%, of RIE versus Treatment, Concentration mg/l

```
Method

Factor coding  (-1, 0, +1)


Factor Information

Factor              Type   Levels  Values
Treatment           Fixed       7  AC, CNTs, CNTs-COOH, CNTs-NH3, CNTs-OH, Graphene,
PVPP
Concentration mg/l  Fixed       5  200, 400, 800, 1000, 2000


Analysis of Variance

Source                           DF   Adj SS   Adj MS  F-Value  P-Value
  Treatment                       6   3868.6  644.765   126.77    0.000
  Concentration mg/l              4   3542.0  885.512   174.11    0.000
  Treatment*Concentration mg/l   24   2526.4  105.268    20.70    0.000
Error                            70    356.0    5.086
Total                           104  10293.1


Model Summary

      S    R-sq  R-sq(adj)  R-sq(pred)
2.25521  96.54%     94.86%      92.22%
```

General Linear Model: Ferulic reduction %, of RIE versus Treatment, Concentration mg/L

```
Method

Factor coding  (-1, 0, +1)


Factor Information

Factor              Type   Levels  Values
Treatment           Fixed       7  AC, CNTs, CNTs-COOH, CNTs-NH3, CNTs-OH, Graphene,
PVPP
Concentration mg/l  Fixed       5  200, 400, 800, 1000, 2000


Analysis of Variance

Source                           DF  Adj SS   Adj MS  F-Value  P-Value
  Treatment                       6   67373  11228.9  1493.26    0.000
  Concentration mg/l              4   28532   7133.1   948.59    0.000
  Treatment*Concentration mg/l   24    5175    215.6    28.68    0.000
Error                            70     526      7.5
Total                           104  101607


Model Summary

      S    R-sq  R-sq(adj)  R-sq(pred)
2.74221  99.48%     99.23%      98.83%
```

Appendix 31: Comparisons of the Gallic acid reduction percentage of RIE

Tukey Pairwise Comparisons: Response = Gallic acid RIE, Term = Treatment

```
Grouping Information Using the Tukey Method and 95% Confidence

Treatment   N     Mean   Grouping
AC         15  19.7607  A
PVPP       15  15.6918     B
CNTs-NH3   15  15.3494     B
CNTs       15   7.0547        C
Graphene   15   5.2775        C  D
CNTs-COOH  15   4.4281           D
CNTs-OH    15   3.6894           D

Means that do not share a letter are significantly different.
```

Appendix 32: Comparisons of the Ferulic acid reduction percentage of RIE

Tukey Pairwise Comparisons: Response = Ferulic reduction % of RIE, Term = Treatment

```
Grouping Information Using the Tukey Method and 95% Confidence

Treatment   N     Mean     Grouping
Graphene   15  81.6643  A
AC         15  79.6888  A
CNTs-OH    15  39.3296     B
CNTs       15  32.6629        C
CNTs-NH3   15  32.1672        C
CNTs-COOH  15  24.0698           D
PVPP       15  10.5249              E

Means that do not share a letter are significantly different.
```

Appendix 33: Cost comparison of commercial scale, assuming commercial wine treating 10,000L of wine at 1000mg/L.

Finning agents	Cost (A$)	Savings vs. PVPP(A$)	Saving percentage vs. PVPP (%)
PVPP	22,000.00	-	
AC	48,00.00	17,200.00	78.18
G	12,900.00	9,100.00	41.36
CNTs	12,500.00	9,500.00	43.18
OH-CNTs	24,700.00	-2,700.00	-12.27
COOH-CNTs	10,300.00	11,700.00	53.18
NH_2-CNTs	2,125,200.00	-2,103,000.00	95 * times more costly